Stochastic simulation models of *Plasmodium falciparum* malaria epidemiology and control

INAUGURALDISSERTATION
zur
Erlangung der Würde eines Doktors der Philosophie

vorgelegt der
Philosophisch-Naturwissenschaftlichen Fakultät
der Universität Basel

von
Nicolas Maire
aus Basel (BS)

Basel, 2008

Genehmigt von der Philosophisch-Naturwissenschaftlichen Fakultät auf Antrag von Prof. Dr. M.Tanner, Prof. Dr. T.Smith und Dr. A.Saul.

Basel, den 11.12.2007

Prof. Dr. H.-P. Hauri
Dekan

Summary

Every year malaria causes an estimated 1.3–3 million deaths and around half a billion clinical episodes. The majority of deaths occur in children under the age of 5 years. Malaria today occurs mostly in tropical and subtropical countries, particularly in sub-Saharan Africa and Southeast Asia. In developing countries malaria may account for as much as 40% of public health expenditure, 30-50% of hospital admissions, and up to 50% of outpatient visits to health facilities.

Malaria is a vector borne disease caused by the protozoan parasites of the genus *Plasmodium*. *Plasmodium falciparum* causes the most severe form of the disease, and is responsible for half of the clinical cases and 90% of the deaths from malaria.

Malaria control interventions in countries where the disease is endemic currently include personal protection against mosquito bites, vector control, and prophylactic drugs. There is currently no registered malaria vaccine, but this is an active field of research. The vaccine that is furthest advanced in clinical development is called RTS,S/AS02A. This is a pre-erythrocytic vaccine, which aims to kill the parasites before they enter the red blood cells.

Predictive models can provide a rational basis for decisions on how to allocate resources for malaria control. Mathematical modeling of malaria has a long history, starting with the first models of malaria transmission dynamics by Ross a century ago. At the Swiss Tropical Institute, a malaria modeling project has generated algorithms for rational planning of malaria control. This model is implemented as an individual-based discrete-time simulation model. The behaviors and state changes of simulated human individuals are governed by a minimal set of sub-models that are considered crucial for making quantitative predictions of the impact of malaria control interventions.

The integrated model includes components that capture relevant aspects of malaria transmission and epidemiology in the absence of control: the relationship between the entomologic inoculation rate and the force of infection; epidemiologic models for acute illness, severe morbidity, and mortality; infectiousness of human population. Another central model component, for natural immunity to asexual blood stages of *P. falciparum*, is described in this thesis. The use of the model for making quantitative predictions requires reliable estimates of the values of the parameters of the mathematical functions. The different model components were therefore fitted to a number of datasets from studies in various ecological settings and for various epidemiologic outcomes using a simulated annealing algorithm. Comparison of the model predictions with field data show that the model appears to reproduce reasonably well the parasitologic patterns seen in malariologic surveys in endemic areas.

Epidemiologic patterns can be modified by control interventions. Because of the individual-based approach chosen, a number of different simulated interventions can be introduced by making assumptions on how they modify the processes described above. This thesis describes a model for case management to predict the impact of improved case management on incidence of clinical episodes and mortality while incorporating effects on persistence of parasites and transmission. It allows the simulation of different rates of treatment coverage and parasitologic cure rates, and makes it possible to look at how variations in transmission intensity might affect the impact of changes in the health system. It also defines a baseline environment that can be used the predict the impact of other control interventions.

The second part of the thesis focuses on the prediction of the impact of a pre-erythrocytic stage vaccine. Different assumptions about how such a vaccine may lead to a measured reduction in the incidence of new infections in vaccinated individuals are discussed. The vaccine profile was chosen to match data from clinical trials of RTS,S/AS02A. The results demonstrate that an adequate simulation of the first two RTS,S/AS02A trials published can be achieved by assuming that vaccination completely blocks a certain fraction of infections that would otherwise reach the erythrocytic stages.

The impact that such a vaccine would have on the epidemiology if introduced via the Expanded Program on Immunization (EPI) is then predicted. This is the first major attempt to combine dynamic modeling of malaria transmission and control with predictions of parasitologic and clinical outcome. The results suggest a significant impact on morbidity and mortality for a range of assumptions about the vaccine characteristics, but only small

effects on transmission intensities.

To make predictions of the cost-effectiveness of such a vaccination program, costing data are incorporated into a model of a health system that is currently in place in a low-income country context, based largely on data from Tanzania. Depending on the assumed vaccine characteristics and cost, the predicted cost-effectiveness ratios would make vaccination campaigns an attractive choice for health planners compared with other malaria control interventions.

In addition to making quantitative predictions, the model points to data that may be important to make accurate predictions. In order to make mid- to longterm predictions, more data on the clinical epidemiology of malaria in adolescents and adults would be desirable.

The work reported here creates a sound foundation for measuring the effects of introducing new antimalarial interventions, or scaling-up those that are already known to be efficacious and cost-effective. A challenge that remains is to make a comprehensive set of model predictions available to a non-modeler audience so it can be valuable both for informing malaria control strategies and research funding policy.

Zusammenfassung

Malaria verursacht jedes Jahr schätzungsweise 1.3–3 Millionen Todesfälle und etwa eine halbe Milliarde Neuerkrankungen. Der Grossteil der Todesfälle betrifft Kinder unter fünf Jahren. Malaria kommt heute vor allem in tropischen und subtropischen Ländern vor, am stärksten betroffen sind Südostasien und Afrika südlich der Sahara. In Entwicklungsländern ist Malaria für bis zu 40% der Gesundheitskosten, 30-50% der Einweisungen in ein Krankenhaus, und 50% der Arztbesuche verantwortlich.

Malaria wird durch Parasiten der Gattung *Plasmodium* verursacht, welche von Stechmücken übertragen werden. *Plasmodium falciparum* verursacht die schwerste Form der Krankheit, und ist für die Hälfte der Neuerkrankungen und 90% aller Todesfälle verantwortlich.

Die Bekämpfung der Krankheit in malariaendemischen Gebieten umfasst den Schutz von Individuen gegen Mückenstiche (z.B. mit Hilfe von Moskitonetzen), die Bekämpfung des übertragenden Vektors, sowie die medikametöse Prophylaxe. Bis heute ist kein Malaria-Impstoff zugelassen, aber die Impstoff-Entwicklung ist ein aktives Forschungsfeld. Der in der Entwicklung am weitesten fortgeschrittene Impfstoff heisst RTS,S/AS02A. Es handelt sich dabei um eine prä-erythrozytische Impfung, welche die Bekämpfung des Erregers vor dessen Eintritt in die roten Blutkörperchen zum Ziel hat.

Mathematische Modelle können eine Basis für die Planung von Programmen zur Malaria-Bekämpfung und die Priorisierung der eingesetzen Mittel darstellen.

Mathematische Modelle der Malaria-Übertragung sind seit langem etabliert. Ronald Ross publizierte das erste Model im Jahr 1911. Am Schweizerischen Tropeninstitut wurde ein integriertes Model der Malaria-Übertragung zur Evaluation verschiedener möglicher Bekämpfungsstrategien entwickelt. Das Modell ist als individuen-basierte Computersimulation implementiert. Dabei werden eine Anzahl von Prozessen simuliert, die als für das

Verständnis der Malaria-Epidemiologie und die quantitative Voraussage des Effekts von Bekämpfungsstrategien als zentral angesehen werden.

Das integrierte Modell umfasst Komponenten, welche alle wichtigen Aspekte der Malaria-Übertragung und Epidemiologie beschreiben: Der Zusammenhang zwischen der Infektionsrate (Entomologic Inoculation Rate) und der Übertragungsintensität (Force of Infection), ein epidemiologisches Modell für den Zusammenhang zwischen Infektion und Erkrankung, schwerer Erkrankung und Todesfolge, sowie die Infektivität des menschlichen Wirtes. Eine weitere zentrale Komponente, die sich mit der natürlich erworbenen Immunität gegen die asexuellen Blutstadien des Parasiten befasst, wird in dieser Arbeit vorgestellt.

Um ein mathematisches Modell für quantitative Voraussagen benutzen zu können, muss eine zuverlässige Schätzung der Parameter der dem Modell zu Grunde liegenden mathematischen Funktionen erfolgen. Die Parameter der verschiedenen Modell-Komponenten wurden deshalb mit Hilfe eines Optimierungs-Algorithmus basierend auf Daten aus einer Reihe von verschiedenen Feldstudien geschätzt. Ein Vergleich der Modell-Voraussagen mit Daten aus weiteren Feldstudien bestätigt, dass das Modell die parasitologischen Muster in malariaendemischen Gebieten zufriedenstellend reproduzieren kann.

Die Epidemiolgie der Malaria kann durch deren Bekämpfung verändert werden. Aufgrund des in dieser Studie gewählten individuen-basierten Ansatzes können der Effekt einer Reihe verschiedener möglicher Bekämpfungsstrategien untersucht werden. Diese Arbeit beschreibt ein Modell für die medizinische Versorgung von an Malaria erkrankten Patienten. Das Modell erlaubt die Simulation verschiedener Annahmen über die Wirksamkeit der Behandlung und deren Zugänglichkeit für Malaria-Patienten. So kann vorausgesagt werden, wie sich Investitionen in eine verbesserte medizinische Versorgung von Malaria-Patienten abhängig von der Übertragungsintensität auswirkt. Das Modell definiert damit auch eine Referenz-Umgebung, welche für Studien der Auswirkungen anderer Bekämpfungsstrategien dienen kann.

Der zweite Teil dieser Arbeit befasst sich mit der Voraussage der Auswirkungen eines prä-erythrozytischen Impfstoffs.

Es werden verschiedene Hypothesen besprochen, welche den beobachteten Effekt eines solchen Impfstoffs auf die Inzidenz von Neuinfektionen zu erkären versuchen. Die Computersimulationen stützen sich dabei auf Daten aus klinischen Studien des Impstoffs RTS,S/

AS02A. Die Resultate zeigen, dass ein einfaches Modell der Interaktion zwischen erworbener und Impfstoff-induzierter Immunität genügt, um die aus den klinischen Studien publizierten Erkenntnisse zufriedenstellend zu erklären.

Als nächstes wird untersucht, welche Auswirkung die Einführung eines solchen Impstoffs mittels eines bestehenden Impfprogramms für Kleinkinder (das Expanded Program on Immunization) haben könnte. Damit wurden zum ersten Mal die potentiellen Auswirkungen eines Impfprogramms mit Hilfe eines dynamischen Modells der Malaria-Übertragung vorausgesagt. Die Resultate zeigen eine deutliche Reduktion der Morbidität und Mortalität als Folge des Programms, aber nur einen kleinen Effekt auf die Intensität der Malaria-Übertragung. Um Voraussagen über die Kosteneffizienz eines solchen Impfprogramms machen zu können, wurden ein Modell des Gesundheitssystems in einem Entwicklungsland und dessen Kosten ins Modell integriert. Als Datenbasis diente Tansania. Abhängig davon, welche Annahmen über die Eigenschaften und Kosten getroffen werden, kann die Einführung eines Malaria-Impfstoffs in ein bestehendes Impfprogramm im Vergleich mit anderen Bekämpfungsstrategien als kosteneffizient gelten.

Das Modell kann auch zur Identifizierung von Daten dienen, welche zur Planung effektiver und kosteneffizienter Bekämpfungsstrategien hilfreich wären. Die Analyse der Modellvorhersagen zeigt, dass verlässliche Voraussagen über einen weiteren Zeithorizont zuverlässige Daten zur klinischen Epidemiologie der Malaria bei Jugendlichen und Erwachsenen voraussetzen. Das vorgestellte Modell bietet eine solide Basis, um den Effekt und die Kosteneffizienz zukünftiger Möglichkeiten zur Malariabekämpfung mit bestehenden Methoden zu vergleichen. Eine verbleibende Herausforderung stellt die Aufgabe dar, die Resulte und Voraussagen der Modelierungs-Studie für die Verantwortlichen von Programmen zur Malaria-Bekämfung zugänglich zu machen.

Acknowledgements

I would like to thank my supervisor, Prof. Dr. Tom Smith, for his personal and scientific contributions. I have profited tremendously from his experience and skills in malaria epidemiology and related fields. His enthusiasm, patience, and sense of humor were invaluable during the more difficult times.

A special thank you goes to Prof. Dr. Allan Saul, who agreed to act as a co-referee in the role of an external expert.

I wish to express my sincere thanks to Prof. Dr. Marcel Tanner, Director of the STI, for establishing an excellent working environment at the Institute level and Prof. Dr. Mitchell Weiss at the Department level.

I am grateful to Prof. Dr. Tom Smith and Prof. Dr. Marcel Tanner for giving me the opportunity to work on the modeling study as a member of a great team: Amanda Ross, Gerry Killeen, Jürg Utzinger, Fabrizio Tediosi, Guy Hutton, Dan Anderegg, Melissa Penny, Nakul Chitnis, Alain Studer, Allan Schapira, Don de Savigny, Matthias Bischof, Penelope Vounatsou, Josh Yukich, Michael Bretscher, Lesong Conteh, Blaise Genton, and Christian Lengeler. My contributions included the development of models; the implementation of models; software architecture and design; software configuration management; preparation of simulation input data; running of simulations for parameter estimation and predictions; analsysis of simulation results; writing of manuscripts. Tom Smith, Amanda Ross, Fabrizio Tediosi, Jürg Utzinger, Guy Hutton, and Marcel Tanner also contributed to the writing of and critically reviewed the published work in this thesis. Fabrizio Tediosi and Guy Hutton were responsible for the costing data and the interpretation of the economic evaluation.

I would like to thank the members of the Technical Advisory Group (TAG) Michael Alpers, Paul Coleman, David Evans, Brian Greenwood, Carol Levin, Kevin Marsh, F Ellis McKenzie, Mark Miller, Brian Sharp, and of the Project Management Team at the PATH Malaria

Vaccine Initiative and GlaxoSmithKline Biologicals S.A.

The mathematical modeling study was financially supported by th PATH Malaria Vaccine Initiative and GlaxoSmithKline Biologicals S.A. The contents of this thesis do not necessarily reflect the endorsement, opinion, or viewpoints of the PATH Malaria Vaccine Initiative or GlaxoSmithKline Biologicals S.A.

Current funding support is from the Bill & Melinda Gates Foundation and the Swiss National Science Foundation (3300C0-105994).

I wish to thank Prof. Dr. Klaus Dietz and Dr. Louis Molineaux for many long inspiring discussion during their visits to Basel.

I gratefully acknowledge the individuals and institutions of the africa@home collaboration who laid the foundation for malariacontrol.net, and all malariacontrol.net users who are helping to take this to the next level.

Thanks are also expressed to the senior scientists, staff and my fellow students at STI who helped in one way or another. My warmest thanks are addressed to Margrith Slaoui, Eliane Ghilardi, and Christine Walliser for professional administrative support throughout. A special thank you goes to the STI library team of Heidi Immler, Fabienne Fust and Andrea Wirth. Many thanks go to the IT team for their valuable support: Simon Roelly, Martin Baumann, Lukas Camenzind, Brice Matter, Dominique Forster, Simon Schlumpf and Marco Clementi.

Contents

List of Figures

List of Tables

Chapter 1

The use of mathematical models to predict the impact of malaria interventions

This chapter is based on the book chapter: Using volunteer computing to simulate the epidemiology and control of malaria: malariacontrol.net. Nicolas Maire.

In press: Distributed & Grid Computing. Principles, Applications and Supporting Communities, Tectum Verlag, Marburg

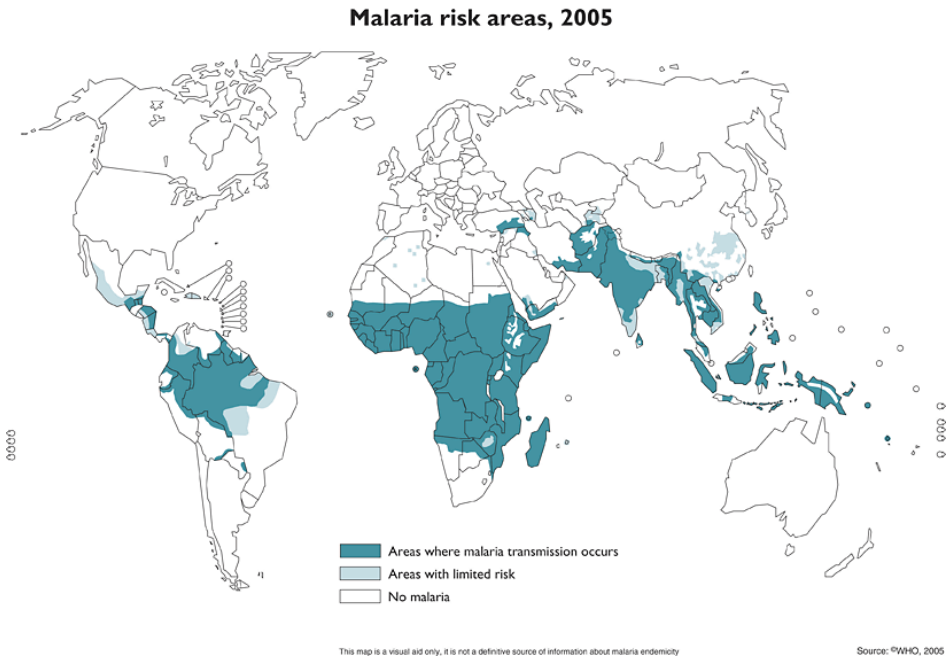

Figure 1.1: Map of malaria risk areas. Source: World Health Organization, 2005. `http://www.who.int/mediacentre/events/2006/g8summit/malaria_large.gif`

1.1 Malaria

Some of the most challenging problems requiring urgent solution in the contemporary world are those of infectious diseases in the developing world. These problems primarily result from lack of resources, from poverty per se. One of the most pervasive diseases of poverty is malaria. Every year malaria causes an estimated 1.3–3 million deaths and around half a billion clinical episodes [Breman et al., 2001]. The majority of deaths occur in children under the age of 5 years. There are no accurate statistics available, as most cases occur in rural areas, where a large proportion of the population does not have access to hospitals or health care in general. Malaria today occurs mostly in tropical and subtropical countries, particularly in sub-Saharan Africa and Southeast Asia (Figure 1.1).

Malaria is a vector borne disease caused by the protozoan parasites of the genus *Plasmodium*. There are four species that can infect humans, of which *Plasmodium falciparum* causes the most severe form of the disease. It is responsible for half of the clinical cases

and 90% of the deaths from malaria. [Gilles and Warrell, 1993]. Figure 1.2 shows the life cycle of the parasite.

P.falciparum is transmitted from person to person by female mosquitoes of the genus *Anopheles*. Inside the human host the parasite undergoes a series of changes. Within half an hour of inoculation of the parasites, the sporozoites infect the liver via the blood stream (Figure 1.2 (a)). Here they divide repeatedly into about 30,000-40,000 merozoites over the course of one or two weeks. Merozoites are released into the blood stream where they invade red blood cells. Inside these blood cells they grow and divide, eventually causing the rupture of the cell and the release of more merozoites, which can go on to invade new blood cells (Figure 1.2 (b)). A small proportion of merozoites develop into gametocytes, and can be taken up by a subsequent mosquito bite. Inside the mosquito the parasite undergoes sexual reproduction and then invades the salivary gland (Figure 1.2 (c)). The cycle completes when the infected mosquito bites another human.

Typically, malaria produces fever, headache, vomiting and other flu-like symptoms. If effective drugs are not available for treatment, the infection can progress rapidly to become life-threatening. Residents of malaria-endemic regions acquire immunity to malaria through natural exposure to malaria parasites. After continued exposure from multiple infections immunity generally provides protection against severe effects of malaria but fails to provide strong protection against infection with malaria parasites.

In developing countries malaria may account for as much as 40% of public health expenditure, 30-50% of hospital admissions, and up to 50% of outpatient visits to health facilities [RBM WHO, 2006]. Critically, malaria is not just caused by poverty; the burden of malaria disease is also an important factor contributing to that poverty. Economic growth in countries with high malaria transmission has historically been lower than in countries without malaria. Some economists believe that malaria is responsible for a growth penalty of up to 1.3% per year in some African countries [Gallup and Sachs, 2001]. Not only does malaria result in lost life, and lost productivity due to illness and premature death, malaria also hampers children's schooling and social development through both absenteeism and permanent neurologic damage [Holding and Snow, 2001].

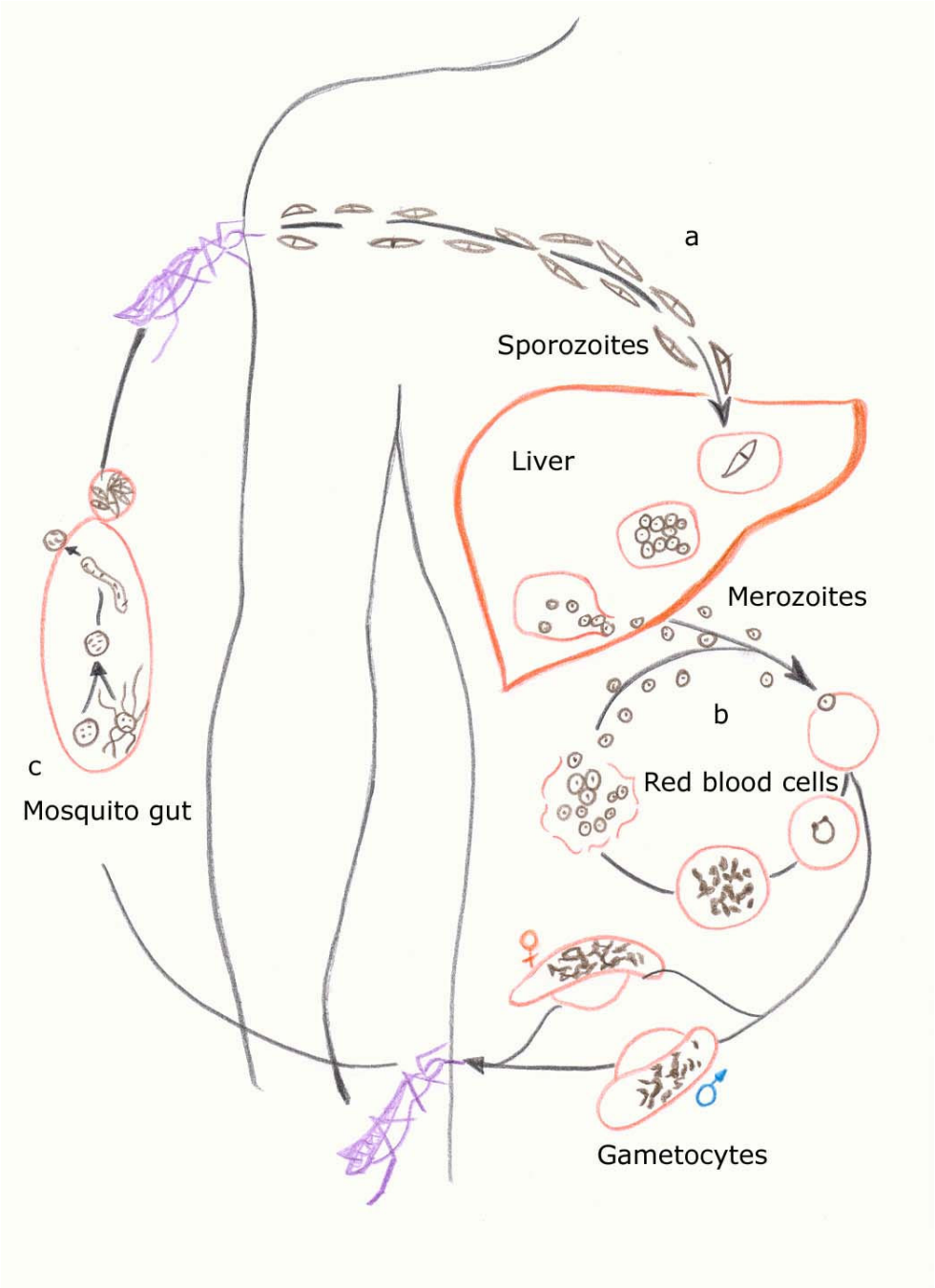

Figure 1.2: The life cycle of *P. falciparum*. A detailed description of the different stages is in the text.

1.2 Malaria control interventions.

Malaria control interventions in countries where the disease is endemic currently include personal protection against mosquito bites, vector control, and prophylactic drugs. There is currently no registered malaria vaccine, but this is an active field of research.

Vector control and protection against mosquito bites. Very soon after the discovery in 1897 that malaria is transmitted by mosquitoes [Gilles and Warrell, 1993], attempts to prevent malaria by killing the mosquitoes vector began. Source reduction is the method of choice for mosquito control when the mosquito species targeted are concentrated in a small number of discrete habitats. Larval habitats can be destroyed by filling depressions that collect water or by draining swamps to remove standing water [Gilles and Warrell, 1993]. Another approach is to cover the walls and other surfaces of a house with a residual insecticide. This method does not prevent people being bitten, but can prevent transmission of infections to another person, as mosquitoes often rest inside houses after taking a blood meal [World Health Organization, 2006]. Mosquito nets help prevent mosquitoes reaching people when they are sleeping, because *A. gambiae*, the most important vector species, mainly bite humans at night [Gillies, 1988, Geissbuehler et al., 2007]. Thus, mosquito nets can greatly reduce the transmission of malaria. The nets are not a perfect barrier, so they are often treated with an insecticide designed to kill the mosquito before it can find a way past the net. These nets have the advantage of also providing some protection to others, including people sleeping in the same room but not under the net. The distribution of mosquito nets impregnated with insecticide has been shown to be an extremely effective method of malaria prevention [Lengeler, 2004, World Health Organization, 2006].

Case management. Improving the management of acute malaria can reduce the malaria-induced burden because infections are cleared before they can cause severe malaria and potentially lead to death. There is also an indirect protective effect as infections are cleared and therefore there is a reduction of the infectious reservoir of people who may transmit to mosquitoes. The management of acute malaria cases can be improved in a number of ways, for example by using more effective drugs or combinations of different drugs, improving access to health facilities, patient compliance to treatment schedules, or strengthening diagnosis [Goodman et al., 1999].

Prophylactic drugs. Several drugs, most of which are also used for treatment of malaria, can be taken preventively. Use of prophylactic drugs is seldom practical for full-time residents of malaria-endemic areas, and their use is usually restricted to short-term visitors and travelers to malarial regions. As opposed to continuous chemoprophylaxis, Intermittent Preventive Treatment (IPT) reduces the number of times an individual has to be given the antimalarial and circumvents the problem of delivery as it is given at routine health visits or times of vaccination. In addition, this intervention can easily be targeted to the most vulnerable population groups. Such an approach has been shown to yield benefits for malaria prevention in pregnant women and infants living in endemic areas [Greenwood, 2006, Meremikwu et al., 2006].

Vaccination. At present, vaccines for malaria are under development, with no completely effective vaccine yet available. The vaccine that is currently furthest advanced in clinical development is RTS,S/AS02A . This is a pre-erythrocytic vaccine, which aims to kill the parasites before they enter the red blood cells. A recent study that looked at over 2000 Mozambican children and demonstrated reduction in the infection risk of approximately 45% [Alonso et al., 2004]. The vaccine has also been shown to be safe and partially effective in infants [Aponte et al., 2007], the age group that will most likely be targeted by a vaccine campaign. Other vaccines currently under development target either the blood stages of the parasite or the stages that are transmitted to the next host by a mosquito [Ballou et al., 2004].

1.3 Mathematical models for decision making in malaria control

Recently, governments in industrialized countries, international agencies, and philanthropic bodies like the Bill & Melinda Gates foundation, have begun to take seriously the need to invest in malaria control, but where should they be putting their resources? To decide on how to allocate resources for malaria control, predictive models are needed to infer what is likely to happen if any of a large array of possible malaria control strategies is adopted. The problem is a similar to that of predicting climate change. Although the dynamics of malaria are qualitatively well understood, and mathematical models of malaria epidemiology have been around for a century [Ross, 1911], the science of quantitatively predicting what

will happen when we intervene against malaria is not well established. While there are many different kinds of interventions possible, their likely effects are difficult to quantify, especially when they are combined. These effects are difficult to quantify for short time scales and even more difficult for longer time-spans of interest, which may be up to decades in length. The likely impact of malaria control interventions has generally been inferred from intervention trial results, which assess only short-term effects using well controlled delivery systems. The long term effectiveness in programs will be reduced because of less than perfect access, compliance, targeting accuracy, and consumer adherence. There will also be longer term dynamic effects due to changes in the immune status of the population, and benefits due to herd immunity (in the case of vaccines) and community effects of vector control.

It seems unlikely that any of the strategies listed above will prove to be a magic bullet that will solve the problem of malaria for good, but well-planned integrated control may be able to capitalize on the advantages of each individual intervention. Since *Plasmodium falciparum* malaria is one of the most frequent causes of morbidity and mortality in areas where it is endemic [Breman et al., 2001, Greenwood et al., 2005, Snow et al., 2005], even a partially protective intervention may be a critically important public health tool.

Mathematical modeling of malaria has a long history, starting with the first models of malaria transmission dynamics by Ross [1911]. Macdonald [1957] built on Ross' work and identified the importance of mosquito longevity for the basic reproductive number (R_0). R_0 is the number of secondary cases following the introduction of a single infected individual into a susceptible population, an important measure in studies of infection dynamics. Macdonald was also among the first to recognize the potential of using computers in the study of malaria transmission models [Macdonald et al., 1968]. They also included the first stochastic malaria simulation model published. Dietz and Molineaux extended on these compartmental models by adding immunity, and emphasized the need of estimating model parameters from field data [Dietz et al., 1974, Molineaux and Gramiccia, 1980]. Up to that point, malaria eradication was at the focus of interest in malaria modeling. After the realization in the 1970s that global malaria eradication was an unrealistic goal [Gilles and Warrell, 1993], the focus of malaria models shifted towards control, and as a consequence models of clinical epidemiology [Rowe et al., 2007] and models of comparative cost-effectiveness [Goodman et al., 2000]. In terms of the methodology, the limitations of

continuous-time compartmental methods became apparent [Saul, 1998, Molineaux and Dietz, 1999, Paget-McNicol et al., 2002, Gatton and Cheng, 2004]. Models were extended to include discrete time steps, and complemented with individual-based approaches [McKenzie, 2000], which at that point had gained popularity in ecology and other research fields [Grimm and Railsback, 2005].

1.4 Overview of the modeling strategy

At the Swiss Tropical Institute (STI), a malaria modeling project has generated algorithms for rational planning of malaria control [Smith et al., 2006a]. This integrated model is implemented as an individual-based discrete-time simulation model [Grimm and Railsback, 2005], where the predictions result from the overall consequences of processes involving individuals of a population. Individuals are characterized by a set of properties and behaviors. This allows for an intuitive translation of reality into the implementation domain by mapping real world entities onto abstract datatypes (or programming objects). The simulated population consists of a collection of these objects. Individuals are updated over time, using discrete time steps with intervals appropriate to capture the dynamics of the system. Currently, a temporal resolution of five days per simulated interval is used. Characteristics of each individual are tracked through time, and relevant events recorded. The behavior is determined by mathematical description to specify functional relationships between the variables of the system. A summary of the simulated events of interest is output at the end of a simulation run.

1.4.1 Model components

The behaviors and state changes of simulated human individuals are governed by a minimal set of sub-models that are considered crucial for making quantitative predictions. All relevant modules are briefly discussed in the following section, and later chapters contain full descriptions of some of the model components.

Relationship between the entomologic inoculation rate and the force of infection. The process of infection of human individuals through bites of infected mosquitoes is considered the most upstream component of the model framework. The seasonal pattern

and magnitude of the entomologic inoculation rate (EIR) is the main simulation input and in the absence of simulated interventions determines the epidemiologic predictions. Underlying the simulation of the infection process is a stochastic model for the relationship between the EIR for *P. falciparum* malaria and the force of infection in endemic areas [Smith et al., 2006b]. The model incorporates effects of increased exposure to mosquito bites as a result of the growth in body surface area with the age of the host. The number of new infections in a human host at any simulated time interval is drawn from a Poisson distribution, where the mean is the age-adjusted EIR corrected for the survival probability of the inoculum as a consequence of naturally acquired pre-erythrocytic immunity and the reduction in the proportion of entomologically assessed inoculations leading to infection, as the EIR increases.

A model for natural immunity to asexual blood stages of *P. falciparum*. Successful inoculations pass into blood-stage infections after a fixed pre-patent period of 3 five-day intervals. Asexual blood-stage infections are characterized by hypothesized traces of parasite densities of individual infections over time. The densities are based on a description of the time courses of parasite densities in immuno-naïve, untreated patients who received therapeutic *P. falciparum* infections [Eyles and Young, 1951]. While most mathematical models for acquired immunity to *P. falciparum* consider effects of immunity on duration of infection and infectiousness, the most evident effect of immunity is to reduce parasite densities. Chapter 2 describes a stochastic simulation model to predict the distributions of *P. falciparum* parasite densities in endemic areas, with the parasite densities modified depending on immunity parameters determined from the individual's history of infection. The model for asexual blood-stage parasite densities is a central link between the different sub-models. Downstream components like the models for morbidity, mortality, and the infectiousness of humans to mosquitoes all directly depend on the predicted parasite densities.

An epidemiologic model for acute illness. Whereas most previous malaria models were concerned with threshold analyses of the conditions necessary for the interruption of malaria transmission, predictions of the clinical epidemiology of malaria are crucial for models which look at malaria control. Here, the probability of a clinical attack of malaria is assumed to be a function of the peripheral parasite densities. A pyrogenic threshold that responds dynamically to the parasite load determines how likely a certain parasite

load is to lead to a clinical episode at any simulated time interval. The pyrogenic threshold increases with exposure and decays in the absence of parasites [Smith et al., 2006c]. The severity of the episode and the clinical outcome as well as the probability of the episode being treated depend on the model components described below.

An epidemiologic model for severe morbidity and mortality. Severe malaria episodes are defined as events that would have been diagnosed as severe malaria, had the patient presented to a health facility [Ross et al., 2006b]. The model considers two subcategories of severe malaria episodes. These comprise episodes with extremely high parasite densities in hosts with little previous exposure, and acute malaria episodes accompanied by co-morbidity or other risk factors enhancing susceptibility. In addition to direct malaria mortality from severe malaria episodes, the model also considers the enhanced risk of indirect mortality following acute episodes accompanied by co-morbidity after the parasites have been cleared. Due to the limited availability of data on severe malaria in adults, the model predictions for children are likely to be more reliable than those for older people.

Infectiousness of human population. Models of infectious diseases need to consider the interdependence of hosts, which is what distinguishes them from models of non-infectious diseases. Control interventions against infectious diseases can benefit individuals even if they are not covered by the intervention itself through the indirect effect on transmission intensity. In the current model, the indirect effect depends on the nature of the simulated intervention. In the case of interventions that have a vector control component, the effect on vectorial capacity must be considered. Such entomologic models are currently being developed (Chitnis et al, in preparation). Predictions of the impact of interventions that do not affect the vector population, such as vaccines, can make simplifying assumptions that allow the simulation of indirect intervention effects without the need to explicitly model the vector population [Killeen et al., 2006]. Assuming constant vectorial capacity, the effect of the intervention is captured by scaling the EIR by the relative infectiousness of the human population. Relative infectiousness here means the probability of a mosquito biting human to become infected during the intervention period compared with this probability at the same point in the year in a non-intervention scenario.

The transmission cycle is therefore closed using a statistical model for the relationship

between asexual parasite densities of *P. falciparum* and the infectivity of the host to mosquitoes [Ross et al., 2006a]. This model takes into account the delay between asexual parasitemia and infectivity resulting from the time course of gametocytemia. It also allows for the need for the blood meal to contain gametocytes of both sexes if infection is to take place.

Predictions of the impact of control interventions. The model components described so far provide a framework for simulations of malaria transmission in the absence of control. Epidemiologic patterns can be modified by control interventions. Because of the individual-based approach chosen, a number of different simulated interventions can be introduced by making assumptions on how they modify the processes described above.

Among the possible interventions, the first that is discussed in this thesis is case management (Chapter 3), which has implications on disease outcomes, and potentially indirect effects by reducing the infectiousness of humans if treatment drugs have a gametocytocidal effect, treatment is prompt and coverage is high [Butcher, 1997]. The integration of a model for case management into the stochastic simulation framework allows us to predict the impact of improved case management on incidence of clinical episodes and mortality while incorporating effects on persistence of parasites and transmission.

Figure 1.3 shows the points at which different malaria vaccine types act. The predictions

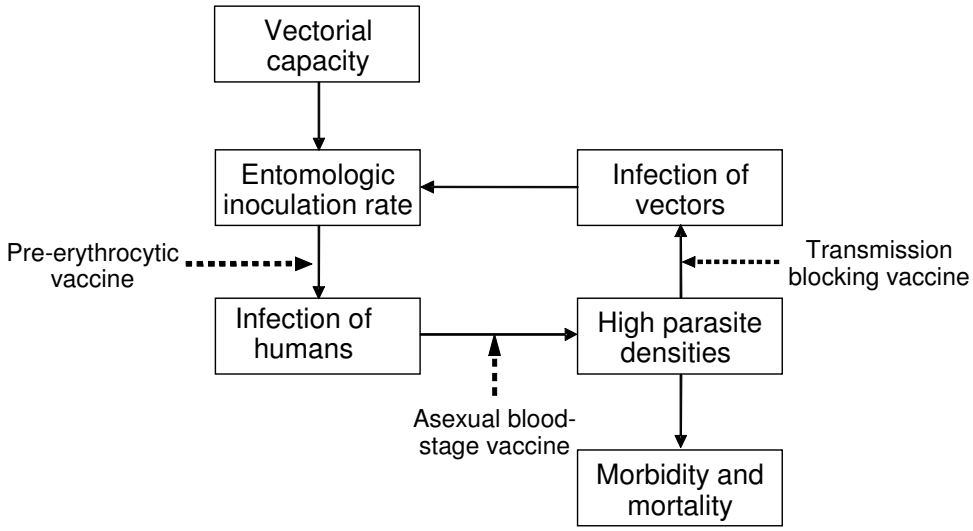

Figure 1.3: Vaccine points of action. Modified from Smith et al. [2006a]

of the impact of vaccines discussed in this thesis are all based on the assumption that the vaccine acts on the pre-erythrocytic stages of the parasite. Chapter 4 discusses different assumptions on how such a vaccine may lead to a measured reduction in the incidence of new infections in vaccinated individuals. The vaccine profile was chosen to match data from clinical trials of RTS,S/AS02A [Alonso et al., 2004]. Chapter 5 predicts the impact that such a vaccine would have on the epidemiology if introduced via the Expanded Program on Immunization (EPI). To make predictions of cost-effectiveness, costing data on the vaccine is incorporated into the model, together with a description of a health system that is currently in place in a low-income country context, based largely on data from Tanzania (Chapter 6). The cost-effectiveness of such a vaccination program results from the epidemiologic impact and the net cost of the intervention.

The standard outcome of all predictive scenarios presented are predictions of three-monthly patterns of parasitemia, age-incidence of clinical episodes, severe malaria, and death over a 20-year time horizon, so as to cover a period at least as long as those that might usually be considered by health planners.

1.4.2 Estimation of model parameters

The use of the model for making quantitative predictions requires reliable estimates of the values of the parameters of the mathematical functions. The different model components were therefore fitted to a number of datasets from studies in various ecological settings and for various epidemiologic outcomes using a simulated annealing algorithm [Kirkpatrick et al., 1983, Press et al., 1988]. Even though the simulations could be distributed over STI's local network the computing resources were limiting the optimization process because of the high dimensionality of the parameter space and the stochastic nature of the model predictions. For this reason, downstream model components were fitted conditional on upstream parameters. Table 1 in [Smith et al., 2006a] lists all model parameters, together with the values estimated from fitting to field data.

1.5 Goals and objectives

In summary, the goals of this research project are

- the development of models for the natural history and epidemiology of *P. falciparum* malaria.
- the development of models for malaria control interventions.
- the prediction of the epidemiologic impact and cost-effectiveness of control interventions.

The specific objectives addressed in this thesis are

- a model for natural immunity to asexual blood stages of *P. falciparum* malaria (Chapter 2).
- a model for the case management of *P. falciparum* malaria in sub-Saharan Africa (Chapter 3).
- a model for a pre-erythrocytic vaccine, and estimates of the vaccine characteristics of a real vaccine (Chapter 4).
- predictions of the epidemiologic impact of introducing a pre-erythrocytic vaccine into the Expanded Program on Immunization in sub-Saharan Africa (Chapter 5).
- predictions of the cost-effectiveness of introducing a pre-erythrocytic vaccine into the Expanded Program on Immunization in Tanzania (Chapter 6).

Chapter 2

A model for natural immunity to asexual blood stages of *Plasmodium falciparum* malaria in endemic areas

Nicolas Maire[1], Thomas Smith[1], Amanda Ross[1],
Seth Owusu-Agyei[2], Klaus Dietz[3], Louis Molineaux[4]

This article has been published:
American Journal of Tropical Medicine and Hygiene 2006, 75, Suppl 2, 19-31

[1]Swiss Tropical Institute, Basel, Switzerland
[2]Navrongo Health Research Centre, Navrongo, Ghana
[3]University of Tübingen, Tübingen, Germany
[4]World Health Organization, Geneva, Switzerland

Abstract

Most mathematical models for acquired immunity to *Plasmodium falciparum* consider effects of immunity on duration of infection and infectiousness, but do not consider the most evident effect of immunity, which is to reduce parasite densities. Few attempts have been made to fit such models to field data. We propose a stochastic simulation model to predict the distributions of *P. falciparum* parasite densities in endemic areas, in which acquired immunity acts by reducing parasite densities. We have fitted this model to age-specific prevalence and geometric mean densities from settings in Ghana, Nigeria, and Tanzania. The model appears to reproduce reasonably well the parasitologic patterns seen in malariologic surveys in endemic areas and is appropriate for predicting the impact of interventions such as vaccination in the context of continual exposure to *P. falciparum*.

2.1 Introduction

In areas endemic for *Plasmodium falciparum* malaria, many people are subjected to frequent re-infection; thus they develop partial immunity that leads to control of parasite densities and to reduction in the frequency of clinical episodes [Molineaux et al., 1988]. However the level of acquired immunity does not reach a state of absolute resistance to infection. Mathematical models that capture these effects of immunity are needed to predict the potential epidemiologic impact of partially effective interventions against the parasite, such as current formulations of malaria vaccines [Alonso et al., 2004].

Within-host models for individual *P. falciparum* infections have considered how partial immunity affects parasite densities as an explicit consequence of differential survival of the circulating asexual parasites as the infection develops [Molineaux et al., 2001, Paget-McNicol et al., 2002]. However, models for the dynamics of *P. falciparum* in populations, including those modeling acquired immunity [Aron, 1988, Dietz et al., 1974, Struchiner et al., 1989], have generally not considered the densities of asexual parasites. We are aware of only one population model for *P. falciparum* malaria that explicitly considered the effects of immunity on parasite densities [Elderkin et al., 1977]. The lack of models of parasite density is surprising because effects on densities are the clearest evidence for an effect of naturally acquired immunity. The existence of such natural immunity represents some of the strongest evidence that development of an efficacious malaria vaccine is possible.

One of the major effects of immunity in most epidemiologic models of malaria [Aron,

1988, Molineaux and Gramiccia, 1980, Struchiner et al., 1989] is to reduce the duration of infections and consequently the number of infections of the vector resulting from one human infection. This quantity, following the report of Macdonald [Macdonald, 1957], is generally assumed to be proportional to infection duration, which leads to a formula that makes the basic reproductive number proportional to the infection duration. However, there is little empirical evidence on the effect of acquired immunity on duration of infection [Sama et al., 2004]. Some models [Gupta and Day, 1994] and empirical studies [Smith et al., 1999, Smith and Vounatsou, 2003] have even suggested that in the semi-immune host, chronic malaria infection may persist longer than in naïve hosts.

We now propose a new model for natural immunity to the asexual blood stages of *P. falciparum* that specifically focuses on the effect on parasite densities, since it is undoubtedly the case that the major impact of acquired immunity is to reduce the overall parasite load in infected individuals. This model makes predictions of the age patterns of patent parasitemia and of the geometric mean parasite density. Infections in naïve hosts mimic the levels of parasitemia reached by *P. falciparum* infections induced to treat neurosyphilis in the United States (Milledgeville Hospital, GA and National Institutes of Health Laboratories, Columbia, SC during 1940-1963, Figure 2.1) [Collins and Jeffery, 1999b]. In previously exposed hosts, we model a reduction in the densities that depends on the host's history of infection. This simulated acquired immunity does not affect the duration of the infections although it can reduce the period for which parasite density is above the detection limits used in field malariology.

We implement the model by stochastic simulation of each individual infection in a human population using a five-day time-step, and introduce infections by a process dependent on the temporal pattern of the entomologic inoculation rate (EIR) modulated as described in [Smith et al., 2006b].

Here, we present how the model has been fitted to prevalence, density, and multiplicity data of *P. falciparum* obtained from different epidemiologic settings in Ghana, Nigeria, and Tanzania, and show that it gives realistic predictions of age-prevalence and age-density relationships across a range of transmission intensities. This model forms one component of a comprehensive dynamic model for the transmission cycle of the *P. falciparum* parasite, and of malaria morbidity, and mortality, as well as of cost-effectiveness of control strategies.

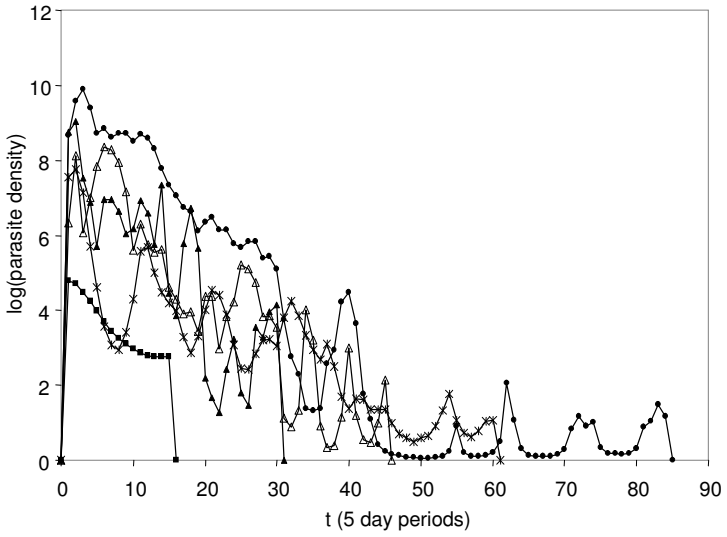

Figure 2.1: Parasite density as a function of time since infection in malaria-naïve individuals. Geometric mean parasite density as a function of time since start of patency and depending on the duration of patent infection. The figure shows examples from five individual patients.

2.2 Methods

Epidemiologic data. The model was fitted simultaneously to six datasets of pre-intervention cross-sectional malariologic surveys from four different field studies of *P. falciparum* malaria in Africa (Tables 2.1 and 2.2), that were chosen to represent a range of transmission intensities. In addition, datasets from Saradidi, Kenya and from interventions carried out in Matsari village (Garki project, Nigeria), were used to fit the model for the incidence of infection, as described in the accompanying paper [Smith et al., 2006b]. Data from the pre-intervention phase of the Garki project collected in Rafin Marke, Matsari, and Sugungum villages, and from Navrongo, Idete, and Namawala were used to fit the model for three distinct cross-sectional outcomes in the absence of intervention; 1) age-specific prevalence of patent parasitemia, 2) age-specific geometric mean density of parasitemia in positive individuals, and 3) age-specific multiplicity measured by polymerase chain reaction-restriction fragment length polymorphisms (PCR-RFLP) of the merozoite surface protein 2 gene [Smith et al., 2006b] (data from Navrongo only).

In all of these field-studies, entomologic surveys had been carried out to determine the annual cycle of the inoculation rate (Figure 2.2; Table 2.1) and these entomologic data were used as input to the simulation model.

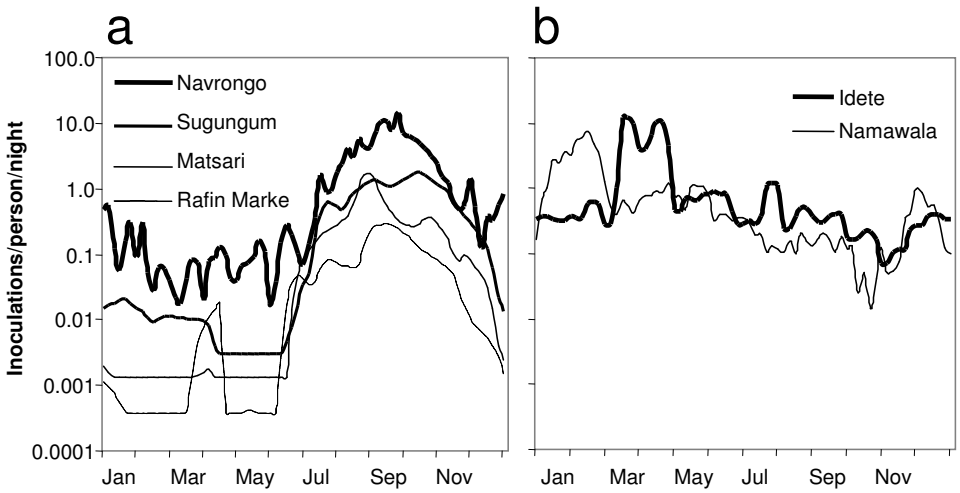

Figure 2.2: Entomologic input data. Annual cycle of the entomologic inoculation rate. a) West African sites. b) East African sites.

Table 2.1: Datasets included in the fitting of the model to field data

Site / Reference	Description of the data	Purpose of inclusion	EIR*	Quantities fitted
Rafin-Marke, Garki, Nigeria (pre-intervention)‡ / 1§	8 cross-sectional surveys of entire village population, at 10-week intervals (total 2,593 blood slides)	Age-prevalence and density at lowest EIR in the Garki project.	1§	Age- and season-specific parasite prevalence†, age-specific parasite density†
Matsari, Garki, Nigeria (pre-intervention)‡ / 1§	8 cross-sectional surveys of entire village population, at 10-week intervals (total 2,963 slides)	Age-prevalence and density at circa the median EIR for the Garki project	1§	Age- and season-specific parasite prevalence†, age-specific parasite density†
Sugungum, Garki, Nigeria (pre-intervention)‡ / 1§	8 cross-sectional surveys of entire village population, at 10-week intervals (total 4,487 blood slides)	Age-prevalence and density at highest EIR in the Garki project.	1§	Age- and season-specific parasite prevalence†, age-specific parasite density†
Saradidi, Kenya / 2§	21 cohorts each of approximately 50 children aged between 6 months and 6 years whose parasites were cleared and who were then followed-up with 2 weekly surveys.	Incidence of infection in relation to EIR	2§	Incidence risk of infection over 2-week periods.

Continued on next page

Table 2.1: Datasets included in the fitting of the model to field data

Site / Reference	Description of the data	Purpose of inclusion	EIR*	Quantities fitted
Matsari, Garki, Nigeria (intervention phase) / 1§	8 cross-sectional surveys of entire village population, at 10-week intervals. Mass treatment with sulfamine-pyrimethamine 10-weeks prior to each survey (total 2,663 blood slides)	Incidence of infection allowing for patency of infections	1§	Age- and season-specific incidence risk of patent infection†
Namawala, Tanzania / 3§	12 cross-sectional surveys of an age-stratified sample, at 2-month intervals (total 3,901 blood slides)	Age-prevalence and density at very high EIR	3§	Age- and season-specific parasite prevalence†, age-specific parasite density†
Idete, Tanzania / 4§	Surveillance of a rolling cohort of infants (1,382 blood slides over 16 months). Also 1 cross-sectional survey of 312 children 1-5 years old. 5§	Effects of maternal immunity	6§	Age- and season-specific parasite prevalence†, age-specific parasite density†

Continued on next page

Table 2.1: Datasets included in the fitting of the model to field data

Site / Reference	Description of the data	Purpose of inclusion	EIR*	Quantities fitted
Navrongo, Ghana / 7§	6 cross-sectional surveys of an age-stratified sample, at 2-month intervals (total 522 slides/DNA samples)	Age-multiplicity and seasonality of multiplicity.	8§	Age-specific parasite prevalence and density, age-specific multiplicity of *msp*-2, by PCR-RFLP

* Entomologic inoculation rate (inoculations per person per year, estimated for adults as described in the cited references)

† by microscopy. The simulations assumed limits of detection of parasites by microscopy to be 2 parasites/μl of blood for the Garki study, and 40 parasite/μl of blood for the other sites, corresponding to the nominal limits of methods for quantifying parasitemia used in the sites.

‡These surveys were carried out prior to the introduction of residual insecticide spraying and of mass anti-malarial treatment in some of the villages.

§1: [Molineaux and Gramiccia, 1980]; 2: [Beier et al., 1994]; 3: [Smith et al., 1993]; 4: [Alonso et al., 1994, Kitua et al., 1996]; 5: Placebo group from the trial of Alonso and others [1994]; 6: [Charlwood et al., 1998]; 7: [Owusu-Agyei et al., 2002]; 8: Owusu-Agyei and others, unpublished data

Table 2.2: Overall data summary and log likelihoods for each site

	Data summary			Loss functions for best fitting model		
	Annual EIR*	% Prevalence †	Geometric mean density (parasites/μl)‡	Log likelihood for prevalence	Log likelihood for Geometric mean density	Log likelihood for Multiplicity
Sugungum	132	48.3	22.4	-2,830.4	-116.6	-
Rafin Marke	18	44.2	17.8	-1,722.4	-131.2	-
Matsari (pre-intervention)	68	41.6	18.4	-1,895.9	-122.8	
Matsari (intervention phase)	5.5§	8.5	-	-782.4	-	-
Idete§§	584	59.6	3,146.8	-1,124.3	-132.7	-
Navrongo	405	54.8	336.1	-341.7	-116.1	-276.8
Namawala	329	77.3	1,111.3	-2,007.7	-92.1	-

*EIR = entomologic inoculation rate.

†Overall proportion of slides positive for *P. falciparum.*

‡Geometric mean of recorded parasite densities on positive slides. The substantial difference between the Garki study and other datasets partly reflects different parasitologic methods and is allowed for by the bias adjustment in the models.

§Arithmetic mean of estimated daily inoculation rate for the whole intervention period, based on re-analysis of the original data.

§§Average parasite densities in Idete are much higher because this dataset comprises predominantly data for very young children. In all cases the models were fitted to the age group- and survey- specific data, not to the overall means. The data from Saradidi and the fit to those data are described in an accompanying paper [Smith et al., 2006b]

In all sites except Idete, the health system at the time of the surveys treated only a small proportion of the clinical malaria episodes; in the Idete study, we calculate from the published results [Kitua et al., 1996, Vounatsou et al., 2000] that the village dispensary treated approximately 64% of clinical malaria attacks and our simulations assume this coverage of effective treatment. Parasite densities in the Garki dataset were recorded by scanning a predetermined number of microscope fields on the thick film and recording how many had one or more asexual parasites visible. We converted these values to numbers of parasites/μl by assuming a Poisson distribution for the number of parasites per field and a blood volume of 0.5 mm^3 per 200 fields [Molineaux and Gramiccia, 1980]. In the other field studies, parasites were counted against leukocytes and converted to nominal parasites/μl assuming the usual (though biased) standard of 8,000 leukocytes/μl [Shute, 1988].

The biases in density estimates resulting from these different techniques was accounted for by multiplying the observed parasite densities with constant values estimated for Garki (ν_0) and non-Garki (ν_1) field studies to rescale them to the values in the malariatherapy patients (determined using the methods of Earle and Perez [1932]).

Hypothesized set of processes controlling asexual parasitemia. For every individual in the simulated population each discrete infection is characterized by simulated duration and densities at each five-day time point. The host acquires immunity as a function of exposure and this in turn modifies the density of subsequent infections.

Durations of infection. We treat each infection as monoclonal, but note that the infection process allows multiple infections during the same time interval. Each new infection j, initiated in individual i at time t_0, is assigned a duration, i.e. $t_{\max}(i,j)$. The duration is defined as the time interval between the first and last days of patent parasitemia that would be observed in the absence of adjustments to allow for host immunity. The present model does not allow the immune status of the host to affect the simulated period for which the infection persists, although the immune status does affect the duration of patent infection by modifying the proportion of time points for which the parasites are at detectable densities.

The simulated infection starts after the pre-erythrocytic latent period l_p, set to three time intervals, i.e. 15 days which correspond to the hepatic stage of the life cycle plus the pre-patent blood stage infection. We use the index τ to denote the time since the start

of patent infection, i.e. $\tau = 1$ corresponds to the first five-day interval when the infection becomes patent, three time units after the infection event.

The duration of infection is randomly sampled from a distribution equivalent to that of malariatherapy patients treated in Milledgeville, Georgia [Collins and Jeffery, 1999b]. Infections in patients from this hospital persisted for longer than those in South Carolina and this appears to reflect more conservative policies (more treatment) in the latter hospital. We therefore assume that the Georgia infections were more similar to untreated natural infections in a typical malaria-endemic setting of Africa. The period of follow-up after the last positive slide also varied. Thus, confidence that an infection was spontaneously cleared also varied. We considered only patients who did not receive any anti-malarial treatment on their last day of positivity, and for each of these determined $t_1(i)$, the duration of follow-up after the last recorded day of positivity. For a series of cutoffs, t_1*, we considered that subset of patients for whom $t_1(i) > t_1*$, and calculated the mean of the logarithm of the observed durations for those patients who were included. We surmise that the subset giving the highest value of this mean best approximates the behavior of untreated natural infections. The maximum value of this mean was 5.13 (corresponding to a geometric mean of 169.0 days), which was computed from a subset comprising those 47 patients for whom $t_1(i) > 2$ months. In this set of patients, the standard deviation of the natural log of the duration was 0.80, and the distribution of durations in this subset of patients was approximately log normal. In the simulations we therefore sampled the durations of untreated infections using

$$\ln(t_{\max}(i,j)) \sim Normal(5.13, 0.80) \tag{2.1}$$

Expected densities of single infections. At each time point, $\tau = 0, 1, ..., t_{\max}(i,j)$, the density, $y(i,j,\tau)$, of the infection j in host i, is set by first determining the expected log density, $E(\ln(y_0(i,j,\tau)))$, that would apply in the absence of previous exposure. To determine $E(\ln(y_0(i,j,\tau)))$ we first determine the mean logarithm of the densities of malariatherapy patients in the Georgia hospital, specific for the age of the infection (τ) and for the pre-defined duration ($t_{\max}$). The distributions of densities for the Georgia patients were summarized by grouping the data into five-day categories according to the time since the first day of patent asexual parasitemia and according to durations, and then using moving average smoothing of the logarithmically transformed densities to obtain a function, $y_G(\tau, t_{\max})$ (Figure 2.1), which is a simple description of average densities experienced in

the course of a single malaria infection of a previously naïve host.

The actual densities experienced by different malariatherapy patients varied widely even when the inocula were of the same strain, and were not greatly affected by the size of the inoculum [Glynn and Bradley, 1995]. In our model this between-host variation is captured by assigning to each individual i in the simulated population a value, $(d(i))$, drawn from a log-normal distribution (geometric mean 1, variance σ_i^2), which multiplies the densities so that

$$E(\ln(y_0(i,j,\tau))) = \ln d(i) + \ln(y_G(\tau, t_{\max})) \tag{2.2}$$

This empirically determined function provides a description of single infections that thus captures the effects of blood-stage immunity that the infection stimulates against itself. This includes effects of innate immunity, antigenic variation, and variant independent anti-merozoite immunity [Molineaux et al., 2001].

Adjustments are then applied to $E(\ln(y_0(i,j,\tau)))$ to allow for immunity acquired as a result of exposure to previous infections and for co-infection in hosts with multiple infections. These determine the adjusted expected value, $E(\ln(y(i,j,\tau)))$. The simulated density $y(i,j,\tau)$ is then determined by sampling its logarithm using normal distributions centered on $E(\ln(y(i,j,\tau)))$.

Effects of acquired immunity on the expected parasite density. Acquired immunity to erythrocytic stages of the parasite is related to cumulative exposure to asexual parasites. In our model the extent of acquired immunity depends both on the diversity of the parasites to which the host has been exposed and on the cumulative density of total parasitemia. In the current version we assume no decay of this component of natural immunity in the absence of infections.

The first trigger function is the cumulative density (parasites/μl of blood $\times$ days) of asexual parasitemia since birth up to time t for individual i, i.e.

$$X_y(i,j,t) = \int_{t-a}^{t} Y(i,\tau)d\tau - \int_{t_{0,j}}^{t} y(i,j,\tau)d\tau \tag{2.3}$$

where $Y(i,\tau)$ is the total parasite density of individual i at time τ, and a is the age at time t. $X_y(i,j,t)$ measures the total antigenic stimulus to which the host has been exposed less the exposure due to infection j, which is measured by the term $\int_{t_{0,j}}^{t} y(i,j,\tau)d\tau$. The

latter term must be subtracted to avoid allowing twice for acquired immunity stimulated by infection j itself.

We parameterize the effect D_y of this exposure on parasite densities with a Hill function of the form:

$$D_y = \frac{1}{1 + \frac{X_y}{X_y^*}} \tag{2.4}$$

where we omit the indices from $X_y(i, j, t)$ to simplify the notation, and where X_y^* is a parameter to be estimated, which takes a real positive value, and where D_y consequently takes a value 1 when $X_y = 0$, and is small but positive when X_y is large.

The second trigger function is the cumulative number of prior infections that the host has experienced, i.e.

$$X_h(i, t) = \int_{t-a}^{t} h(i, \tau) d\tau - 1 \tag{2.5}$$

This term monotonically increases with the size of the repertoire of non-variant polymorphic antigens to which the host has been exposed, and therefore provides a measure of the antigenic stimulus that they provide. We assume that the effect of this on parasite densities can be measured by a further, one-parameter sigmoidal function where the further parameter X_h^* is constrained to take a positive value, i.e.

$$D_h = \frac{1}{1 + \frac{X_h}{X_h^*}} \tag{2.6}$$

The third trigger function is the age of the host a, which is inversely related to the extent of maternally derived protection. We treat the level of maternal protection as independent of maternal exposure. In case of a low transmission level, few infants will be exposed during the first few months of life, so maternal immunity is irrelevant. If transmission is frequent, then all mothers will have similar immune status [Ross and Smith, 2006].

We parameterize the multiplication factor that models the effect of maternal immunity D_m, with a decay function that lies between 0 (maximal effect, corresponding to the status at birth), and 1 (no reduction in density), such that

$$D_m = 1 - \alpha_m \exp(-\frac{0.693a}{a_m^*}) \tag{2.7}$$

where a_m^*, the half-life of the maternal immunity, and α_m, the maternal protection at

birth, are additional parameters to be estimated. We then compute the expected density for single infections as

$$E(\ln(y(i,j,\tau))) = D_y D_h D_m \cdot \ln(y_0(i,j,\tau)) \tag{2.8}$$

Effects of concurrent infections. When the host is infected with more than one infection at the same time, innate immunologic responses, together with other density-dependent regulatory mechanisms, lead to a reduction in the overall density to below that expected if the infections did not interact. We estimate this effect by assuming the density of each component infection to be multiplied by a term constrained to take a value between 1 (no interaction between co-infections) and $1/M(t)$, where $M(t)$ is the total multiplicity of concurrent infections at time t. The value $1/M(t)$ corresponds to reduction of the total density to that expected if there was only a single infection. To achieve this we define a further parameter D_x, constrained to be between 0 and 1 and set

$$E(\ln(y(i,j,\tau))) = D_y D_h D_m \cdot \ln(y_0(i,j,\tau)) + \ln(\frac{D_x}{M(t)} + 1 - D_x) \tag{2.9}$$

Distributions of parasite densities and determination of expected prevalence. The predicted densities for each individual in the simulated population, $y(i,j,\tau)$, are sampled around the expectations of their logarithms, using log-normal distributions. The variance of these log-normal distributions, which is estimated from the field data during the fitting process, comprises both variation between hosts, and variation within individual hosts.

Variation between hosts is quantified by the term σ_i^2, while variation within individual hosts is quantified by a term $\sigma_y^2(i,j,\tau)$, which includes an effect of the cumulative exposure of the host, and is necessary to obtain a good fit. Thus,

$$\sigma_y^2(i,j,\tau) = \frac{\sigma_0^2}{1 + \frac{X_h(i,t)}{X_v^*}} \tag{2.10}$$

where the parameters σ_0^2 and X_v^* need to be estimated.

It follows that the simulated densities are distributed as

$$\ln(y(i,j,\tau)) \sim Normal(E(\ln(y(i,j,\tau))), \sigma_y^2(i,j,\tau)) \tag{2.11}$$

The total density at time t in host i is then the sum of the densities of the various co-infections j.

$$Y(i,t) = \sum_j y(i,j,\tau(i,j)) \tag{2.12}$$

Entomologic inoculation rate. The input to the model is the annual cycle of the EIR. In the case of the Garki sites in Nigeria, the EIR was assessed using human night bait collections and dissections of the salivary glands of the *Anopheles* mosquitoes to give the sporozoite rate. A random effects logistic model was used to give season- and village-specific estimates of the sporozoite rate. The EIR values were then rescaled so the annual totals corresponded to the published values of 18, 68, and 132 for the villages of Rafin Marke, Matsari, and Sugungum respectively [Molineaux and Gramiccia, 1980]).

In the cases of Idete (annual EIR = 584) and Namawala (annual EIR = 329) in Tanzania and Navrongo in Ghana (annual EIR = 418), the human biting rate was calculated using light trap collections, with adjustment for the relative numbers of mosquitoes caught by human landing and light traps [Charlwood et al., 1998, Smith et al., 1993]. The sporozoite rates were estimated by using an enzyme-linked immunosorbent assay (ELISA) to test the heads and thoraces of the captured anophelines for sporozoites.

For each of the sites, which were assumed to be at equilibrium, an estimate of the daily inoculation rate was assigned to each five-day period, based on re-analysis of the original data, and averaging estimates for the same season, where data were available from multiple years. Where the observed dry season biting rate was too low for an estimate of the EIR to be made, a value was assigned equal to 1% of the average rate for the rest of the year. The inoculation rate estimates for Saradidi in Kenya, based on human landing collections and sporozoite ELISA techniques, were taken directly from the report by Beier and others [1994].

Implementation and fitting of the model. Since the model parameters are not identifiable from the data from single transmission settings or from single outcome measures, estimates were made by maximizing the joint likelihood for all of the quantities listed in Table 2.1. Each likelihood evaluation required a stochastic individual-based simulation of a human population comprising 10,000 individuals for each of the 6 datasets (corresponding

to the malariologic patterns in 6 different African villages). These simulations were implemented in Fortran 95 using five-day time steps, with as input the EIR for each five-day period. Each simulation began by simulating the exposure of the population over a whole lifetime prior to the period for which the data applied (to ensure the correct values of the cumulative exposure variables at the start of the monitoring period). For this warm-up period the same average annual cycle of the EIR (estimated from the available entomologic data) was assumed to have recurred since the birth of the oldest member of the simulated population. A demographic model was used that ensured that the simulated population remained stable with the same age-distribution throughout (see 2.5 Appendix).

The actual surveys carried out in the six villages were simulated, and predictions thus made for the distribution of parasite densities in each age group at each survey. Simulated prevalence was defined by comparing each predicted parasite density with the limit of detection used in the actual field study. By comparing observed and simulated geometric mean densities we were able to optimize the parameters of our model for immunologic control of parasite densities. The comparison of the observed with simulated prevalence allowed us at the same time to estimate the variances of the parasite density distributions.

The likelihood was computed for each of the outcomes listed in Table 2.1 separately for each age group and each survey. Binomial likelihoods were used for the prevalence of patent parasitemia, and a normal likelihood for the mean log parasite density among slides positive by microscopy. For the Navrongo dataset Poisson likelihoods were calculated for the total numbers of distinct parasite infections detected by polymerase chain reaction-restriction fragment length polymorphism in the sampled individuals in each age group, and at each survey.

The overall loss function was computed as a weighted sum of the negative log likelihoods for each of these components across all age-groups, surveys, and sites (Table 2.1; Table 2.2). Each age-specific prevalence or multiplicity assessment was given unit weight, but we weighted the log likelihoods for parasite densities by a factor of 10 (so that the prevalence and density had roughly equal weight in the final loss function). We also included in the fitting process simulation of the infection process during the intervention phase in Matsari village [Smith et al., 2006b] (Model B). The log-likelihood for the prevalence data from this simulation was also subtracted from the overall loss function (Table 2.2). The goodness of fit of the model to the data was assessed graphically.

Simulated annealing [Kirkpatrick et al., 1983, Press et al., 1988] was used to identify

the values of the parameters that minimized the loss function (Table 2.3). Approximate confidence intervals were obtained by estimating the Fisher information for the parameters. This was done by least squares fitting of local quadratic approximations to the (stochastic) log likelihood surface.

Table 2.3: Fitted values of the parameters*

Parameter	Process quantified	Units / dimension	Equation	Point estimate (95%CI)
Y_h^*	Critical value of exposure to parasites for liver stage immunity	Parasite-days/ μL	Equation 9†	∞
X_y^*	Effect of exposure on parasite density, critical value	Parasite-days/ $(\mu L x 10^{-7})$	2.3	3.5 (2.9, 4.2)
X_h^*	Effect of exposure on number of infections, critical value	Infections	2.5	97.3 (20.0, 474.5)
α_m	Maternal protection at birth	Proportion	2.7	0.90 (0.88, 0.93)
a_m^*	Decay of maternal protection	Per year	2.7	2.53 (2.33, 2.75)
D_x	Effects of concurrent co-infections on density	Dimensionless	2.8	0
σ_i^2	Variation between individuals in densities	Dimensionless	2.2	10.2 (9.7, 10.7)
σ_0^2	Fixed variance component for densities	ln(density)	2.10	0.66 (0.54, 0.79)
X_v^*	Critical value of the exposure in the model of variance	Infections	2.10	0.92 (0.82, 1.03)
ν_0	Bias adjustment for observed parasite densities in sites from Garki	Dimensionless	-	4.80 (4.28, 5.38)
ν_1	Bias adjustment for observed parasite densities in non-Garki sites	Dimensionless	-	0.18 (0.17, 0.19)

*CI = confidence interval.

†[Smith et al., 2006b]

Validation of model for age-prevalence. In addition to fitting the model to data we compared the predicted relationship between prevalence in children less than five years of age and EIR with the meta-analysis of Beier and others [1999].

2.3 Results

We optimized our model for the control of asexual blood stages of *P. falciparum* in terms of the biologic plausibility of the mechanisms for the control of parasites, the agreement with gross features of the actual field data, and the fit to six datasets across a range of transmission intensities as measured by the joint log likelihood.

The final model that we propose incorporates most of the processes that we initially envisaged. In particular, it includes stochastic variation in the duration of infections, and in the densities that they achieve at each time point. These densities decrease in general as a sigmoidal function of the cumulative density experienced by the host (Equation 2.4, Figure 2.3a), with the critical value of the curve, X_y^*, which correspond to a mean age of 7.1 years (SD=10.1) in the lowest EIR setting (Rafin Marke) and to 5.3 years (SD=8.5) in Navrongo. The densities also decrease with the cumulative numbers of infections experienced (Equation 2.6, Figure 2.3b) with the critical value of this curve, X_h^*, which corresponded to a mean age of 27.5 years (SD=2.5) in Rafin Marke and 11.4 years (SD=1.2) in Navrongo. The predicted age-pattern of the effects of maternal immunity on the densities (Equation 2.7, Figure 2.3c) shows the expected decay of this component of immunity in the first few months of life. The distributions of the densities vary by individual host (Equation 2.2), and there is also stochastic within-host variation in the densities by exposure (Equation 2.10, Figure 2.3d).

The model did not include any explicit effect of parasite density on the infections emerging from the liver (see Smith and others [2006b]), and the best fitting value of D_x, explicitly quantifying interactions between co-infections (Equation 2.9), was 0, which limited the interactions between concurrent infections to those induced by acquired immunity. We explored several different parameterizations to try to capture interactions between co-infections, but we were not able to improve the fit of our models.

The model also assumed that each inoculation behaves as a single parasite clone. This is a simplification since many oocysts in the field are heterozygous [Babiker et al., 1994,

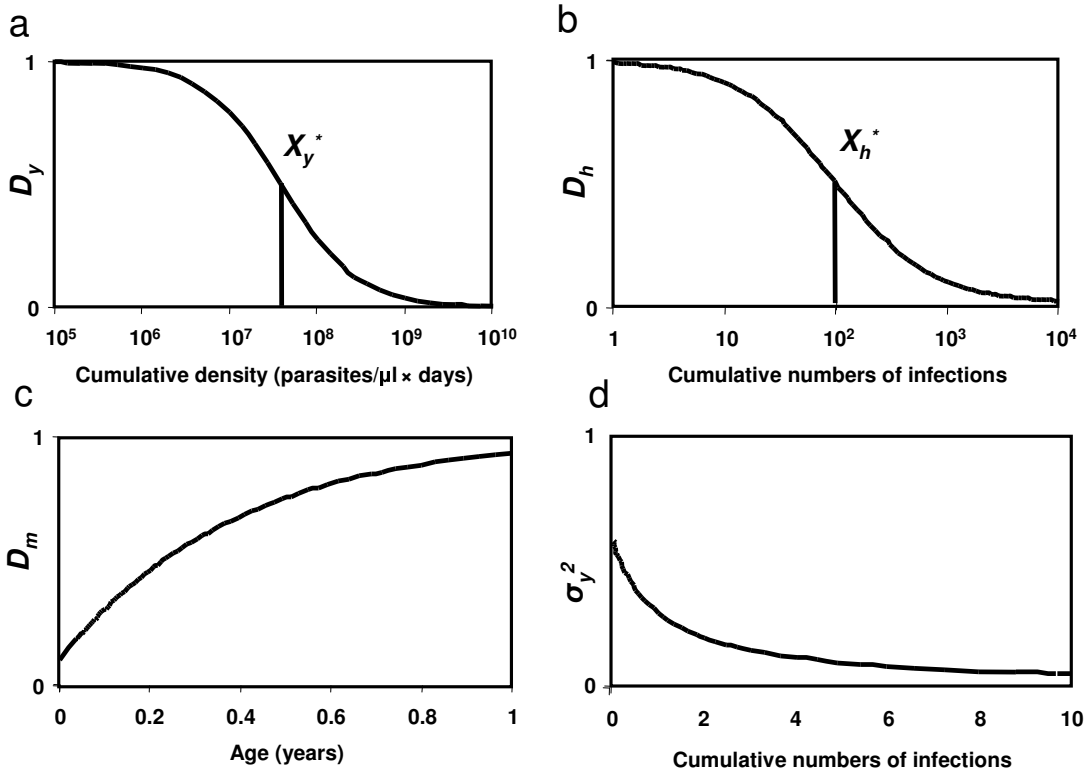

Figure 2.3: Effects of acquired immunity on parasite density. a) Cumulative density of asexual parasitemia. Relationship between the cumulative density of parasites experienced and the trigger D_y (Equation 2.4). b) Cumulative number of infections. Relationship between the cumulative number of infections and D_h (Equation 2.6). c) Age of the host. Age-dependent decay of maternal immunity (Equation 2.7). d) Within-host variation of parasite densities. Variation around expected parasite densities within individual hosts as function of cumulative parasite densities experienced (Equation 2.10).

Paul et al., 1995], and result in mixed populations of sporozoites (Ranford-Cartwright L, unpublished data). However, we were not able to improve the fit of the model by allowing for diversity in the inoculum.

A good fit of the model to the parasite densities could only be achieved by including parameters to allow for biases introduced by different methods for quantifying parasite densities. We aimed to adjust all the modeled densities to the same scale as that in the malariatherapy studies by introducing two parameters ν, one for the Garki dataset (where the nominal densities were much lower than our model predicted), and one for the other field studies, where the nominal densities were higher than our predictions (Table 2.3). These adjustments ensured that our predicted densities in naïve individuals corresponded on average to those in malariatherapy patients but do not allow us to separate ethnic variations from effects of differences among study sites in the quantification of parasitemia.

In all settings, *P. falciparum* showed the characteristic age-prevalence pattern found in malaria-endemic areas, with the highest prevalence in young children, reaching almost 100% in those sites with EIRs>200 infectious bites per person per year (Figure 2.4).

The age of peak prevalence was younger in the highest transmission sites and moves to older ages in lower transmission settings, but there is little difference between sites in the prevalence in older children and adults. These patterns were well reproduced by our model, with clear separation between the sites in the predicted age-prevalence curves in young children at all except the highest transmission rates, with peak prevalence at the age of one year in the highest transmission sites and in adolescents in the lowest transmission site of Rafin Marke.

Despite the highest recorded EIR in Navrongo, the prevalence of *P. falciparum* was relatively low in the young children; thus, this setting had an anomalously high age of peak prevalence (Figure 2.4) [Owusu-Agyei et al., 2002]. The age at which the multiplicity reaches a peak is also anomalously high in Navrongo, in comparison to other sites that have been studied (Figure 2.5) [Owusu-Agyei et al., 2002, Smith et al., 1999].

The highest geometric mean parasite densities rather than the peaks in prevalence were found in younger children, with gradual decreases with age in the geometric mean densities among the infected individuals (Figure 2.6). There was little peak shift in the geometric mean densities in either the data or the model predictions, which suggested that the highest densities should be found in the 1-2-year-old children.

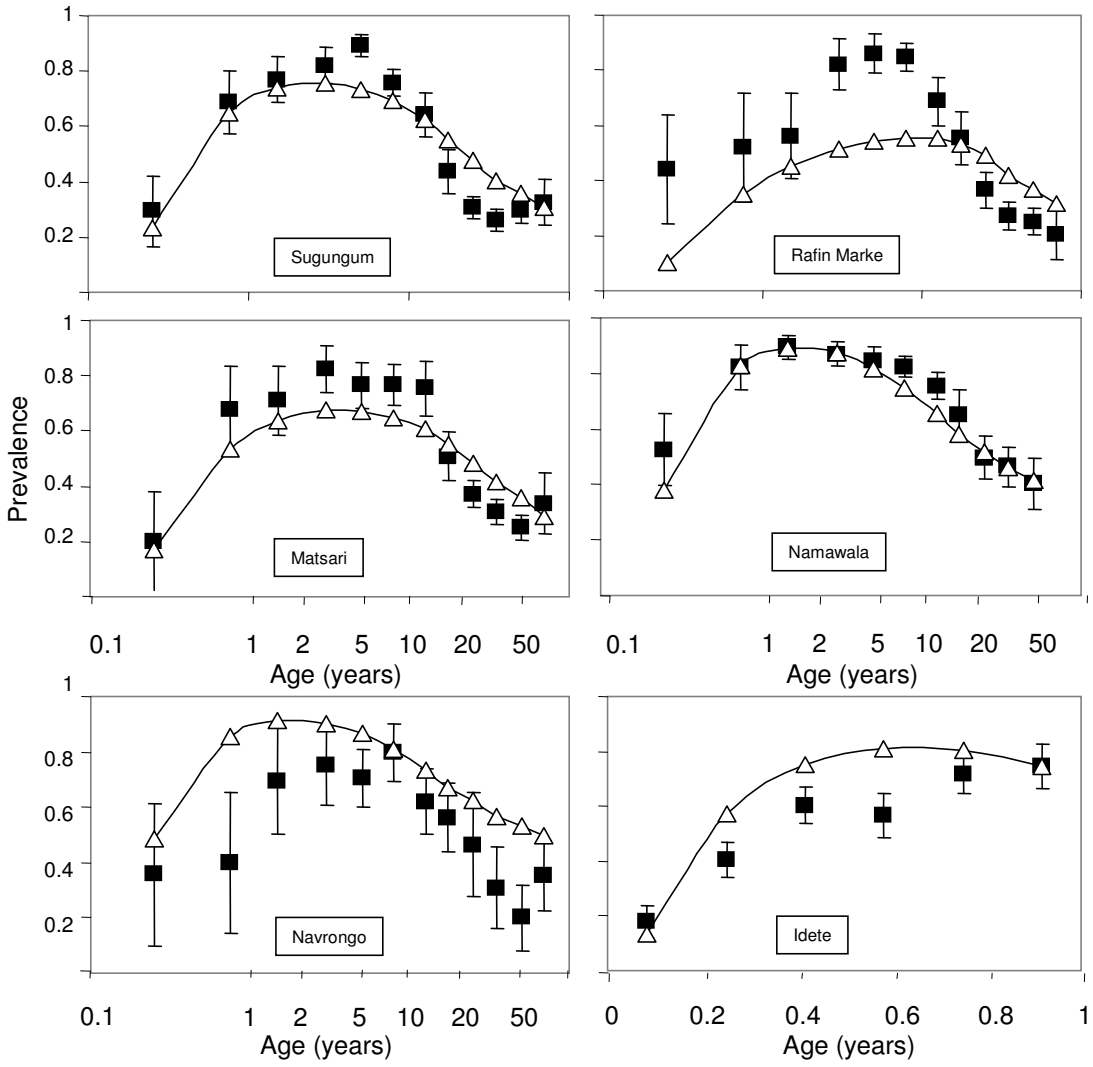

Figure 2.4: Comparison of predicted and observed age-prevalence curves. ■ = data (error bars are 95% confidence intervals); Δ = model predictions.

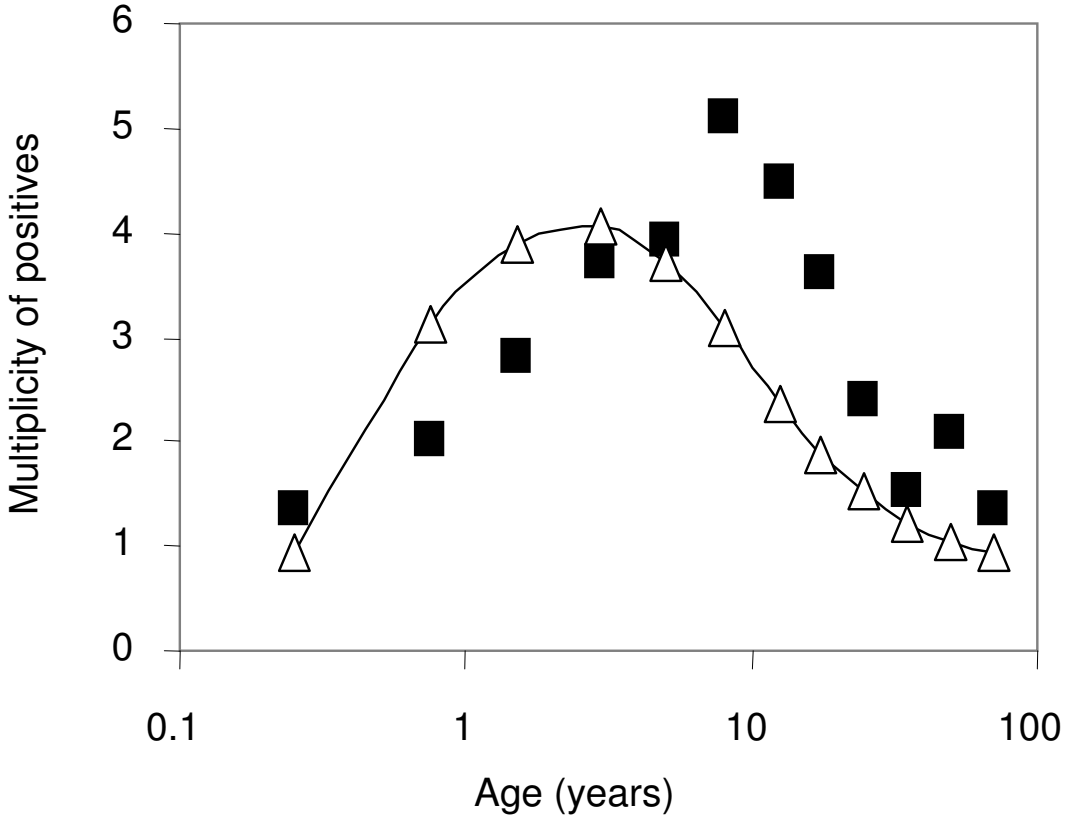

Figure 2.5: Comparison of predicted versus observed multiplicity of infection. ■ = data for Navrongo; Δ = model predictions

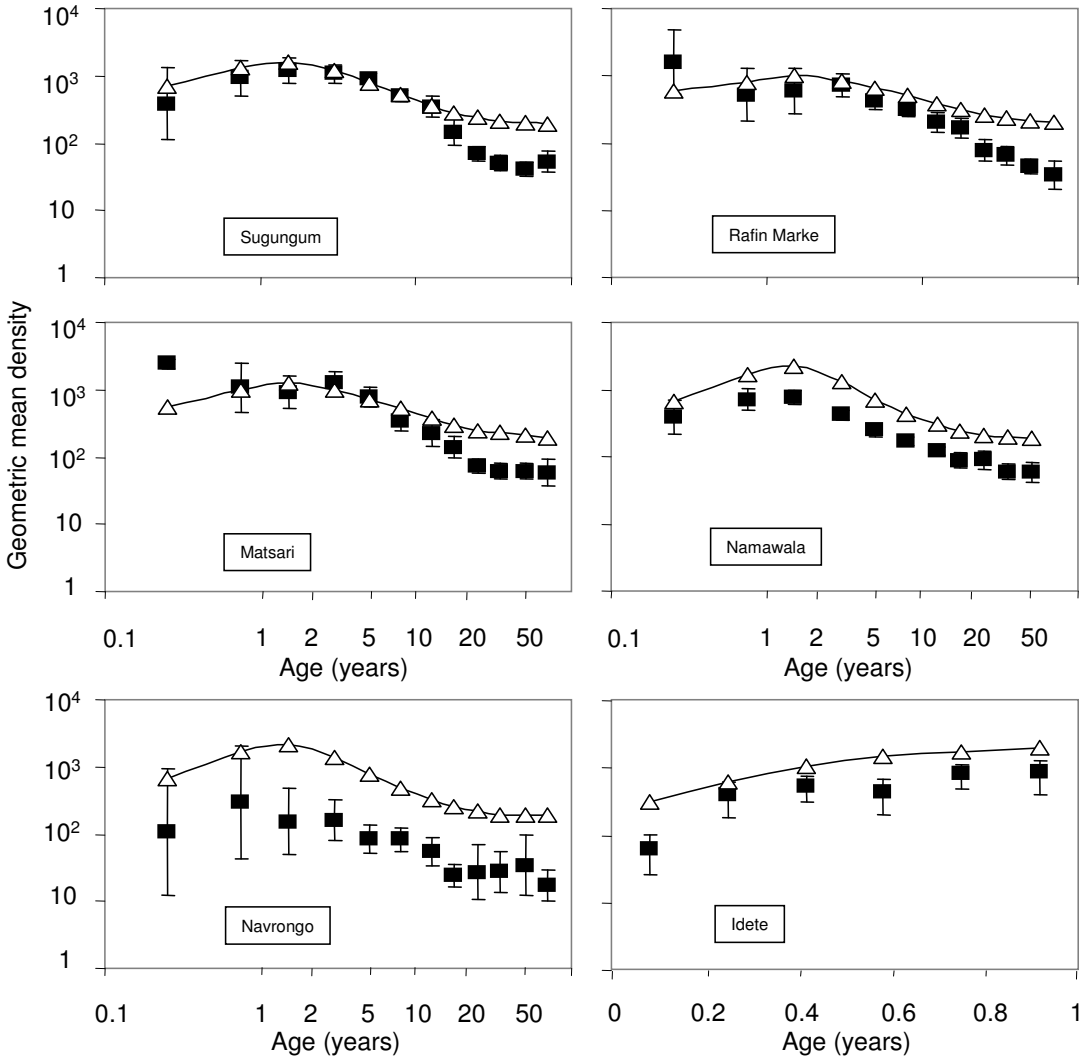

Figure 2.6: Comparison of predicted versus observed age-density curves. ■ = data (error bars are 95% confidence intervals); Δ = model predictions.

Comparison of the model predictions with the summary of field studies of prevalence in children less than five years found a good fit, with only a small tendency for the predicted prevalence to be below that observed (Figure 2.7).

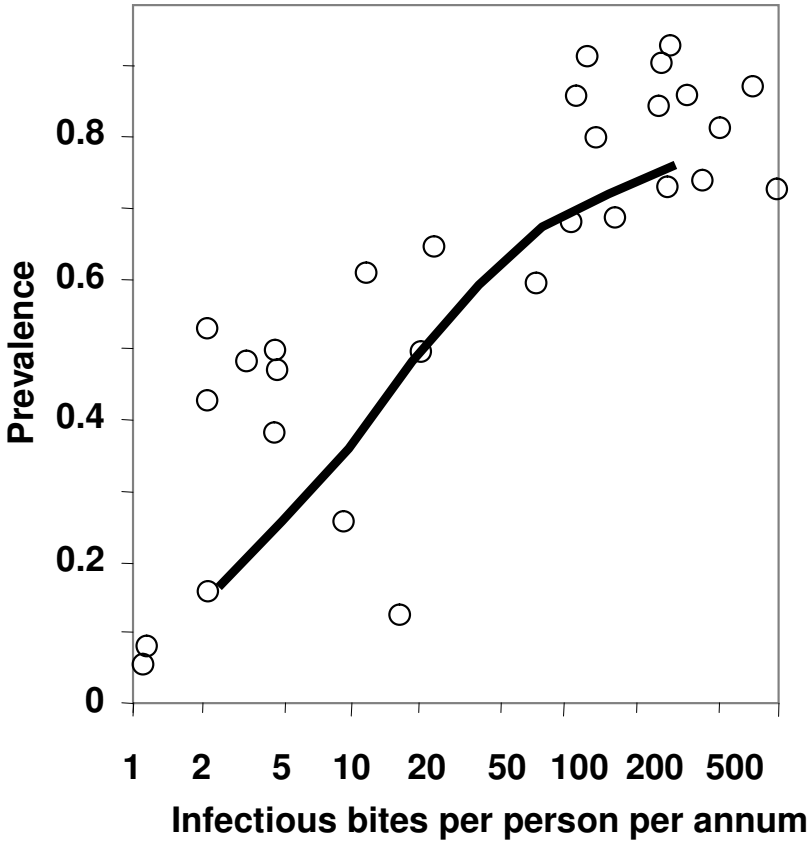

Figure 2.7: Comparison of model predictions with observed prevalence in children under five years of age in 31 sites across Africa. ∘ = field data reported by Beier and others [1999]. The line corresponds to predictions of our model made using the seasonal pattern of inoculations in Namawala scaled to different values of the annual entomologic inoculation rate.

Since the model was fitted only to cross-sectional data, it was not expected to give good predictions of longitudinal patterns within individual hosts. Comparison of individual parasitologic profiles with the patterns observed in malariatherapy patients confirmed that within host variation was less than that observed in actual infections of naïve hosts.

2.4 Discussion

The model we present for the processes involved in controlling the asexual blood stages of *P. falciparum* infections provides a foundation for estimating the likely impact of variations in malaria transmission and of control of parasite densities on the parasitologic burden in endemic areas. It forms a central component of a comprehensive model to assess and quantify the epidemiologic and economic effects of introducing malaria vaccines [Smith et al., 2006a]. In addition to these applications, our analyses of models for the control of asexual blood stages can also be used to test hypotheses about the nature of acquired immunity and malaria transmission dynamics.

The realism of the model presented here is limited by a number of gaps in our current knowledge of malaria. For example, no attempt has been made to simulate detailed immunologic processes. This is justified by the lack of agreed immunologic proxy markers for protection in malaria. Thus, models of malaria immunity that aim to predict morbidity and mortality cannot be validated against immunologic data. Modeling T-cell dynamics or antibody levels would thus serve only to increase the complexity of the models without adding to the validity. Our model assumed that the main mechanisms controlling parasite densities do not decay in the absence of stimulation because we have no comprehensive database from which to estimate rates of decay. It would be possible to analyze predictions from sets of models fitted to the same data, assuming different rates of decay, but this would require substantially more computing power than the analysis of a single model.

Inhabitants of endemic areas who temporarily move away are more vulnerable to malaria when they return, but it is unclear whether this results from loss of anti-parasite immunity or of parasitologic tolerance. Some specific immune responses against *P. falciparum* have been shown to be highly labile (e.g. Kinyanjui and others [2003]), but the epidemiologic consequences of this are yet to be elucidated. Even after several decades free of malaria, people in the central highlands of Madagascar retained some protective immunity to *P. falciparum* [Deloron and Chougnet, 1992].

To reproduce realistic age-prevalence and age-density curves, we required only to simulate effects of acquired immunity on parasite densities, without any decay in immunity over time or any explicit effect on duration of infection. In common with many other diseases with acquired immunity, [Anderson and May, 1991, Woolhouse, 1998] as *P. falciparum* transmission increases, there is a characteristic decrease in the age at which the maximum

prevalence is reached and increases in the actual peak prevalence. Our model was also able to reproduce these shifts.

Terms both in the cumulative parasite load, X_y, and cumulative number of infections, X_h, were needed, which confirmed that models are inadequate in which acquired immunity is a simple function only of the number of strains to which the host has been exposed. The quantitative load of parasites resulting from repeated inoculations is also important in our proposed model. This could reflect effects of the repertoire of antigen variants that have been expressed in the host, as well as undifferentiated effects of the actual number of parasites. Our formulation differs from models that assume the parasite population to comprise a limited number of strains, or that strain-specific immunity can lead to complete protection.

As with all mathematical models for infectious diseases, we made a number of simplifications. First, we assumed that ethnic differences in the response to *P. falciparum* malaria between sites are small, although such differences are known to occur in sub-Saharan Africa [Greenwood et al., 1987, Modiano et al., 1996].

Although our model showed satisfactory overall fits to the various datasets across a wide range of transmission intensities, a somewhat poorer fit was observed with the Navrongo data. A likely explanation for this relatively poor fit to this more recently collected dataset is that we assumed that the impact of anti-malaria treatment was negligible. This assumption is clearly appropriate in the case of the historical data from sites where there was little or no effective treatment, and enabled us to avoid the need to model treatment effects. However, in sub-Saharan Africa early diagnosis and treatment is currently the backbone of malaria control [World Health Organization, 1993]. We needed to use recent data to fit the model to age-multiplicity patterns because genotyping techniques have only recently become available. The data from Navrongo that we used for this come from an area with generally poor access to primary health services, although there are four health centers and a hospital. A fraction of the population sleeps under mosquito nets after a successful trial carried out a decade ago [Binka et al., 1996], and a pilot community health program has treated many of the acute illnesses, including fever episodes in young children [Binka et al., 1995]. The poorer fit of our model to the Navrongo data than to the other datasets suggests that these interventions have reduced levels of malaria infection in Navrongo below those to be expected at the high inoculation rates observed there.

Other limitations arise because our model was fitted to cross-sectional data, rather than

to patterns of variation in parasitemia within individuals, and therefore it is more successful in reproducing the former than the latter. Longitudinal patterns within individuals might be better reproduced by fitting within-host models explicitly incorporating effects of antigenic variation to repeated assessments of parasitemia with short time-intervals. Such models have been fitted to data from malariatherapy patients [Molineaux et al., 2001, Paget-McNicol et al., 2002, Recker et al., 2004] but there is no agreement that any particular such model is appropriate. By basing the time-course of parasitemia on an empirical description of the malariatherapy data, we attempted to incorporate the dynamics of antigenic variation without explicitly modeling the processes that lead to it. Because our model is individual-based and therefore makes predictions of sequential patterns of parasitemia within simulated hosts, it would be possible to amend it to include a more realistic model of within-host dynamics but there are few datasets from endemic areas to which longitudinal patterns of parasitemia with short time-intervals can be fitted.

We conclude that this model appears to reproduce reasonably well the parasitologic patterns seen in malariologic surveys in endemic areas. Development of improved models will require fitting to data on longitudinal patterns of parasitemia in semi-immune individuals, in particular to data from people whose exposure is interrupted by well-documented periods of protection from infection. Such models are needed to understand the consequences of malaria interventions in areas of infrequent or unstable transmission. The present model is appropriate for predicting the impact of interventions such as vaccination in the context of continual exposure to *P. falciparum*.

2.5 Appendix

The simulation requires a demographic model for the human population in which the following are needed:

1. Population size is held constant (this ensures that the computational effort and denominators remain similar throughout the simulation. In some applications we do not know at the outset how much time we must simulate; we do not want the simulated population to be continuously growing).

2. The age-distribution remains approximately constant, so that models for parasite dynamics can reach equilibrium (assuming constant host/vector ratios). The infectious

reservoir depends on the age distribution of the human population so a stable age distribution is required for parasitologic equilibrium.

3. The age distribution reflects that of actual contemporary populations, to ensure correct overall measures of disease burden and transmissibility.

Real populations are created by processes which vary over time, and in sub-Saharan Africa they are growing [United Nations, 2002]. In a simulated population it is not in general possible to keep the age distribution stable by applying current birth and death rates. Usually a stable age distribution can only be maintained by removing more simulated individuals at each age and time point than the deaths predicted by a realistic mortality model. We separate processes maintaining the age-distribution of the human population from the demographic effects of malaria, which we do not aim to model, by simulating out-migration. We use age-specific out-migration rates to those needed to maintain a stable population. In fitting our parasitologic model we do not simulate any mortality. The same approach is used in models that do simulate mortality, in which the out-migration rates are reduced to compensate for the deaths.

Age-distribution of the simulated human population. We simulate age-distributions based on the those recorded for African demographic surveillance sites [INDEPTH Network, 2002]. Stable life tables cannot be constructed for these age distributions without including age-specific immigration. We avoid simulating immigration because this would require us to clone simulated individuals, altering the variance structure. We fit a continuous parametric curve to smooth the age distribution because the distributions summarized in published data are themselves smooth, and fewer in-migrations are needed. A bath-tub function for mortality rates (higher in infants and older people) gives a good fit to historical European data (M. Safan, unpublished data) and separates parameters of the age-distribution from those of population growth.

If ρ is the Malthusian parameter, corresponding to the exponent of an exponential growth model, then a stationary age-distribution is given by $f(a)$ where:

$f(a) = \frac{e^{-\rho a - M(a)}}{\int_0^\infty e^{-\rho a - M(a)} da}$ and $\mathrm{M(a)} = \mu_0 \frac{1-e^{-\alpha_0 a}}{\alpha_0} + \mu_1 \frac{e^{\alpha_1 a}-1}{\alpha_1}$

Fitting the parameters of the age distribution. We set ρ, the population growth rate, to 0 and estimate the parameters μ_0, μ_1, α_0 and α_1 and by least-squares fitting of

the logarithmically transformed percentages of the population in each age group to those of real African populations. Because the observed age distribution is aggregated into a limited number of groups, the parameters μ_0 and α_0 are difficult to fit. We require a high number of removals in the first year of life, so models with high infant mortality do not require immigration of infants. We specify a high removal rate of infants and constrain the age-specific removal rates in the first year of life so that there are four neonatal removals for every six post-neonatal one. The age-specific removal rates of the simulated population are then:

$$\mu(\mathrm{a}) = \mu_0 e^{-\alpha_0 a} + \mu_1 e^{\alpha_1 a}$$

At each five-day time point, we compare the age-specific cumulative numbers of individuals to that of the target population, and excess individuals are out-migrated. After a run-in period, the age distribution based on Tanzanian data (Figure 2.8a) is approximately stable (Figure 2.8b).

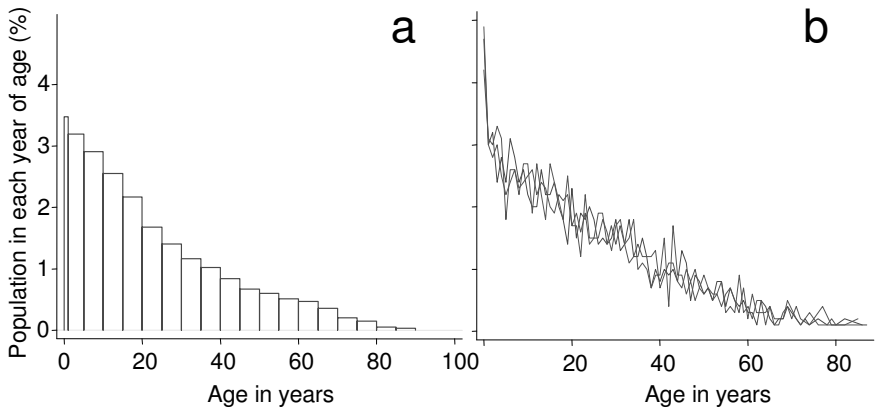

Figure 2.8: Age distributions of the population. a) Field data from Ifakara, Tanzania [INDEPTH Network, 2002]. b) Simulated population distributions of 1,000 individuals at 3 cross-sectional time points (t=10,000, 50,000 and 100,000).

Chapter 3

An approach to model the costs and effects of case management of *Plasmodium falciparum* malaria in sub-Saharan Africa

Fabrizio Tediosi, Nicolas Maire, Thomas Smith,
Guy Hutton, Jürg Utzinger, Amanda Ross, Marcel Tanner
Swiss Tropical Institute, Basel, Switzerland

This article has been published:
American Journal of Tropical Medicine and Hygiene 2006, 75, Suppl 2, 90-103

Abstract

An important shortcoming of existing methods for estimating the cost-effectiveness of malaria control interventions is that the incidence of illness and transmission dynamics are assumed to be independent of the case management system. We have developed a model for case management and integrated it into a stochastic simulation of *Plasmodium falciparum* malaria dynamics. This allows us to predict the incidence of clinical episodes and of mortality while incorporating effects of case management on persistence of parasites and transmission. We make predictions for a range of different transmission intensities in sub-Saharan Africa and simulate a range of case management scenarios with different coverage rates. The model predicts that high treatment rates have a proportionately greater epidemiologic impact at low transmission levels. Further development is needed for models for health-seeking behavior and referral patterns. The current model is a first step towards useful predictions of the epidemiologic and economic consequences of introducing and/or scaling-up of malaria control interventions.

3.1 Introduction

Models for the cost-effectiveness of different disease control strategies generally, and malaria control interventions in particular, usually assume the incidence of illness and transmission dynamics to be independent of the prevailing case management system [Drummond et al., 1997, Gold et al., 1996]. Decision trees typically start with the observation of an illness episode and consider how the episode is managed subsequently, but do not consider whether management itself affects the incidence of the disease. With infectious diseases such as malaria, this approach ignores the feedback that may arise from an effective case management system, which in turn reduces the frequency of infection, and thus impacts transmission dynamics.

Models for nosocomial infections and those recently developed to simulate the severe acute respiratory syndrome epidemic [Cooper and Lipsitch, 2004, Lipsitch et al., 2003] provide examples of approaches in which the operation of the health system interacts in a dynamic fashion with the biology of the infecting organism. In these models, prompt treatment of infections reduces epidemic spread, and thus results in both reductions in the subsequent burden of disease and in the requirements for treatment of secondary cases.

When the infection has a long time course, which may encompass several illness episodes,

treatment may also reduce the subsequent burden of disease independently of its effect on transmission. In malaria, untreated *Plasmodium falciparum* infections can persist for many months, during which clinical attacks recur at irregular intervals [Collins and Jeffery, 1999a]. One of the current mainstays of malaria control is access to early diagnosis and effective treatment [World Health Organization, 1993]. Prompt and effective treatment not only reduces the reservoir hosts who are infective to mosquitoes, but also prevents recurrences. Longitudinal studies of malaria in endemic populations frequently record declines in incidence over time. A major reason for this is likely to be that study participants receive more frequent treatment and this reduces the incidence of subsequent malaria fever attacks, irrespective of any effect on transmission. Conventional cost-effectiveness analysis of treatment does not consider these effects.

Malaria control interventions, such as source reduction by means of environmental management, increasing the coverage of insecticide-treated nets (ITNs), indoor residual spraying, and (potentially) the introduction of a malaria vaccine, modify the demands on the health system, and thus affect both immediate direct impact and longer-term indirect effects of case management. This applies even when the intervention, such as vaccination, does not directly modify case management. It follows that prediction of the impact of preventative and curative interventions against malaria must take into account these dynamic effects.

This report presents a first attempt to develop a dynamic model including case management of *P. falciparum* malaria in a typical setting of sub-Saharan Africa. It has been integrated into a model for the clinical epidemiology and natural history of *P. falciparum* malaria [Smith et al., 2006a]. We compare the outcomes of different case management regimens in settings of different transmission intensities.

3.2 Materials and Methods

Epidemiologic model. The epidemiologic model is a stochastic individual-based simulation of *P. falciparum* malaria in endemic settings that uses a five-day time step. The primary input is the pattern of the entomologic inoculation rate (EIR) in the absence of malaria control interventions, with separate values of the EIR specified for each of the 73 five-day periods during the year [Smith et al., 2006b,a]. For the present analyses, we simulate populations of 100,000 individuals, with an approximately stationary age distribution matching that of the demographic surveillance site in Kilombero, Tanzania in 1997-1999

(Chapter 2).

For every individual in the simulated population, each discrete *P. falciparum* infection is characterized by a simulated duration and parasite density at each five-day time point (Chapter 2). The host acquires immunity as a function of exposure and this in turn modifies the parasite density, and infectivity to mosquitoes [Killeen et al., 2006, Ross et al., 2006a] at subsequent time-points. At each time point, a clinical event, either uncomplicated clinical malaria, severe malaria, or death from either malaria or other causes, may occur. Probabilities for occurrence of these events depend on the parasite density, recent exposure, and age-dependent co-morbidity. They have been determined by functions that have been fitted to field data across a wide range of transmission settings [Ross et al., 2006b, Ross and Smith, 2006, Smith et al., 2006c]. In addition, the prevalence of anemia (hemoglobin levels less than 8 g/dL) is assigned at the population rather than the individual level, as a function of simulated age and parasite prevalence [Carneiro et al., 2006].

Clinical events. There are five different entry points into the case management tree: no event, uncomplicated malaria, severe malaria, indirect malaria death, and non-malaria death or out-migration. They are defined as follows.

No event, includes asymptomatic malaria infections. In this case, the simulated individual continues to the next time point, with the natural history of *P. falciparum* infections unmodified by the case management model.

Uncomplicated clinical malaria comprises *P. falciparum* infections that may be treated either at home or in peripheral health facilities. The model assumes that the risk of uncomplicated clinical malaria depends on whether the parasite density exceeds a critical threshold, which in turn is a function of past exposure [Smith et al., 2006c]. The case management implications of uncomplicated clinical malaria further depend on whether the host has recently been treated for malaria. Two possibilities were considered, as follows. The first is uncomplicated clinical malaria in the absence of recent treatment. This is defined by no treatment over the previous 30 days (6 time points). The decision tree pathways for this scenario are shown in Figure 3.1a. They include entry into the formal health care system and receiving the first-line drug, self-treatment at home with the recommended first-line drug, or absence of seeking of malaria treatment. The second is an uncomplicated clinical malaria episode that occurs despite recent treatment history. Figure 3.1b shows the decision tree pathways for this scenario. An uncomplicated malaria

case that was treated in the past 30 days is assumed to either seek care or not. If care is sought, it is assumed to take place in the formal health care system, with treatment being based on the second-line drug. We do not consider the possibility that patients self-treat after drug failure because this would very likely involve ineffective re-treatment with the first-line drug, with no epidemiologic consequences.

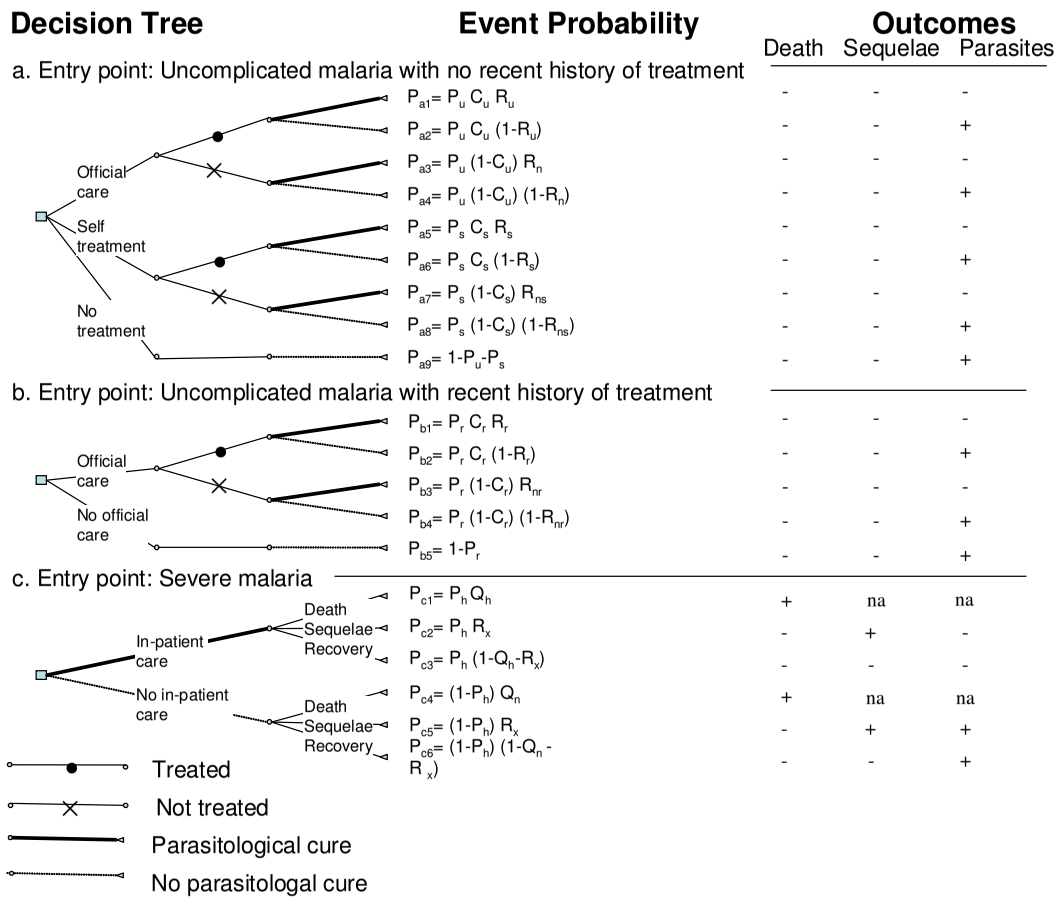

Figure 3.1: Decision tree pathways. na = not applicable.

Severe malaria episodes are those clinical malaria episodes that are life-threatening if they are left untreated. We consider these as equivalent as those events that would have led to an admission diagnosis of severe malaria, had the patient presented to a health facility [Ross et al., 2006b]. The current model assumes that a severe malaria case can either be treated as an in-patient or not be treated at all. In the former case it is assumed that compliance is 100%. There are three possible clinical outcomes for treatment of a severe malaria episode, namely, death, recovery with neurologic sequelae, or full recovery (Figure 3.1c).

Indirect malaria death considers those deaths that would not have occurred in the absence of prior malaria exposure but which do not meet the criteria for severe malaria [Ross et al., 2006b].

Non-malaria death and out-migration correspond to events that occur independently of the parasitologic status of the host. These events are simulated to maintain the correct age-structure of the simulated population.

When more than one simulated clinical attack occurs within 30 days of another attack, these are counted as the same episode. Thus, there can be several treatments for one episode. The severity assigned to the episode is assigned to that of the most severe malaria attack within the 30-day period.

Each decision tree pathway predicts the outcome in terms of whether the parasites are cleared, and the clinical outcome (i.e. death, recovery with long-term sequelae or full recovery). The epidemiologic effects of the case management depend stochastically on the values of the joint probabilities of the clinical and parasitologic outcomes, conditional on the clinical event. These conditional probabilities are computed by calculating the probabilities for each branch of the decision tree pathways (Figure 3.1). For the model of uncomplicated malaria, the probabilities associated with each branch in the decision tree were obtained from the literature (Table 3.1).

Table 3.1: Model inputs used for efficacy and malaria treatment-seeking behavior*

Symbol	Description	Case management scenarios					Reference
		No treatment	Reference	Moderate coverage	Complete coverage	Effective treatment	
	Uncomplicated malaria						
P_u	Probability of seeking care in the formal health sector	0.0	0.04	0.27	1.0	1.0	-
P_s	Probability of self-treatment	0.0	0.01	0.13	0.0	0.0	-
P_r	Probability of seeking out-patient care in case of treatment failure	0.0	0.04	0.27	1.0	1.0	-
	Compliance						
C_u	SP: formal health sector	n.a.	0.90	0.90	0.90	1.00	1§
C_r	Amodiaquine	n.a.	0.45	0.45	0.45	1.00	1§
C_s	SP: self-treatment	n.a.	0.85	0.85	n.a.	n.a.	1§

Continued on next page

Table 3.1: Model inputs used for efficacy and malaria treatment-seeking behavior*

Symbol	Description	Case management scenarios					Reference
		No treatment	Reference	Moderate coverage	Complete coverage	Effective treatment	
	Cure rate†						
R_u	SP: formal health sector	n.a.	0.93	0.93	0.93	1.00	1§
R_r	Amodiaquine	n.a.	0.85	0.85	0.85	1.00	1§
R_s	SP: self-treatment	n.a.	0.63	0.63	n.a.	n.a.	1§
	% of non-compliers for whom treatment is effective						
R_{ns}	SP	n.a.	0	0	n.a.	n.a.	-
R_{nr}	Amodiaquine	n.a.	0.20	0.20	n.a.	n.a.	1§
	Severe malaria						
P_h	Probability of inpatient care	0.0	0.48	0.48	1.0	1.0	2§
R_q	Cure rate (Quinine)	n.a.	0.998	0.998	0.998	0.998	1§

Continued on next page

Table 3.1: Model inputs used for efficacy and malaria treatment-seeking behavior*

Symbol	Description	Case management scenarios					Reference
		No treatment	Reference	Moderate coverage	Complete coverage	Effective treatment	
R_x	Probability of neurologic sequelae for severe episodes for age-group <5 years of age‡	0.0132	0.0132	0.0132	0.0132	0.0132	3§,1§
R_x	Probability of neurologic sequelae for severe episodes for age-group ⩾5 years of age‡	0.005	0.005	0.005	0.005	0.005	3§,1§

*The values for the reference scenario are adapted from those used in our simulation of a field trial of a malaria vaccine; those for the moderate coverage scenario are based on the data of the Tanzanian National Malaria Control Program [NMCP, 2003]. SP = sulfadoxine-pyrimethamine; n.a. = not applicable.

† The cure rate refers to the "adequate clinical response rate".

‡ The same probabilities are used for neurologic sequelae for both in-patients and non-hospitalized severe episodes.

§ 1: Goodman et al. [2000]; 2: McCombie [1996]; 3: Brewster et al. [1990]

For the severe malaria model, we used in-patient case fatality rates, $Q_h(a)$, from a recent study in Tanzania [Reyburn et al., 2004], and estimated corresponding community case fatality rates, $Q_c(a)$. $Q_h(a)$ varies with age a, taking values from 3% to 13%. $Q_c(a)$ takes values estimated previously using our model for severe malaria and mortality assuming the two risks to be related via a constant odds ratio, φ_1, taking a value of 2.09 [Ross et al., 2006b], i.e.

$$Q_c(a) = \varphi_1 Q_h(a) \frac{1 - Q_c(a)}{1 - Q_h(a)} \tag{3.1}$$

We assume negligible drug-resistance to quinine, so that parasites are cleared in all hospitalized cases who survive. We assign a probability of sequelae, R_x, with a value independent of treatment (Table 3.1).

Disability adjusted life-years (DALYs). Years of life lived with disability are calculated using standard methods [Murray and Lopez, 1996b] on the basis of the duration of disability, and respective disability weights (Table 3.2). These weights for different malaria-attributable disease conditions have been obtained from the Global Burden of Disease (GBD) study [Murray and Lopez, 1996a].

Table 3.2: Disability weights and duration of disability used to calculate YLDs*

Disease condition	Disability weight	Duration (years)
Untreated neurologic sequelae	0.473	35.4
Neurologic sequelae (treated)	0.436	35.4
Uncomplicated malaria episode	0.211	0.01
Anemia	0.012	ND
Low birth weight	ND	ND
Others	ND	ND

*YLDs = years of life with disability; ND = not defined

Years of life lost (YLLs) and DALYs (age-weighted) are calculated assuming age-specific life expectancies based on the life-table from Butajira, Ethiopia, with an average life expectancy of 46.6 years at birth [INDEPTH Network, 2004]. This life-table represents that of an east African setting, but is characterized by low malaria transmission. For example, it is very similar to that for Hai district, a high-altitude site in Tanzania [INDEPTH Network, 2002].

In a first step, YLLs and DALYs are presented with no discounting. Subsequently we compare the results with those obtained using a 3% discount rate, which is the one most commonly used in cost-effectiveness analyses [Drummond et al., 1997, Gold et al., 1996].

Malaria transmission intensity. The introduction of changes in case management (or of other interventions) leads to transient behavior, which may in principle modify the level of *P. falciparum* transmission. These effects on transmission are captured in the model by the effects on infectiousness of the human population resulting from clearing parasites. The simulation model predicts for time point t the proportion $\bar{\kappa}_m(t)$ of vectors that become infected at each feed on a human host [Killeen et al., 2006] [Ross et al., 2006a]. We adjust this to give $\kappa_u(t) = 0.56\bar{\kappa}_m(t)$ to allow for the bias arising because $\bar{\kappa}_m(t)$ is estimated from artificial feed data [Killeen et al., 2006]. We record the value $\kappa_u^{(0)}(t)$ that $\kappa_u(t)$ takes in the simulation of the reference scenario to which a change in the case management model has been applied, and compare this value to $\kappa_u^{(1)}(t)$, the prediction of $\kappa_u(t)$ for the same time-point in the simulation with a change in case management. The effect of the change in case management on transmission is then modeled by a change in the EIR in adults at l_v time units later ($E_{\max}(t + l_v)$), such that

$$E_{\max}^{(1)}(t + l_v) = \frac{E_{\max}^{(0)}(t + l_v)\ \kappa_u^{(1)}(t)}{\kappa_u^{(0)}(t)} \tag{3.2}$$

where l_v corresponds to the duration of the sporogonic cycle in the vector, and where $E_{\max}^{(0)}(t + l_v)/\kappa_u^{(0)}(t)$ is the overall vectorial capacity. The consequences for the infection rates follow from details of the epidemiologic model [Smith et al., 2006b].

We considered four different intensities of transmission, each with the same seasonal pattern as that in Namawala, Tanzania [Smith et al., 1993] (Table 3.3). For the reference scenario, we used an overall annual EIR of 21 infectious bites per year which represents a typical level of transmission for a mesoendemic setting [Hay et al., 2000, Robert et al., 2003].

Health systems. Uncomplicated malaria patients seeking formal health care in Tanzania are usually diagnosed during an out-patient visit either in a health center, a dispensary, or a hospital. A diagnostic test (normally light microscopy of finger prick blood smears) is performed on less than 10% of treated cases (National Malaria Control Program, 2004, unpublished data). Current Tanzanian national treatment guidelines recommend that an

Table 3.3: Scenarios modeled: health systems and transmission intensities*

Scenario	Annual EIR
Very low	1.3
Low	5.2
Reference	21
High	83
Very high	329
Health system	
No treatment	
Reference	
Moderate coverage	
60% Abuja target coverage	
Full coverage	
Effective treatment	
Antipyretic treatment	

*EIR = entomologic inoculation rate. EIR changes over time in these scenarios.

uncomplicated malaria episode be treated with sulfadoxine-pyrimethamine (SP) as the first-line drug. Amodiaquine serves as the second-line drug, and quinine is used for treatment of severe malaria [Ministry of Health, Tanzania, 2000]. Our models assume that formal-sector treatment adheres to these practices (Tables 3.4 and 3.5). We also assume that SP is used as the drug of choice for self-treatment, but the efficacy is assumed lower to account for lower quality of drugs purchased in the private sector. The levels of compliance and of drug resistance that we assume are given in Table 3.1.

Table 3.4: Sulfadoxine-pyrimethamine and amodiaquine doses and costs, by age and weight*

Regimen, age and weight categories	Number of tablets	Cost per course in Tshs.	Cost per course in US$ 2004
Sulfadoxine-pyrimethamine			
< 1 year (<11 kg)	0.5	12.4	0.012
1 to 5 years (11-19 kg)	1	24.8	0.024
6 to 9 years (19-30 kg)	1.5	37.2	0.035
10- 14 years (30-45 kg)	2	49.6	0.047
15 and above (> 45 kg)	3	74.4	0.071
Amodiaquine			
< 1 year (<11 kg)	1.25	18.75	0.018
1-3 years (11-15 kg)	1.75	26.25	0.025
4-5 years (15-19 kg)	2.25	33.75	0.032
6-8 years (19-25 kg)	3	45	0.043
9-11 years (25-36 kg)	4.25	63.75	0.061
12-14 years (36-50 kg)	6.25	93.75	0.089
15-16 years (50-60 kg)	7.5	112.5	0.107
17 and above (> 60 kg)	8	120	0.114

*Sulfadoxine-pyrimethamine is administered as a single dose. Amodiaquine values are the number of 200-mg tablets in a three-day course [MSD, 2004].

Table 3.5: Intravenous quinine doses and costs, by age and weight

Age and weight categories	Dose	Cost per day in Tshs.	Cost per day in US$ 2004	Cost per course in US$ 2004
Initial dose (20 mg/kg over 4 hours)				
< 1 year (< 11 kg)	180	54	0.051	
1-3 years (11-15 kg)	240	72	0.069	
4-5 years (15-19 kg)	360	108	0.103	
6-8 years (19-25 kg)	420	126	0.120	
9-11 years (25-36 kg)	600	180	0.171	
12-14 years (36-50 kg)	840	252	0.240	
15-16 years (50-60 kg)	1,080	324	0.309	
17 and above (> 60 kg)	1,200	360	0.343	
Dose per day thereafter (10 mg/kg every 8 hours for 6 days)				
< 1 year (<11 kg)	270	81	0.077	0.514
1-3 years (11-15 kg)	360	108	0.103	0.686
4-5 years (15-19 kg)	540	162	0.154	1.029
6-8 years (19-25 kg	630	189	0.180	1.200
9-11 years (25-36 kg)	900	270	0.257	1.714
12-14 years (36-50 kg)	1,260	378	0.360	2.400
15-16 years (50-60 kg)	1,620	486	0.463	3.086
17 and above (> 60 kg)	1,800	540	0.514	3.429

We evaluate the effects of different case management in our model by varying either malaria treatment seeking-behavior or availability of treatment. Table 3.3 summarizes the set of scenarios considered that include seven different sets of assumptions for the level of treatment.

No treatment. In this model, we assume no access to antimalarial treatments.

Reference case management. In this model, we took the same probability of seeking treatment of uncomplicated malaria as in our recent simulation of a malaria vaccine trial (Chapter 4), but assume 20% of treatments to be self-treatment and 80% to use formal care. We use a value of 48% for the probability of seeking treatment of severe malaria (Table 3.1) [McCombie, 1996, 2002]. The treatment rates for uncomplicated episodes are low because the model for clinical episodes was fitted to very intensive surveillance data from Senegal, which included minor fevers that would be very unlikely to lead to treatment seeking [Smith et al., 2006c]. The treatment rates were estimated by triangulating the predictions of this model for clinical episodes with health system attendance data from Manhiça, Mozambique (Chapter 4).

Moderate coverage. In this model, we use recent data from the Tanzanian National Malaria Control Program of the Ministry of Health [NMCP, 2003]. This report states that 27% of children less than five years of age were treated within 24 hours in health facilities, 13% at home, and 2% at traditional healers. The remaining 58% received no treatment within 24 hours from the onset of disease [NMCP, 2004]. We use these percentages of 27% of children receiving formal care, and 13% self-treatment of uncomplicated malaria episodes (Table 3.1). We use the same coverage of formal care for severe malaria as in the reference model. In the context of our five-day time-step we do not distinguish in our simulations whether treatment is within 24 hours or not.

Abuja target coverage. Sixty percent of uncomplicated episodes are treated with the appropriate drug. The simulated coverage of hospital treatment of severe episodes remains at 48%.

Complete coverage. We assume that 100% of uncomplicated clinical episodes are treated with formal-sector care. We also assume that 100% of severe malaria episodes are treated.

Effective treatment. We assume that 100% of clinical episodes are treated with formal-sector care and that there are no treatment failures. Moreover, we assume that all severe episodes receive in-patient treatment.

Anti-pyretic treatment. We assume the same anti-malarial treatment coverage as in the reference scenario, but in addition we assume that 50% of episodes are treated at home by paracetamol. The paracetamol is assumed to provide only symptomatic relief and thus to have no effect on the epidemiologic outcomes.

This defined the baseline status of the simulated populations. We ran simulations over a 90-year period at different transmission intensities under the assumptions of the reference case management scenario. The rather low level of treatment in this scenario is intended to approximate conditions prevailing in many areas studied in Africa of limited drug availability, drug resistance, and non-treatment or undertreatment of minor febrile attacks.

To explore the dynamic impact of different case management options, we then simulated the transient behavior over the next 5-, 10-, and 20-year periods for different case management scenarios, assuming the vectorial capacity for *P. falciparum* transmission to follow the same seasonal pattern as during the baseline period. We compared outcomes with those of scenarios in which the reference case management regimen continued.

Costing. Both marginal and average costs of health care were computed. The marginal cost of treatment is the additional financial or opportunity costs that is incurred when treating each additional case, but does not include the fixed cost of the infrastructure. The average costs include all those costs involved in delivering the intervention, including the use of spare capacity, and those health care resources diverted from other uses [Hutton and Tediosi, 2006].

Uncomplicated malaria. Direct costs of an uncomplicated malaria case seeking care at formal-sector facilities, C_{do}, comprise the cost of an out-patient visit, the cost of drug treatment, and other costs incurred by the patients, i.e.

$$C_{do} = D_o + V_o + H_o \tag{3.3}$$

where H_o is the patient (household) cost when visiting formal-sector outpatient facilities (excluding fees), and D_o is the cost of out-patient drug treatment, and V_o is the non-drug costs of an out-patient visit. D_o is computed as

$$D_o = D_{od} L_d (1 + W) \tag{3.4}$$

where D_{od} is the cost of drug per day and L_d is the number of days of therapy. The drug regimens and hence price depend on patient age and weight (Table 3.4), with the prices, which include distribution costs to districts, corresponding to those in the medical store department catalog [MSD, 2004] of the Tanzanian Ministry of Health. W, the % additional cost of drug wastage, takes a value of 25% throughout [Goodman et al., 2000].

The non-drug cost of an outpatient visit is computed from published data on proportions of out-patients reporting at different levels of the health system, on the proportion, p_t, of cases undergoing diagnostic tests, and on unit costs after exclusion of drug costs (Table 3.6). In the average analysis, the non-drug cost, V_{ao}, is thus given by

$$V_{ao} = p_{hc}V_{hc} + p_hV_h + p_dV_d + p_tT. \tag{3.5}$$

In the case of marginal costs there is an adjustment for the proportion of recurrent non-fixed costs, i.e.

$$V_{mo} = V_{ao}p_{ro}(1 - p_{rfo}). \tag{3.6}$$

The patient (household) costs per outpatient visit, H_o, comprise travel expenses, expenses related to medical supplies, H_m, and non-medical supplies, H_n, such as the purchases of food and drinks or costs of spending the night away from home while seeking care [Adam et al., 2004] (Table 3.6), so that

$$H_o = H_t + H_m + H_n \tag{3.7}$$

In case of self-treatment it is assumed that patients do not incur in any additional costs to purchase the drug because the drugs are likely to be purchased from a private shop close to the patient's home.

Table 3.6: Health-seeking behavior and unit cost assumptions

Item	Description	Value	Reference
	Household (patient costs)*		
H_t	Travel cost (US$)	0.08	[Adam et al., 2004]
H_m	Medical supplies (US$)	0.03	[Adam et al., 2004]
H_n	Non medical supplies (US$)	0.19	[Adam et al., 2004]
	Uncomplicated malaria		
p_{hc}	% of out-patient visits that take place at health centers	18%	[GFATM, 2004]
p_d	% of out-patient visits that take place at dispensaries	72%	[GFATM, 2004]
p_h	% of out-patient visits that take place at hospitals	10%	[GFATM, 2004]
V_{hc}	Cost per out-patient visits at health centers (US$)	1.27	[Adam et al., 2004]
V_d	Cost per out-patient visits at dispensaries (US$)	1.02	[Adam et al., 2004]
V_h	Cost per out-patient visits at hospitals (US$)	2.10	[Health Research for Action, 1999]
p_t	% diagnostic tests (proportion of patients)	10%	[NMCP, 2004]
T	Unit cost of diagnostic test (US$)	0.30	[NMCP, 2004]
p_{ro}	% of out-patient visit cost that are recurrent	69%	[NMCP, 2004]
p_{rfo}	% of out-patient visit recurrent cost that are fixed	25%	[Goodman et al., 2000]
H_o	Average patient cost (US$)	0.30	[Adam et al., 2004]
	Severe malaria		
N_i	Non-drug cost per day of stay – (US$)		
	(Capital)	2.30	[Alonso-Gonzalez et al., 2000]
	(Recurrent)	5.50	[Alonso-Gonzalez et al., 2000]
	(Total)	7.80	[Alonso-Gonzalez et al., 2000]
$L_i(1)$	Average length of stay when patient fully recovers	4.50	[Goodman et al., 2000]
$L_i(2)$	Average length of stay when patient recovers with neurologic sequelae	10	[Goodman et al., 2000]
$L_i(3)$	Average length of stay when patient dies	2	[Goodman et al., 2000]
p_{ri}	% of in-patient costs that are recurrent	71%	[Goodman et al., 2000]
p_{fi}	% of in-patient recurrent cost that is fixed	50%	[Goodman et al., 2000]

*Daily average household (patient) out of pocket costs.

Severe malaria. The direct health care costs of a severe malaria case C_{di} are given by

$$C_{di} = D_i + V_i + H_i \tag{3.8}$$

where V_i is the non-drug cost of in-patient care, D_i is the cost of drug treatment, and H_i is the patient (household) cost when visiting formal-sector in-patient facilities. D_i is computed by multiplying the costs by the duration for which they are incurred. During the first day of treatment the drug dosage and consequently the costs are different, so overall D_i is given by

$$D_i = (D_{i1} + D_{i2}(L_i - 1))(1 + W) \tag{3.9}$$

where D_{i1} is the cost for the first day, D_{i2} is the cost per day thereafter, and L_t is the length of treatment (in days) (Table 3.6). The non-drug cost of in-patient care in the average analysis is given by

$$V_i = V_{ai} = N_i L_i(o) \tag{3.10}$$

where $L_i(o)$ is the average length of stay, which varies depending on the outcome o, and N_i is the in-patient cost (see Table 3.6). Correspondingly, in the marginal analysis the non drug cost is

$$V_i = V_{mi} = N_i L_i(o)\ p_{ri}(1 - p_{fi}). \tag{3.11}$$

The costs incurred by patients are the same as for an outpatient visit for the first day. For the subsequent days of stay, we include only the costs of medical and non-medical supplies (H_m and H_n respectively) so that

$$H_i = H_t + (H_m + H_n)L_i(o). \tag{3.12}$$

3.3 Results

The reference scenario simulation. Simulated patterns of age-prevalence and age-incidence for the reference scenario (Figure 3.2) are similar to those for typical mesoendemic settings in Africa to which the models were fitted (Chapter 2, Ross et al. [2006b], Smith et al. [2006c]). The direct cost per capita is stable over time. The predicted infectiousness of the host population, $\bar{\kappa}_u(t)$, fluctuates seasonally around a value of approximately 3% (Figure 3.3a). Since the reference scenario uses the same transmission pattern and health system to construct the baseline population as are applied during the follow-up, there

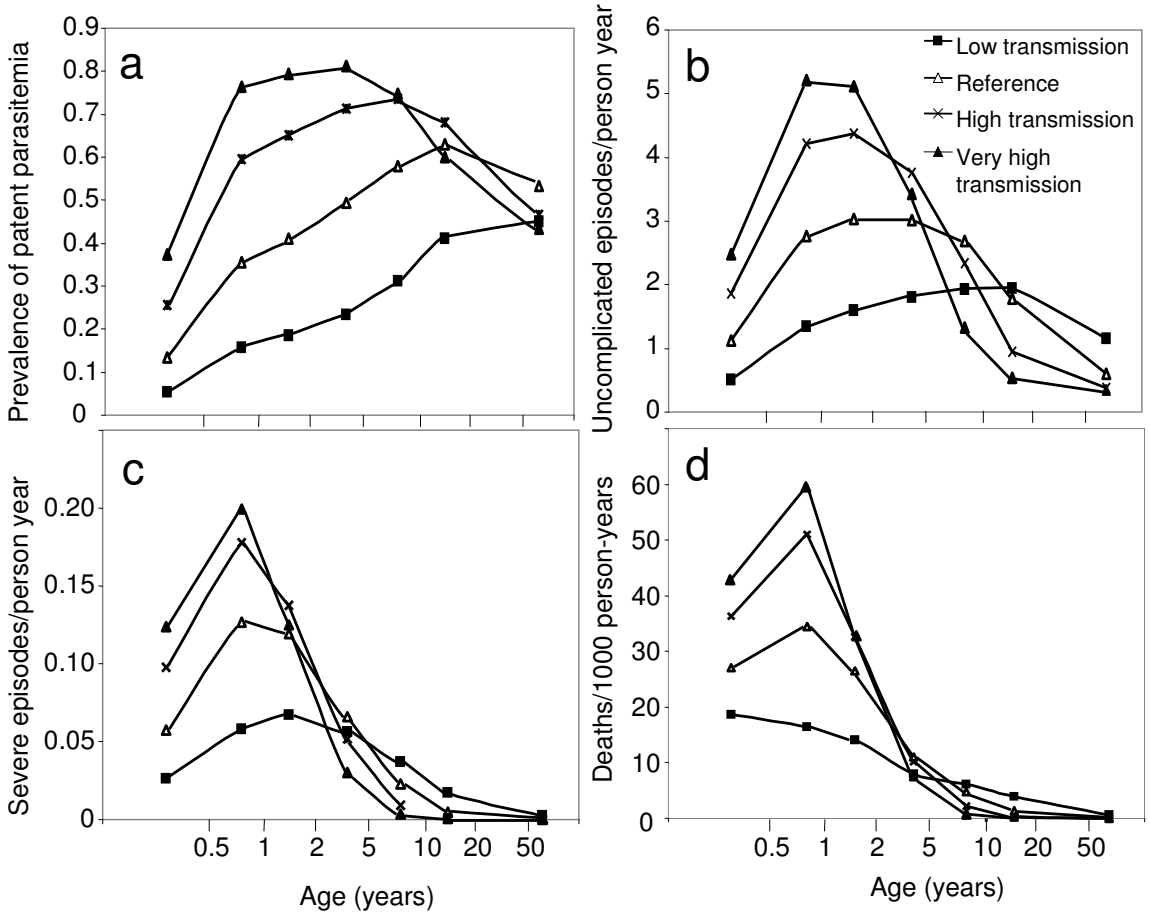

Figure 3.2: Predicted age-prevalence and age-incidence curves by transmission intensities. The reference scenario is the transmission intensity observed at Namawala, Tanzania divided by a factor 16. Low transmission = Namawala transmission divided by 64; high transmission = one-fourth of Namawala transmission; very high transmission = transmission observed at Namawala. a) Age-prevalence curve of patent parasitemia. b) Age-incidence curve of uncomplicated episodes. c) Age-incidence curve of severe episodes. d) Age-incidence curve of mortality.

is no trend over the 20-year simulation period in these epidemiologic variables or in the treatment costs. Over the 20-year simulation period, the total number of undiscounted

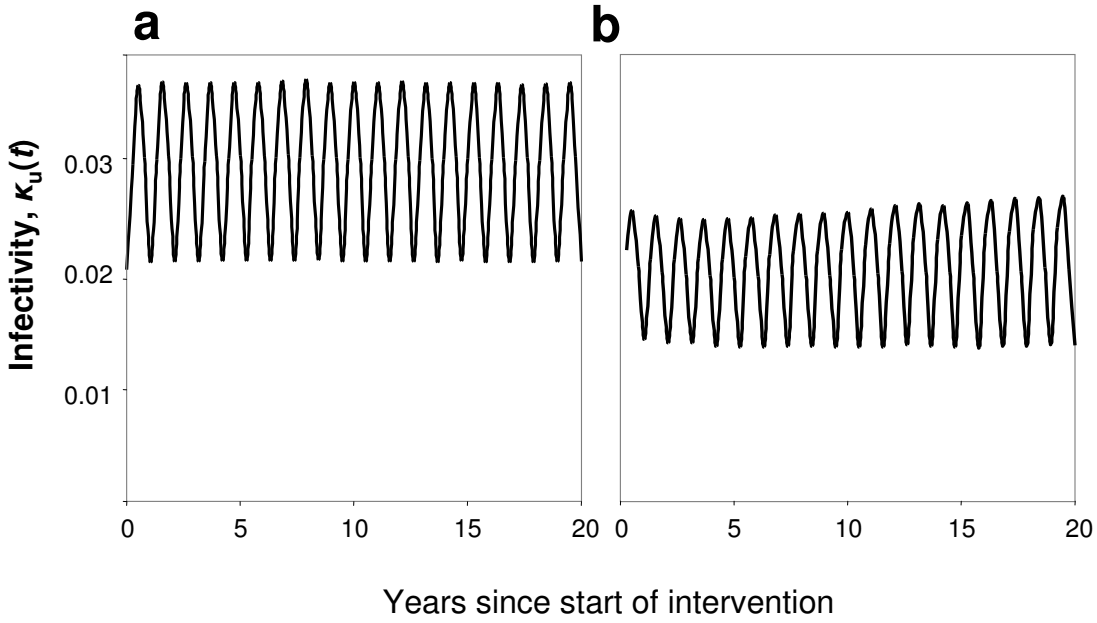

Figure 3.3: Infectivity of the human population. a) Reference scenario. b) Scenario assuming full treatment coverage.

DALYs lost due to malaria in our population of 100,000 people is approximately 481,000, which corresponds to a rate of 0.24 DALYs per capita per year. Since most of these DALYs are due to mortality, the total number of YLLs is very close to that of DALYs (Table 3.7). If YLLs and DALYs are discounted at a standard rate of 3%, the total number of DALYs is considerably lower.

Table 3.7: Years of life lived with disabilities (YLLs)*, disability adjusted life-years (DALYs)*, and direct costs†

	Undiscounted				Discounted (3%)			
	YLLs	DALYs	Average costs	Marginal costs	YLLs	DALYs	Average costs	Marginal costs
Reference	0.238	0.244	0.243	0.142	0.120	0.125	0.184	0.108
Moderate coverage‡	0.217	0.224	1.066	0.736	0.112	0.118	0.809	0.558
60% Abuja target coverage‡	0.160	0.165	1.423	0.946	0.083	0.087	1.053	0.70
Full coverage‡	0.100	0.105	1.807	1.212	0.052	0.056	1.463	0.993
Effective treatment‡	0.081	0.086	1.424	0.918	0.042	0.046	1.054	0.679
No treatment‡	0.276	0.276	-	-	0.138	0.143	-	-
Antipyretic treatment‡§	0.238	0.244	0.266	0.165	0.120	0.125	0.201	0.125
Very low transmission	0.219	0.226	0.285	0.172	0.119	0.125	0.216	0.131
Low transmission	0.224	0.231	0.283	0.169	0.118	0.124	0.215	0.129
High transmission	0.242	0.246	0.204	0.116	0.120	0.123	0.155	0.088
Very high transmission	0.234	0.237	0.169	0.095	0.115	0.117	0.128	0.072
Low transmission, full coverage	0.036	0.038	0.544	0.368	0.017	0.018	0.470	0.321
High transmission, full coverage	0.160	0.165	2.027	1.349	0.068	0.072	1.643	1.109

*Lost per capita per year due to malaria.

†Direct cost per capita in US$ per year.

‡Same transmission level as in reference scenario.

§Epidemiologic outcomes as per reference scenario.

The total undiscounted direct average costs to treat malaria episodes with the reference case management model amounts to US$ 485,793 over the 20-year simulation period. This corresponds to US$ 4.86 per capita and, on average, US$ 0.24 per capita per year (Table 3.7). Out-patient visits account for 32% of total direct costs, drug treatments of both uncomplicated and severe episodes for 7%, hospital admissions of severe episodes for 40%, and patient costs for 22%. The marginal cost, i.e. additional financial or opportunity costs that would be incurred when introducing a new control intervention, is approximately 58% of the average cost.

Effect of changing levels of access to case management. Comparison of the reference scenario with the extreme scenario with no treatment of malaria episodes (either uncomplicated or severe) showed noticeable epidemiologic effects of treatment despite the low attendance rates for uncomplicated episodes in the reference health system. In children less than 10 years of age, the no treatment scenario predicted higher prevalence of infection (Figure 3.4), a higher anemia prevalence (Figure 3.5) and a slight increase in the incidence of clinical episodes, with age patterns as shown in Figure 3.6a,b and c.

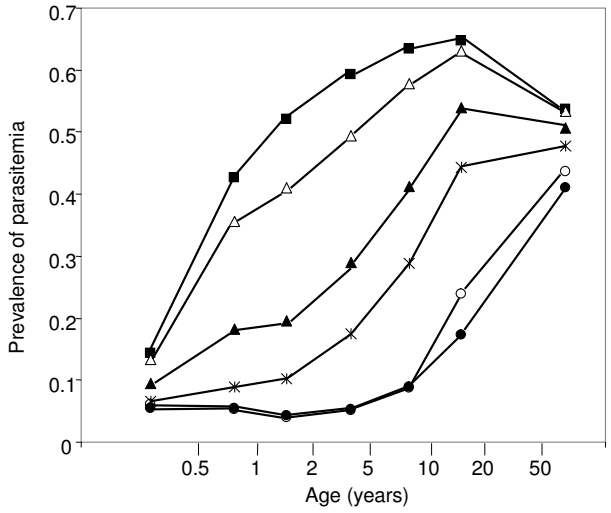

Figure 3.4: Age-prevalence curves of parasitemia under different case management scenarios during a simulated 20-year follow-up period. ■ = no treatment; △ = reference; ▲ = moderate coverage (1^{st} year of follow-up); ⋆ = complete coverage (1^{st} year of follow-up); ∘ = complete coverage (10^{th} year of follow-up); • = complete coverage (20^{th} year of follow-up);

There was only a small effect on the incidence of severe malaria (Figure 3.6d, e and f). Since

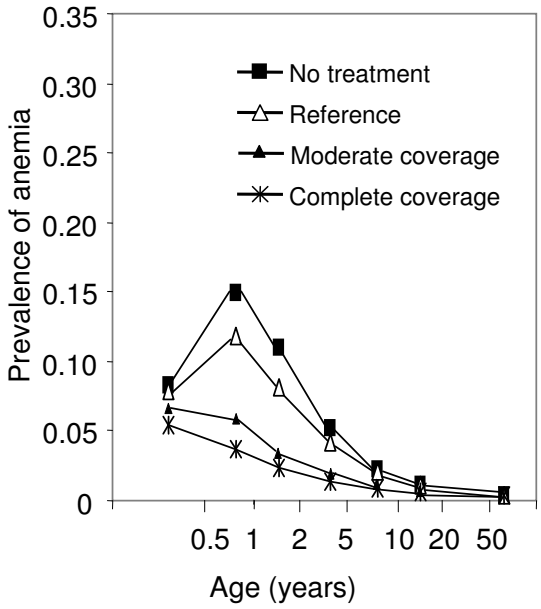

Figure 3.5: Age-prevalence curves of anemia (hemoglobin level < 8g/dL).

the reference health system includes a relatively high treatment rate of severe episodes, the largest differences between the no treatment and reference scenarios were in the mortality rates, with a substantially higher mortality rate predicted with no treatment, especially in the second half of the first year of life (Figure 3.6g, h and i).

The reference scenario is in a state of equilibrium throughout the simulation, although there is stochastic variation over time in the outputs. The no treatment scenario quickly reaches a new equilibrium. Therefore, only the average prevalence over 20 years is shown for this scenario (Figure 3.4), and the effects on incidence of morbidity and mortality do not change much during the follow-up period (Figure 3.6). The total number of DALYs lost over the simulated 20-year period was 13% higher with the no treatment regimen than with the reference. The effect on transmission, as measured by $\bar{\kappa}_u(t)$, is negligible.

The complete coverage scenario for treatment leads to a rapid decrease in transmission, as measured by $\bar{\kappa}_u(t)$ (Figure 3.3b). This stabilizes quickly at a value approximately 60% of that in the reference scenario, implying that treatment of all the clinical episodes (including minor episodes) can reduce the inoculation rate by about 40%. Complete coverage predicted very substantial decreases in prevalence of parasitemia (Figure 3.4), anemia (Figure 3.5), and incidence of uncomplicated episodes (Figure 3.6), but these outcomes, which

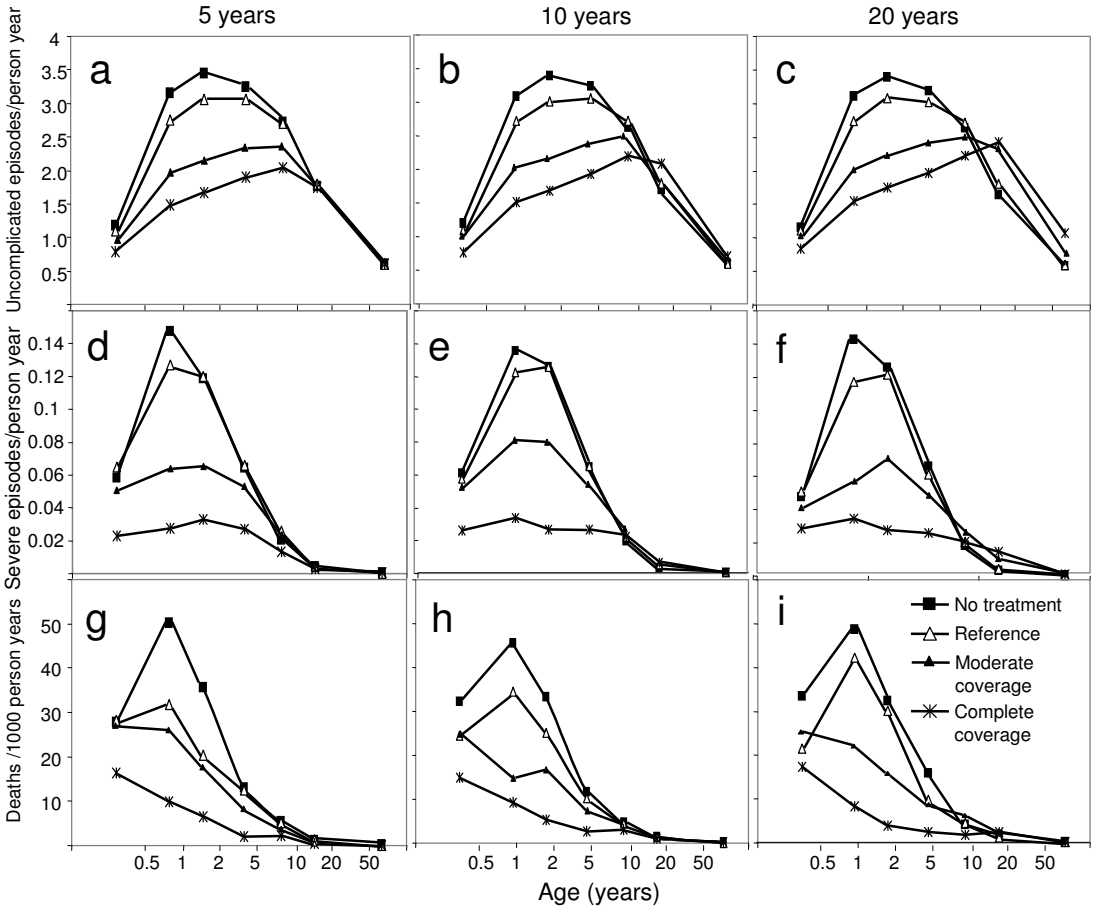

Figure 3.6: Age-incidence curves under different case management scenarios at different durations of simulation during a 20-year follow-up period. a-c) age-incidence of uncomplicated episodes; d-f) age-incidence of severe episodes; g-i) age-incidence of mortality.

reflect the dynamics of immunity, required an extended period to reach equilibrium. Although treatment of severe episodes in the complete coverage health system is no different from the reference, the effects on transmission and persistence of parasites result in substantial reductions in incidence of severe morbidity and mortality (Figure 3.6), leading to a total number of DALYs lost over 20 years of only approximately 45% of those in the reference scenario (Table 3.7).

The epidemiologic effects of high treatment coverage were concentrated in the youngest age groups, resulting in a substantial shift in the age of peak incidence of uncomplicated episodes (to older ages) and of mortality (to younger ages, in which a greater proportion of the mortality is contributed by indirect deaths). Since the changes in the age-prevalence and age-incidence curves caused by complete coverage were also time-dependent, the transient effects can be seen throughout the 20-year follow-up period. As a result of the shifts in age-incidence, 10 years into the simulation an increase in incidence of clinical episodes above baseline levels is evident in individuals more than 10 years of age (Figure 3.6b). Since the shifts in the peak of the incidence curves to older age-groups accumulates over time, the benefit of the intensive treatment regimen decreases with time.

The distribution of direct costs is also changed as a function of treating all malaria episodes with a first-line drug. In the scenarios that we simulated, there would then be little need for second-line treatment; thus, many severe episodes could be prevented, which in turn reduces in-patient costs. Our model predicts that if all uncomplicated episodes were treated with the first-line drug, out-patient visit costs would account for 61% of total direct costs, drug treatments for 7%, in-patients admissions for 3%, and patient costs for 30%. The total direct costs to treat all malaria episodes would be approximately 7.4-times those of the reference scenario.

The moderate coverage scenario predicts effects on prevalence and on the clinical outcomes (Figures 3.4, 3.5 and 3.6) more similar to those for complete coverage than to those for no treatment. This is despite the assumption in the moderate coverage health system of treatment rates for uncomplicated episodes much less than 50% and thus much closer to those for no treatment than those for complete coverage. This implies that within our models, there is a highly non-linear relationship between health outcomes and treatment coverage for uncomplicated malaria, with a very high marginal impact of increases in coverage when it starts from a low level. This conclusion is supported by the simulation of effective treatment, which gave very similar results to that of complete coverage for all the

outcomes except mortality. Mortality rates and thus DALYs lost (Table 3.7) were reduced by the effective treatment health system to substantially below those with the complete coverage health system because all severe cases were assumed to be treated as in-patients.

The Abuja target coverage simulation is intended to simulate the impact of achievement of the coverage of 60% targeted in the Abuja Declaration on Roll Back Malaria in Africa, signed by African Heads of State and Government in April 2000. The YLLs, DALYs, and costs are intermediate between those predicted for the reference and those for full coverage.

The antipyretic treatment simulation is intended to indicate the sensitivity of the costs to allowance for the large number of people who self-treat with anti-pyretics, in addition to those who use anti-malarials. Unfortunately, it is difficult to obtain good estimates for actual levels of self-treatment in sub-Saharan Africa. The coverage of 50% for self-treating with anti-pyretics that we use is associated with an increase in drug costs of between 9% and 16% Table 3.7), which indicates that although this is not likely to be a factor dominating costs, it could be of some importance because these are out-of-pocket expenses paid predominantly by poor patients. It would be important to include better estimates of drug choice and coverage for self-treatment.

Effect of transmission intensity. In higher transmission settings, simulated parasite prevalence was higher, and peaked at a younger age (Figure 3.2a). The incidence of uncomplicated malaria episodes also increased with transmission intensity in young children, but the reverse pattern was observed in older individuals (Figure 3.2b), matching the pattern to which the model was fitted [Smith et al., 2006c]. The incidence of severe episodes showed a similar pattern, but with a steeper decline in incidence with age at high transmission, and consequently a crossing of the age-incidence curves at younger age (Figure 3.2c). The pattern for mortality was similar, with the mortality rate independent of transmission intensity at the age of approximately 3-4 years.

The average level of transmission to the vector, $\bar{\kappa}_u(t)$, was similar to that for the reference scenario for all values of EIR investigated, but the amplitude of the seasonal variation in $\bar{\kappa}_u(t)$ increased with the transmission intensity.

The total number of YLLs and DALYs lost over the simulated 20-year period are only slightly higher in the high transmission settings compared with areas of lower transmission intensity. The total direct costs are determined by the number of uncomplicated and severe

episodes treated, which are higher than in the reference scenario in the low transmission setting and lower in the high transmission setting (Figure 3.7). However, these figures depend strongly on the model predictions for rates of severe malaria in adults, of which we are highly uncertain [Ross et al., 2006b].

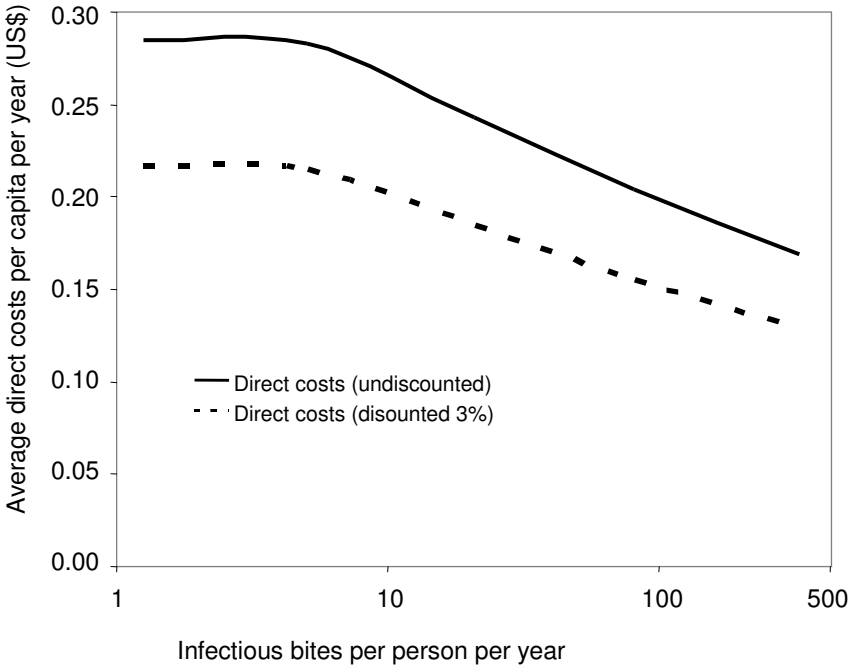

Figure 3.7: Direct costs in relation to transmission intensity. Upper line = undiscounted; lower line = discounted.

Changing access to case management in different malaria transmission intensity settings. The effects of an increased or decreased level of access to case management also vary according to the prevailing malaria transmission intensity (Figure 3.8). In a setting of moderate malaria transmission, treating all uncomplicated episodes over 20 years would lead to only a small difference in the total number of uncomplicated episodes, but reduces incidence of severe episodes by 49%, and the number of deaths and DALYs lost by 57% (Table 3.7).

In the low transmission setting, treating all uncomplicated cases over 20 years reduces incidence of uncomplicated episodes by 71%, severe episodes by 88%, and the number of deaths and DALYs lost by 83%. In the high transmission setting, complete treatment coverage would increase the total number of uncomplicated episodes over time, and would

lead to a reduction of only 31% of severe episodes and DALYs lost and 34% of the number of deaths.

Treating everyone has a much greater effect on incidence at low transmission intensities. At high transmission, a high level of coverage always appears to be beneficial in terms of reducing incidence of severe episodes and of mortality, but may even lead to an increase in incidence of uncomplicated episodes. Within the model, this is because a very high treatment rate is associated with a reduction in exposure to asexual blood stage parasites and thus in acquired blood-stage immunity.

The economic implications of changing levels of access to case-management also differ according to the malaria transmission intensity. Simulation over a 20-year period under the assumption of complete treatment coverage of uncomplicated malaria episodes would increase direct costs by a factor of almost 10 in a highly endemic setting, but the increase would be only 92% in low transmission settings (Table 3.7).

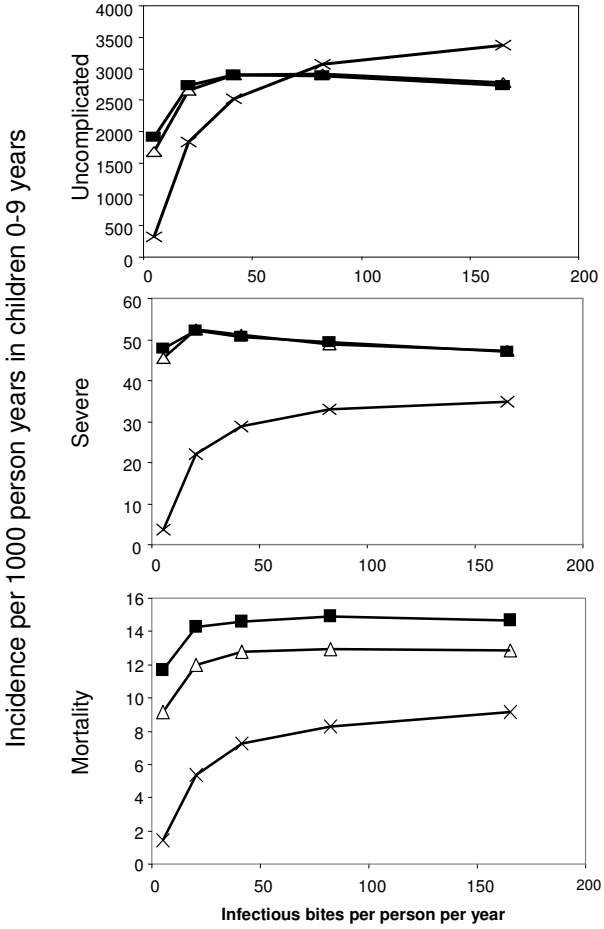

Figure 3.8: The effect of changing case management in different transmission settings. The status of the population at baseline was defined by simulating the reference health system for 90 years for each transmission intensity. The follow-up period then ran for 20 years with the chosen health system, and the results are the average for the 20 years. The incidence rates quickly settled to a new level. Because of the uncertainty in the rates of severe morbidity and mortality in adults, the predictions only for children less than 10 years of age are shown. ■ = no treatment; △ = reference case management; x = full coverage

3.4 Discussion

We present a first attempt to use a dynamic model for case management of malaria in sub-Saharan Africa. For prediction of the effects of the case management, we considered a range of different transmission intensities characteristic for large parts of malaria-endemic Africa, and our simulations are thus likely to be of broad applicability. Lower EIRs than considered here (i.e. less than five infectious bites per person per year) are characteristic of highly urbanized settings, the African highlands, and areas located at the current distribution edges of *P. falciparum* transmission [Keiser et al., 2004, Zhou et al., 2004]. Our model needs further development and validation to make meaningful predictions for such settings.

Our modeling approach expands the scope for predictions of the epidemiologic and economic consequences of malaria interventions as a direct function of the case management. In a first step, we have simulated different rates of treatment coverage, including the most extreme scenarios of either complete lack of treatment or full coverage. These two scenarios, together with a reference scenario largely constructed from real data obtained from Tanzania, were used for simulations up to 20 years. Costs were also built into our dynamic models, which will ultimately make it possible to predict the cost-effectiveness of the case management.

Our immediate purpose is to integrate effects of case management into our dynamic models of the clinical epidemiology and natural history of *P. falciparum* malaria in a typical setting of sub-Saharan Africa. This approach could readily be adapted to assess the costs of scaling up malaria treatment but this would entail more detailed analysis of the activities involved in changing treatment practices.

Our model can be used to make predictions of the effect of introducing a new malaria control intervention (e.g. malaria vaccine) or scaling-up of existing control measures (e.g. ITNs). The former motivated the development of our modeling approach. The current model is probably better at fulfilling this objective than in capturing the impact of changes in case management, including different levels of treatment and changes in national antimalarial drug policies. This is justified because the epidemiologic model was fitted mainly to cross-sectional data from various settings across sub-Saharan Africa. Since it is less able to capture longitudinal patterns within hosts, it does not claim to incorporate realistic patterns of treatment-seeking behavior or of referral patterns. In African settings where patients have limited resources, care-seeking patterns in general and malaria treatment-seeking behavior in particular are complex [de Savigny et al., 2004, Muela et al., 2002, Tanner and

Vlassoff, 1998].

There is a need to build on simple models of the referral system [Goodman et al., 2000], so that we become more confident of the likely impacts of changes in national antimalarial drug policies. For example, parasite resistance to SP has reached critical levels in many parts of central and east Africa, including Tanzania [Mugittu et al., 2004, Talisuna et al., 2004] and this places a question mark against our longer-term predictions of cost-effectiveness which assume that treatment with SP remains efficacious. In view of the public health, social, and economic significance of SP resistance, efforts are underway in Tanzania and elsewhere to change national policies towards artemisinin-based combination therapy (ACT). The Global Fund to Fight AIDS, Tuberculosis, and Malaria has recently approved a project to switch from SP (and amodiaquine) to ACT [GFATM, 2004]. Such a shift in drug policy is of considerable public health significance and will directly affect the case management of *P. falciparum* malaria. There is a need to adapt our model to field data from a range of different settings, and that will make it possible to explore the epidemiologic and economic consequences of the case management system under different scenarios. These should include simulation of the shift from SP to ACT conditional on various levels of SP resistance. All of these simulations need to take into account patterns of self-treatment, for which we currently have only weak data.

Regarding the epidemiologic model, we chose to define the seasonal pattern of *P. falciparum* transmission by using data from the village of Namawala in Tanzania. The high level of transmission measured there, even in comparison to other sites in Tanzania [Drakeley et al., 2003, Hay et al., 2000] , made it possible to measure the intensity of transmission during the dry season. Multiplication of the Namawala rate by a constant therefore provides us with a reasonable estimate of the seasonal pattern, even for lower transmission areas where dry season transmission usually cannot be measured.

The national malaria control program of Tanzania reports that 75% of people live in areas of stable malaria transmission, 17% in areas of unstable transmission (duration of transmission less than one month per year), and the remaining 8% in areas of unstable transmission (highly seasonal) [NMCP, 2004]. However, historic and contemporary maps of malaria endemicity for Tanzania [Clyde, 1967, Craig et al., 1999] do not provide estimates of the inoculation rate with which to determine the distribution of EIR levels among the people within areas of stable transmission.

Our approach makes it possible to look at how such variations in transmission intensity

might affect the impact of changes in the health system. However, our confidence in the present results is limited by uncertainties in our epidemiologic models (especially that for severe malaria and mortality, for which we had no data for older age groups [Ross et al., 2006b]).

Increasing levels of treatment generally shift the age-prevalence and age-incidence curves so that the peaks are in older age-groups. We developed our parasitologic model mainly using archive data that predated the widespread use of anti-malarial chemotherapy. A delayed peak in the age-prevalence curve that we attribute to this effect was already apparent in the dataset from Navrongo, Ghana [Owusu-Agyei et al., 2002] which was from a more recent period than the other studies (Chapter 2). The effect of treatment on reducing acquired blood-stage immunity is very uncertain because asexual blood stage immunity is modeled as a function of both the number of distinct infections and of the cumulative parasite load, and we do not know what should be the relative contributions of these two different components of acquired immunity. The effects of cumulative parasite load are intended to simulate acquisition of immunity to antigenic variants that arise during the course of the infection.

We agree with other models for cost-effectiveness of malaria interventions in attributing most of the burden of disease to mortality rather than to disability associated with acute illness, sequelae, or anemia. Important methodologic issues requiring further investigation arise in the computation of the DALYs. In African populations with high infant mortality, there is generally an increase in life expectancy during the first few years of life, and this leads to perverse outcomes in the computation of DALYs if the effect of an intervention is partly to shift mortality to older ages in childhood. For example, if life expectancy at one year of age is 64 years, and life expectancy at five years of age is 72 years, then the number of life years gained by shifting age at death would be negative: 64-72= -8. This effect is accentuated by discounting or age-weighting of the DALYs, but does not arise with the Japanese life tables used to compute DALYs in the GBD calculations used by the World Health Organization [Murray and Lopez, 1996b]. We did not use these life tables because it is generally considered that local life tables should be used to compute DALYs in cost-effectiveness analyses [Fox-Rushby and Hanson, 2001], but there is a strong case for using death rates that exclude the health effect under investigation. For the present analyses, we used a life table from an east African site with low malaria incidence. In these life tables, where malaria plays only a small role, there is an increase in life expectancy over the first

few years of life.

In conclusion, we have made a first attempt to develop a modeling framework to simulate the dynamic effects of the case management of *P. falciparum* malaria across a wide range of transmission intensities in sub-Saharan Africa. We discovered several deficiencies in our understanding of the relevant health systems. Our simulations of a range of scenarios indicate which of these uncertainties are most likely to be important for the prediction of cost-effectiveness of malaria interventions. Further development of our modeling approach offers more realistic evaluation of the epidemiologic and economic consequences of malaria interventions. This in turn will create a sound foundation for measuring the effects of introducing new antimalarial interventions (e.g. malaria vaccines), or scaling up those that are already known to be efficacious and cost-effective.

Chapter 4

Modeling a field trial of the RTS,S/ AS02A malaria vaccine

Nicolas Maire[1], John J. Aponte[2], Amanda Ross[1], Ricardo Thompson[3], Pedro Alonso[2], Jürg Utzinger[1], Marcel Tanner[1], Thomas Smith[1]

This article has been published:
American Journal of Tropical Medicine and Hygiene 2006, 75, Suppl 2, 104-110

[1]Swiss Tropical Institute, Basel, Switzerland
[2]Center for International Health, Hospital Clinic/Institut d'Investigacions Biomdiques August Pi i Sunyer, University of Barcelona, Barcelona, Spain
[3]National Institute of Health, Ministry of Health, Maputo, Mozambique

Abstract

A double-blind, phase IIb, randomized controlled trial of the malaria vaccine RTS,S/AS02A showed an efficacy of 45.0% in reducing the force of infection for *Plasmodium falciparum* and of 29.9% in reducing incidence of clinical malaria in children 1-4 years of age in Manhiça, Mozambique. We simulate this trial using a stochastic model of *P. falciparum* epidemiology, and the setting-specific seasonal pattern of entomologic inoculations as input. The simulated incidence curve for the control group was comparable with that observed in the trial. To reproduce the observed efficacy in extending time to first infection, the model needed to assume an efficacy of 52% in reducing the force of infection. This bias arises as a result of acquired partial immunity against blood stages, thus suggesting an explanation for the lower efficacy observed in a previous trial in semi-immune adult men in The Gambia. The shape of the incidence of infection curve for the vaccine cohort in Manhiça indicates that the vaccine provides incomplete protection to a large proportion of the vaccinees, rather than offering complete protection to some recipients and none to others. This behavior is compatible with a model of no decay in efficacy over the six-month surveillance period of the trial. The model accurately reproduced the lower efficacy against clinical disease than against infection. In the simulations this finding resulted from loss of acquired clinical immunity as a result of a reduction in the force of infection in the vaccinated cohort. The model also predicted greater efficacy against severe diseases than against clinical disease. The success of the simulation model in reproducing the results of the Manhiça trial encourages us to apply the same model to predict the potential public health and economic impact if RTS,S/AS02A were to be introduced into the existing Expanded Program on Immunization.

4.1 Introduction

A double-blind, phase IIb, randomized controlled trial in Manhiça district, Mozambique, found an estimated 45.0% efficacy of the malaria vaccine RTS,S/AS02A for delaying the time to first *Plasmodium falciparum* infection in children 1-4 years of age[Alonso et al., 2004]. The vaccine efficacy for delaying time to first clinical episodes was 29.9%. In a previous trial carried out with semi-immune adult men in The Gambia, vaccine efficacy for extending time to first infection was 34% [Bojang et al., 2001].

Time to first observed infection is a different outcome from the true proportion of infections prevented by RTS,S vaccination, and there are a number of reasons why these trial estimates of efficacy are likely to be lower. They may be diluted by effects of heterogeneity in vaccine effect between individuals [Halloran et al., 1992]. Pre-existing naturally acquired pre-erythrocytic immunity could also introduce variations between hosts in susceptibility to infection, while asexual blood stage immunity means that some hosts are more likely to appear to be parasite negative, even though they are infected. Such heterogeneities consistently lead to reduction in estimates of efficacy in preventing infection [Halloran et al., 1996].

The different efficacy values all have wide confidence intervals (Table 4.1), and can therefore be reconciled with a statistical null hypothesis that the variation between them represents only a result of chance. However there are good reasons for expecting malaria vaccines to have different efficacies against different outcomes [Alonso et al., 1995]. Acquired immunity is potentially an even more important source of bias in analyses of post-infection outcomes such as incidence of clinical disease, than in those of infection. Post-infection outcomes can also potentially be a cause of attenuated efficacy estimates. The latter is particularly an issue with definitions of clinical malaria episodes used in vaccine trials, which are known to have imperfect specificity [Schellenberg et al., 1994, Smith et al., 1994].

Table 4.1: Efficacy estimates for children 1-4 years of age

Outcome	Manhiça trial [Alonso et al., 2004]		Simulation*	
Prevention of infection	$\widehat{VE}_p$	0.45 (0.31,0.56)	$\widetilde{VE}_p$	0.45¶ (0.42,0.48)
Prevention of clinical episodes	$\widehat{VE}_c$	0.30 (0.11,0.45)	$\widetilde{VE}_c$	0.33 (0.27,0.38)
Prevention of severe malaria	$\widehat{VE}_s$	0.58 (0.16,0.81)	$\widetilde{VE}_s$	0.36 (0.26,0.45)

*Values in parentheses are 95% confidence intervals. Predictions based on 5,400 children per cohort.

¶This value was constrained to be equal to the that of $\widehat{VE}_p$. The remaining efficacy values follow from this constraint, together with the value of 5% for the probability that a malaria fever is treated.

Many of these phenomena lend themselves to simulation-based analyses. We now simulate the Manhiça trial. Our main objective was to test a stochastic model of the primary epidemiologic effect of RTS,S/AS02A. The model makes use of models of malaria incidence [Smith et al., 2006b], parasite densities (Chapter 2) and of clinical malaria [Ross et al.,

2006b, Smith et al., 2006c] to predict the outcomes of the trial. This enabled us to consider the extent to which the trial results can be explained by established features of *P. falciparum* epidemiology in the Manhiça setting. The results also suggest that the model could provide a basis for predicting the potential effects of future malaria vaccine trials elsewhere, and for estimating their potential public health and economic impact.

4.2 Materials and Methods

Study site and trial procedures. The trial [Alonso et al., 2004] was carried out between April, 2003 and May, 2004 among 2,022 children 1-4 years of age living in Manhiça district, Mozambique [Alonso et al., 2002]. Children were randomly allocated three doses of either the pre-erythrocytic malaria vaccine RTS,S/AS02A or control vaccines. The primary endpoint was time to first clinical malaria episode of *P. falciparum*, defined as axillary temperature $\geqslant 37.5$℃ plus *P. falciparum* asexual parasite density >2,500 per μL of blood. Surveillance of this endpoint was in a cohort of 1,605 children recruited from the area around Manhiça itself (cohort I) who were monitored over a six-month period after completion of the vaccination schedule. Vaccine efficacy for prevention of new infections was determined in cohort II, which was composed of 417 children recruited in the area of Ilha Josina located north of Manhiça.

Entomologic inoculation rate. The monthly average entomologic inoculation rate (EIR) was determined for the period of the trial only for the zone around Manhiça where cohort I was recruited. Mosquito densities were determined by sampling the households of a random sample of individuals drawn from the demographic surveillance population. The sporozoite rate was determined using a standard enzyme-linked immunosorbent assay technique, and the EIR was estimated by the product of the human biting rate and the sporozoite rate as described for other entomologic surveys in the area [Aranda et al., 2005]. Transmission in the area of Ilha Josina, where cohort II was recruited, is thought to be higher than around Manhiça.

Simulation of *P. falciparum* incidence and morbidity. We implemented a stochastic simulation model of *P. falciparum* epidemiology [Smith et al., 2006a], using the monthly

pattern of EIR for Manhiça as input to the simulation and making predictions for four simulated cohorts, each of at least 5,000 children 1-4 years of age, the same age-range as in the Mozambique trial [Alonso et al., 2004]. The four cohorts corresponded to the two control and two vaccine cohorts in the actual trial. We used the same computer code, written in FORTRAN, as in our previous simulations [Smith et al., 2006a].

To model the baseline immunologic status of the trial cohorts, we assumed that from birth until to the beginning of the trial these children had been exposed to the same recurring annual pattern of inoculations that was measured during the trial period, and to the drug regimen for treating malaria described previously for the Manhiça district [Saute et al., 2003]. For the simulation of the trial, we reproduced the drug regimen described by Alonso and others [2004]. To estimate the proportion of clinical episodes that were treated, we compared the recorded incidence in the control group with the incidence predicted by the model. The resulting compliance estimate was then applied uniformly to the simulations of both pre-trial and trial periods. In the absence of setting-specific data on the proportion of severe malaria episodes reporting to the formal health sectors, we followed the procedures of Goodman and others [2000] and McCombie [1996] in assuming that half of the severe malaria episodes report to a health facility and compared the observed hospital admission rate with that predicted by this model.

We considered the model predictions of incidence of first *P. falciparum* infection [Smith et al., 2006b], the frequencies and densities of patent parasitemia (Chapter 2), the incidence of acute episodes of clinical malaria [Smith et al., 2006c] and the incidence of severe disease [Ross et al., 2006b]. Our simulations followed the original trial protocol in considering only the time at risk for each individual until their first or only episode (analysis of incidence of acute episodes in cohort I), or first recorded patent infection (cohort II).

Simulation of vaccination. The model for simulation of incidence of first *P. falciparum* infection in the control cohorts is described in an accompanying paper [Smith et al., 2006b]. Briefly, new infections in individual i at time t are modeled via a Poisson process where the force of infection $\lambda(i,t)$ is the product of three independent terms, $E_a(i,t)$, $S_1(i,t)$, and $S_2(i,t)$, where $E_a(i,t)$ is the EIR, adjusted for the expected size of the host, $S_1(i,t)$ captures innate density dependent control, and $S_2(i,t)$ measures the effects of acquired

immunity. In the absence of vaccination, the function for acquired immunity is

$$S_2(i,t) = S_{imm} + \frac{(1 - S_{imm})}{1 + \left(\frac{X_p(i,t)}{X_p^*}\right)^{\gamma_p}},$$

where $X_p(i,t)$ is the level of naturally acquired pre-erythrocytic exposure measured by the cumulative number of entomologic inoculations, X_p^* is a critical value of the level of exposure, γ_p is the steepness of the relationship between exposure and immunity, and S_{imm} determines the survival of inocula in the most highly immune individuals. The fitted curve for $S_2(i,t)$ as a function of $X_p(i,t)$ is given in Figure 4.1, which shows two alternative modifications of this model for application in the vaccine cohorts.

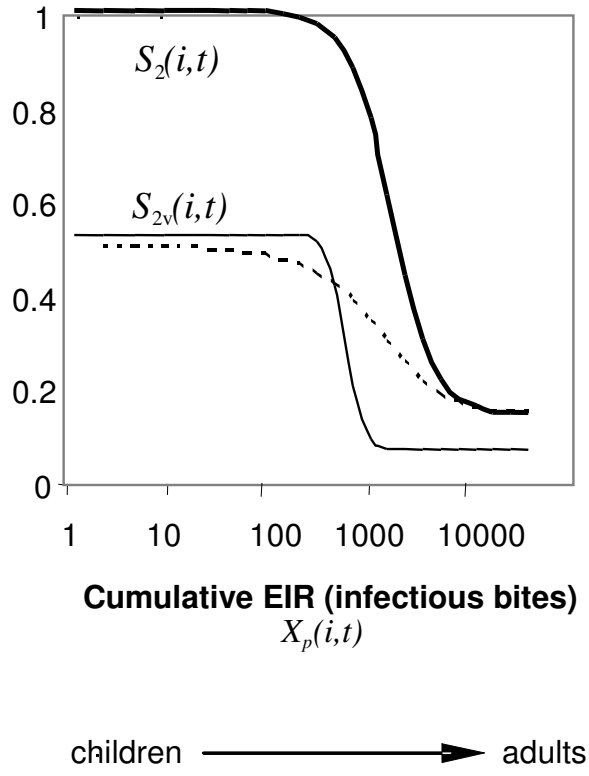

Figure 4.1: Functions used to model acquired immunity. Upper line = value of $S_2(i,t)$ fitted to data from Matsari, Nigeria [Smith et al., 2006b]. Dashed line = $S_{2v}(i,t)$ derived from model (a); X_v=1,800 inoculations. Lower continuous line = $S_{2v}(i,t)$ derived from model (b); $\overline{VE}_0 = 0.52$; EIR = entomologic inoculation rate.

Model A. Vaccination is equivalent to natural exposure to a cumulative total of X_v entomologic inoculations; thus the function becomes

$$S_{2v}(i,t) = S_{imm} + \frac{(1 - S_{imm})}{1 + \left(\frac{X_v + X_p(i,t)}{X_p^*}\right)^{\gamma_p}}$$

We consider briefly the consequences of model A, and conclude that this cannot be distinguished from model B below on the basis of the Manhiça trial data alone.

Model B. Vaccination results in reduction in the probability that an inoculum survives by a proportion that we term the underlying vaccine efficacy in preventing infections, $VE_0(i)$, i.e.

$$S_{2v}(i,t) = S_2(i,t)\,(1 - VE_0(i))$$

To allow for possible variation in efficacy between individuals, i.e. the extent to which the vaccine is leaky [Hudgens et al., 2004], we randomly assign values of $VE_0(i)$ drawn from beta-distributions. We define the underlying overall efficacy, $\overline{VE}_0$, as the mean of $VE_0(i)$ (Figure 4.2). A model with a very low value of the parameter b of the beta distribution corresponds to an all-or-nothing vaccine (i.e. one that offers complete protection to a proportion $\bar{E}_0$ of the vaccinated population ($E_0(i) = 1$ for all i in the protected group), and no protection at all to the others ($E_0(i) = 0$), while a high value of b corresponds to a leaky vaccine.

In both models, we assume that the vaccine efficacy remained constant throughout the surveillance period of the trial. In the main simulations patent parasitemia is assumed to arise at the earliest after a latent period of 15 days (three five-day time units within the simulation).

Fitting of vaccine efficacy to trial results. The original analyses of the trial [Alonso et al., 2004] used proportional hazard survival models to obtain empirical estimates, $\widehat{VE}_p$ and $\widehat{VE}_c$ of the overall vaccine efficacy in preventing infections, VE_p, and in preventing clinical attacks, VE_c, respectively. The efficacy in preventing severe malaria was estimated as:

$$\widehat{VE}_s = 1 - \frac{P_{sv}}{P_{sc}},$$

where P_{sv} is the proportion of children experiencing severe malaria episodes in the vaccine arm and P_{sc} is the corresponding proportion in the control arm.

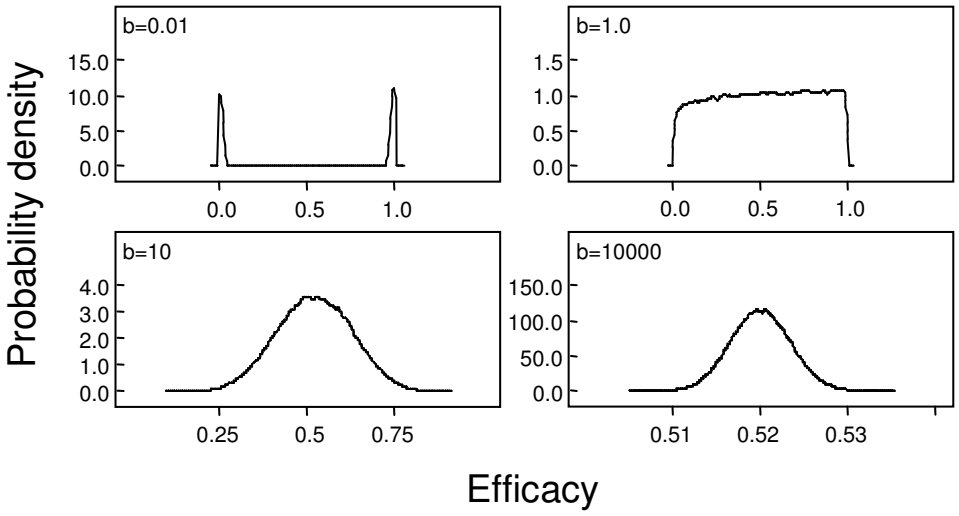

Figure 4.2: Distributions used for simulating the underlying efficacy, $VE_0(i)$.
$VE_0(i) \sim beta(a, b)$, where a and b are two shape parameters, the mean efficacy $\overline{VE_0} = 0.52$ and $a = \frac{b\ \overline{VE_0}}{1-\overline{VE_0}}$

We use the same statistical methods to compute corresponding estimates $\widetilde{VE}_p$, $\widetilde{VE}_c$, $\widetilde{VE}_s$ from our simulated datasets. To determine the best fitting distribution for $VE_0(i)$ we carried out a search using simulations with different efficacy until $\widetilde{VE}_p = \widehat{VE}_p$. Since the immune status of each simulated child is known at each time point, we extract summaries of immune status variables to provide explanations of the patterns observed for the efficacy variables.

4.3 Results

The EIR estimate of 38 inoculations per person per year was higher than that measured in the same area in 1997-1998 [Aranda et al., 2005]. Most of the six-month surveillance period in the Mozambique trial fell during the rainy season, with the peak of malaria transmission during the first half of the surveillance (Figure 4.3). This was reflected in the shape of both observed and predicted infection curves, both of which indicated a very high initial rate of infection, with a tendency to decrease over time. Using this pattern of EIR, we observed that the predicted incidence of infection for the control cohort II was a little lower than that observed in the trial (Figure 4.4a). This discrepancy between the observed and predicted incidence was to be expected because of the higher transmission suspected in the

Ilha Josina zone when compared with Manhiça.

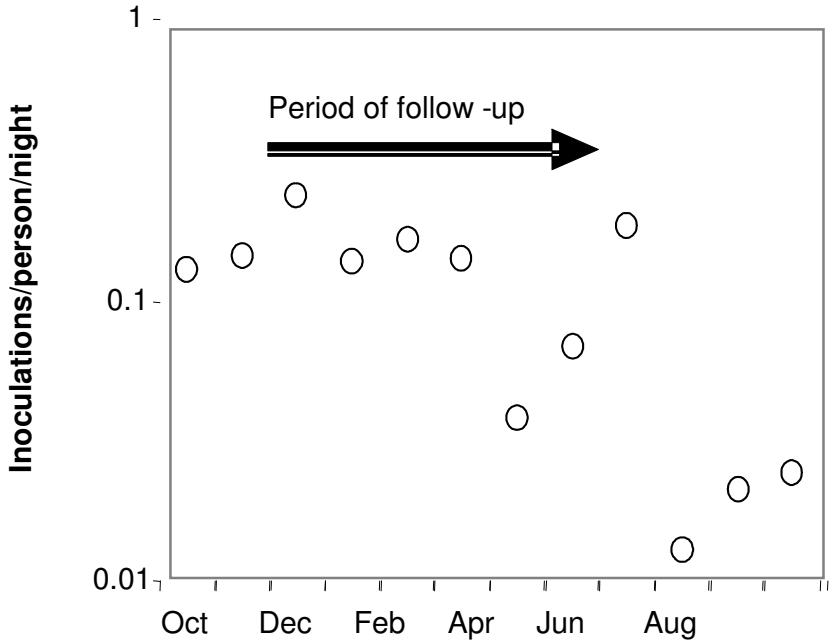

Figure 4.3: Seasonal pattern of the entomologic inoculation rate in Manhiça, Mozambique.

In the control arm of cohort I, the model predicted an overall incidence of malaria fevers that was much higher than the number actually treated during the trial. This is because the simulation, based on a model [Smith et al., 2006c] fitted to intensive surveillance data from Senegal [Rogier and Trape, 1995, Trape and Rogier, 1996] includes minor fevers that would not lead to treatment seeking and would elude detection in all but very active case detection. We assumed these fevers to be treated with a uniform probability and adjusted this probability until the incidence of treatment matched that of 0.5 episodes per child-year recorded in the trial. This was achieved by treating only 5% of the simulated fevers, and corresponded to an overall incidence of 4.2 episodes per child per year. This gave a similar time course of incidence of treated clinical episodes in the simulation to that observed in the trial (Figure 4.4b).

To simulate vaccination, we first considered which version of the model should be used for the action of the vaccine. All versions of our model predict that the effects of naturally acquired pre-erythrocytic immunity are negligible in pediatric populations, except in areas that are very highly endemic for malaria (Smith and others [2006b], Figure 4.1). The Mozambique trial [Alonso et al., 2004] consequently provides us with no information with

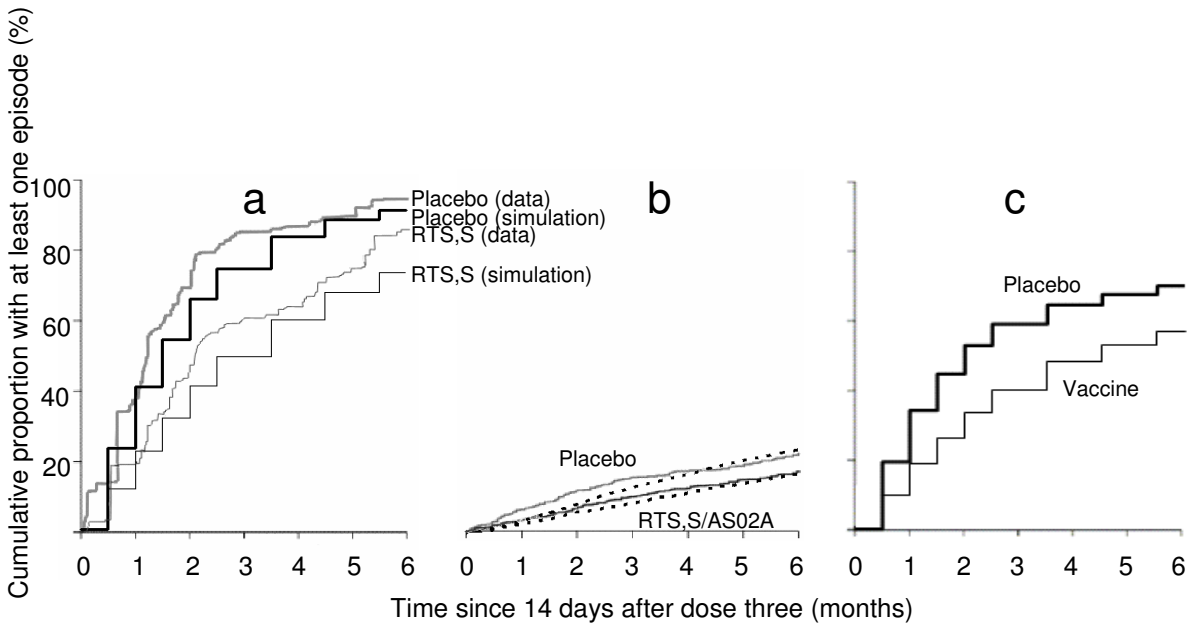

Figure 4.4: Kaplan-Meier survival analysis of time to first events. a) Incidence of first patent infection: the step functions correspond to the results of the simulations, which did not consider the effects of infected children reporting to the health facility between the pre-set survey times. b) Incidence of recorded first clinical episodes (dotted lines indicate simulation). c) Incidence first patent infection in a cohort of adults (simulation only).

which to decide between the two models A or B because the predictions for children are the same, whether the vaccine boosts naturally acquired immunity or acts independently of it. Whatever value we choose to simulate for X_v in model A, we can find a corresponding value for $\overline{VE}_0$ that would enable model B to match the predictions of model A in children. For instance, X_v=1,800 inoculations in model A has almost exactly the same impact as $\overline{VE}_0 = 0.52$ in model B (Figure 4.1).

However, in older people with substantial exposure a vaccine operating by boosting the effect of natural exposure (model A) would have little or no effect (Figure 4.1), because the immune response is already saturated. This has the consequence that development of a malaria vaccine operating as described in model A would very likely be stopped before it was tested in children.

Model B implies that the underlying efficacy is age-independent. Since the RTS,S/AS02A vaccine has already shown efficacy in a group of 250 adult men in The Gambia [Bojang et al., 2001], we argue that model A is a less plausible description of RTS,S/AS02A activity than is model B.

Using model B, a value of $\overline{VE}_0 = 0.52$ was needed to give $\widetilde{VE}_p$=$\widehat{VE}_p$=0.45 (Figure 4.4). When the vaccine arm of cohort II was simulated using this efficacy, the predicted incidence fell just below that observed in the trial vaccine arm. The fit was insensitive to the value of the parameter b of the beta distribution for $VE_0(i)$, providing this was not very low (Figure 4.5). A model with a very low value of b, corresponding to an all-or-nothing vaccine, cannot predict the observed incidence curves because it imposes an upper limit of 1-$\overline{VE}_0$ on the proportion of vaccinees who can become infected. In the trial cohort almost all the vaccinees eventually became infected. We consider it very unlikely that $VE_0(i)$ is constant and therefore adopted an intermediate value of b= 10 for all subsequent simulations.

Using the same model with $\overline{VE}_0 = 0.52$ and b=10, the simulation of cohort I gave an estimated efficacy of 33% against clinical episodes of malaria, which is very similar to the value recorded in the trial, 30% (Table 4.1). The simulated clinical episodes occurred rather uniformly in time during the surveillance period, again mimicking the data of the trial.

Our model was less successful in matching the trial results for severe malaria, predicting an admission rate for severe malaria of 33 per 1,000 child-years in the control arm, compared

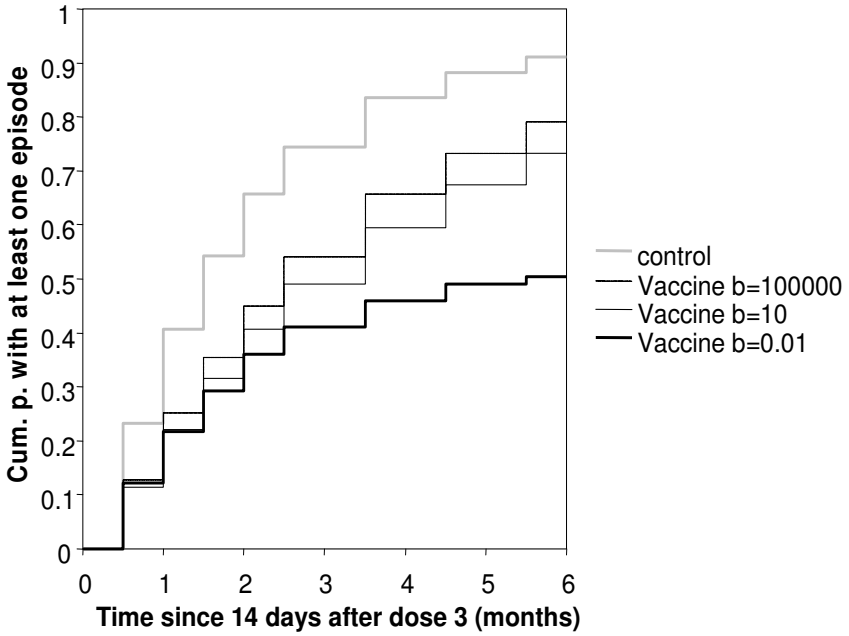

Figure 4.5: Simulated Kaplan-Meier survival analysis of time to first infection for different distributions. The curves for vaccination correspond to different distributions for $VE_0(i)$ (see Figure 4.2). In each case $\overline{VE}_0 = 0.52$.

with the actual admission rate of 70 per 1,000 child-years. We therefore conjecture that almost all severe cases were identified, rather than only approximately half as initially assumed based on previous literature reviews [Goodman et al., 2000]. Such exceptionally high coverage, presumably resulting from increased awareness due to the trial, could also explain why mortality rates in the trial cohorts were very low [Alonso et al., 2004]. As in the trial, predicted efficacy in preventing severe malaria was higher than that for prevention of any clinical episode, but was not as high as the actual value of $\widehat{VE}_s$ (although this estimate was imprecise) (Table 4.1).

We examined the reasons for these variations in efficacy in the simulations. In the model, the lower efficacy against clinical malaria episodes than against incidence of first *P. falciparum* infection was a consequence of a higher simulated pyrogenic threshold in the placebo group (geometric means of 1,617 parasites / μL compared with 1,243 parasites / μL in the vaccine group in a large simulation). Within our model, the pyrogenic threshold responds dynamically to *P. falciparum*, decreasing when individuals are not infected [Smith et al., 2006c]. This led to a small increase in the risk that an infection translated into a clinical attack in vaccinees whose exposure was reduced. The higher efficacy against severe malaria

than against uncomplicated episodes was most obvious in the youngest children in whom there was the least naturally acquired immunity. We used the estimate of $\overline{VE}_0 = 0.52$ to simulate a trial in a cohort of adults and compared the results to those of the Gambian trial [Bojang et al., 2001] in which protection could only be demonstrated for a short period (Figure 4.4c). This simulation gave very similar estimates of both $\widetilde{VE}_p$ and $\widetilde{VE}_c$ to those observed for RTS,S/AS02A among adult men in The Gambia (Table 4.2).

Table 4.2: Efficacy estimates for adults

Outcome	The Gambia trial†		Simulation*	
Prevention of infection	$\widehat{VE}_p$	0.34 (0.08, 0.53)	$\widetilde{VE}_p$	0.33 (0.29,0.37)
Prevention of clinical episodes	$\widehat{VE}_c$	0.31 (-0.07,0.56)	$\widetilde{VE}_c$	0.27 (-0.05,0.49)

*Simulation and monitoring based on the Manhiça pattern of transmission and using the same health system and surveillance patterns as for the simulation of the Manhiça trial; adults 21-24 years of age. Predictions based on 5,400 individuals per cohort. Values in parentheses are 95% confidence intervals.
†[Bojang et al., 2001]

The simulation of adults using the Manhiça pattern of the EIR as input, and the infection incidence curves (Figure 4.4c) were a somewhat different shape to those observed in the Gambian trial, reflecting the different durations and intensity of the transmission seasons in the two sites. However, as in the Gambian data, the simulated curves for vaccine and control groups diverged initially, but seemed to indicate little or no efficacy in the second half of the surveillance period. As in the actual Gambian trial, a large proportion of both control and vaccine groups failed to show infections at the simulated cross-sectional surveys.

4.4 Discussion

Simulation of the outcomes of malaria vaccine trials can help in the design of future trials by indicating which vaccine effects are likely to be measurable with relative ease and at what level of accuracy. It offers a means of deciding which outcomes are important, and also provides insights into vaccine action by indicating which results require further interpretation, and which can be explained by aspects of malaria biology included in the simulations. Such models can be used to predict population effects of a malaria vaccine, taking into account factors such as stage specificity, duration of effectiveness, effect of

natural immunologic boosting, proportion of the population vaccinated, and prevailing entomologic conditions [Halloran et al., 1992]. In addition, models have a role in assessment and quantification of the impact of an efficacious malaria vaccine on public health and on the social and economic development of endemic areas [McKenzie and Samba, 2004].

An important issue for the design of pre-erythrocytic vaccines is whether delays in patency are of consequence even when the host eventually has a blood stage infection. Analyses of malariatherapy data indicate that the infecting dose has little or no impact on the severity of a *P. falciparum* infection [Glynn and Bradley, 1995], but in many infectious diseases the duration of latent periods are of importance for transmission dynamics.

RTS,S/AS02A must reduce the number of infected hepatocytes by a much higher percentage than its efficacy in blocking infections because even a single infected hepatocyte is sufficient to cause a blood stage infection. In RTS,S/AS02A vaccinees given an artificial challenge, many infections that are not blocked completely take a few days longer to become patent than do infections in unvaccinated individuals [Kester et al., 2001] suggesting that they arise from a reduced number of infected hepatocytes. Our simulation of the effect of a five-day extension of the latent period in the vaccine group shows that such delays had a negligible impact on the results of the Mozambique field trial. It follows that an adequate simulation of this trial can be achieved by assuming that vaccination completely blocks a certain fraction, $\overline{VE}_0$, of infections that would otherwise reach the erythrocytic stages, and that no additional terms need to be added to the model to allow for the reduced infectious load in those infections that survive.

We propose that the different efficacy estimates against the different outcomes and in the two field trials carried out thus far in The Gambia and in Mozambique can all be reconciled with the same underlying efficacy of about $\overline{VE}_0 = 0.52$. The extent of variation between individuals in this efficacy is unclear because RTS,S/AS02A protects very few individuals completely. Nearly all vaccine recipients will probably become infected if exposed to sufficient challenge.

To simulate the two efficacy estimates currently available for the randomized controlled trials done in adult men in The Gambia (34%) [Bojang et al., 2001] and children in Mozambique (45%) [Alonso et al., 2004], our model needed to assume a somewhat higher vaccine efficacy (of 52%) for extending time to first *P. falciparum* infection. In the model this difference is an effect of naturally acquired blood-stage immunity. This introduces to both arms of the trial heterogeneity in the probability that an infection will be patent at the

time of a cross-sectional survey, and consequently [Halloran et al., 1996] leads to a small downward bias in $\widehat{VE}_p$. This bias is greater in adults than in children and can thus explain the higher efficacy observed in Mozambique than in the Gambian trial. Similarly, the severe episodes generally occur in the youngest children, who have less acquired blood stage immunity, and this explains the higher efficacy against severe episodes than uncomplicated ones.

The simulations also suggest that the difference observed between $\widehat{VE}_p$ and $\widehat{VE}_c$ are to be accounted for mainly by simulated episodes of clinical malaria occurring at lower parasite densities in the vaccine cohort. This follows from the lower incidence of infection dynamics of our model for clinical episodes [Smith et al., 2006c].

This match between the trial and our predictions both supports the use of the model and demonstrates that the shapes of the incidence curves over time (Figure 4.4) can be explained in the context of our model by the pattern of surveys and the seasonality of the entomologic input. All models agree that the measured efficacy in preventing infections at the start of the follow-up should be equal to $\overline{VE}_0$. We obtained an excellent fit to the time course of efficacy during the trial with a version of our model that assumed no true decay in protection, although the field estimates of efficacy decreased. We conclude that there was no evidence for any decay in underlying efficacy over the six-month surveillance period in the Mozambique trial. Had there been any substantial decay in efficacy, this would have led to a steeper decrease over time in the efficacy measurable in the field. Our simulation of a cohort of semi-immune adult men indicates that the apparently short-term duration of protection in The Gambia could also have arisen as a result of the pattern of seasonality of the inoculations, together with the effects of naturally acquired immunity.

Within the simulations there are no selection biases in the comparison between control and vaccine. This is because we allocate vaccine efficacy, $VE_0(i)$, to individuals independently of their age, previous history of exposure, or of the parameter quantifying individual variation in the ability to control blood-stage parasites.

The close match of the model with the data therefore suggests that the interplay of vaccine-induced and naturally acquired immunity are the main causes of the variations in efficacy between the different outcomes and trials, and that neither selection biases nor random variation need be invoked to account for the differences. The simulation supports the use of our epidemiologic model to make predictions of the potential impact of introducing malaria vaccines into public health programs, but information about the duration of protection will

be important in reducing the uncertainty in these predictions. Longer-term follow-up of trial participants is needed to evaluate the duration of protection. This information can be integrated into the models to simulate the public health and economic implications of malaria vaccine programs implemented together with other control strategies.

Chapter 5

Predictions of the epidemiologic impact of introducing a pre-erythrocytic vaccine into the Expanded Program on Immunization in sub-Saharan Africa

Nicolas Maire, Fabrizio Tediosi, Amanda Ross, Thomas Smith
Swiss Tropical Institute, Basel, Switzerland

This article has been published:
American Journal of Tropical Medicine and Hygiene 2006, 75, Suppl 2, 111-118

Abstract

We predict the effects of introduction of a pre-erythrocytic vaccine against *Plasmodium falciparum* into a malaria-endemic population in Africa. We use a stochastic simulation model that includes components of transmission, parasitology, and clinical epidemiology of malaria and was validated using the results of field trials of the RTS,S/AS02A vaccine. The results suggest that vaccines with efficacy similar to that of RTS,S/AS02A have a substantial impact on malaria morbidity and mortality during the first decade after their introduction, but have negligible effects on malaria transmission at levels of endemicity typical for sub-Saharan Africa. The main benefits result from prevention of morbidity and mortality in the first years of life. Vaccines with very short half-life or low efficacy may have little overall effect on incidence of severe malaria. A similar approach can be used to make predictions for other strategies for deployment of the vaccine and to other types of malaria vaccines and interventions.

5.1 Introduction

The development of a safe and effective vaccine against *Plasmodium falciparum* is recognized as one of the major unmet medical needs in non-industrialized countries [Ballou et al., 2004, World Health Organization, 1996]. As a result of recent funding initiatives, various candidate vaccines targeting different stages of the parasite are in pre-clinical and clinical development [Ballou et al., 2004]. The most advanced vaccine development program is currently that of the pre-erythrocytic vaccine, RTS,S/AS02A, which recently demonstrated an efficacy of 45% in preventing *P. falciparum* infection in children in Mozambique [Alonso et al., 2004].

Partially protective vaccines have complex effects on the dynamic interactions between the host and an infectious agent [Halloran et al., 1994]. It is generally acknowledged that a malaria vaccine is unlikely to be 100% effective and the effects of imperfectly protective malaria vaccines may be particularly complex. To make predictions of the likely public health impact of a range of malaria vaccines, we have developed a stochastic simulation model of the epidemiology of *P. falciparum* in endemic areas [Smith et al., 2006a]. We have now used this model to simulate the likely health impact of introducing the RTS,S/AS02A into malaria-endemic populations via the Expanded Program on Immunization (EPI). The model considers both the short- and long term effects of a vaccination program

on the burden of disease, allowing for the temporal dynamics of effects on immunity and transmission.

5.2 Materials and Methods

Epidemiologic model. The epidemiologic model is a stochastic individual-based simulation of *P. falciparum* malaria in endemic settings that uses a five-day time step with the pattern of transmission as the input. For every individual in the simulated population, each discrete *P. falciparum* infection is characterized by simulated duration, parasite densities (Chapter 2), infectivity [Ross et al., 2006a] and anemia risk [Carneiro et al., 2006]. At each time point, clinical episodes of malaria or malaria attributable mortality may occur with probabilities depending on the simulated parasite density and recent exposure [Ross et al., 2006b, Ross and Smith, 2006, Smith et al., 2006c]. For the present analyses we simulate populations of 100,000 individuals, with an approximately stationary age distribution matching that of the demographic surveillance site in Ifakara, southeastern Tanzania, 1997-1999 [INDEPTH Network, 2002].

We run the model under a series of assumed transmission patterns (Table 5.1). Each simulation assumes a recurring annual pattern of the vectorial capacity. The simulated population has been subjected to this pattern for a lifetime at the start of the vaccination program to ensure that the level of acquired immunity is correct for all ages. We then consider the transient behavior of the model during a follow-up period of 20 years. We simulate case-management and the effects on malaria transmission using a reference scenario as described in an accompanying paper (Chapter 3). This reflects a typical rural setting in Tanzania with mesoendemic malaria transmission.

Reference vaccine scenario. The simulated vaccine is a pre-erythrocytic vaccine that protects vaccinated individual by reducing the force of infection. Relevant characteristics of the simulated vaccine were chosen to match the data from a phase 2b clinical trial in children 1-4 years of age in Mozambique [Alonso et al., 2004]. We have simulated the action of the vaccine in this trial and fitted the efficacy to the trial data (Chapter 4). These simulations suggested that pre-existing semi-immunity leads to a slight underestimation of the underlying efficacy of the vaccine in such a trial. After this, we therefore assume that the vaccine provides an initial reduction in the force of infection of 52% corresponding to

Table 5.1: Variables that vary between scenarios*

Variable	Description	Levels
Coverage	Proportion of eligible individuals who receive all 3 vaccine doses. (coverage with 1^{st} 2^{nd} and 3^{rd} dose).	50% (70%, 85%,85%) **89% (95%, 95%, 99%)** 100% (100%, 100%, 100%)
Initial efficacy of the vaccine	Efficacy in fully vaccinated individuals immediately after 3^{rd} dose. Numbers in brackets show efficacy after 1^{st} and 2^{nd} dose.	0.3 (0.2, 0.25) **0.52 (0.4, 0.46)** 0.8 (0.6,0.7) 1.0 (1.0, 1.0)
Decay of the efficacy of the vaccine	Time after vaccination at which the vaccine efficacy is 50% of initial value, assuming exponential decay of protection.	6 months 1 year 2 years 5 years **10 years** No decay
Variation in vaccine efficacy between hosts (Chapter 4)	b is the parameter of the beta distribution used to describe inter-host variation	All or nothing (b=0.01) **Intermediate(b=10)** Homogeneity(b=100000)
Intensity of transmission	Infectious bites per annum prior to the introduction of the vaccine	High Transmission: 82 **Reference : 21** Low Transmission: 5.1
Seasonality	Source of data for seasonal distribution of inoculations	**Namawala, Tanzania** [Smith et al., 1993], No seasonality

*Each level of each variable defines a scenario that was compared with the reference. In each scenario, the variables not being evaluated were fixed at the reference levels (indicated in **bold**).

the 45% efficacy in extending time to first infection after three doses. There are no data available on the efficacy after one or two doses of RTS,S/AS02A. We assume a reduction in the force of infection of 40% and 46% after the first and the second dose. The Manhiça trial did not demonstrate any decay of the efficacy against infection. However, decay in protection is possible when longer time periods are considered and is likely to have important implications for vaccine effectiveness. We assume an exponential decay of the primary efficacy of the vaccine and set the half-life to 10 years for the reference vaccine.

We expect that the protection provided by the vaccine is not homogenously distributed among the vaccinated individuals. We assign initial values for the efficacy of the vaccine that are drawn from a beta distribution with parameter $b = 10$ (a justification is given in an accompanying paper (Chapter 4).

Simulation approach. We simulate the introduction of vaccination at the target ages of one, two and three months in a random sample of infants. A total of 95% of the infants receiving the first dose, 95% of those receiving the second dose, and 99% of those receiving the first two doses complete the course of vaccination. We assume all vaccines to be delivered at the target age, and that no infant received dose 2 without receiving dose 1, or dose 3 without receiving dose 2. This results in a cohort effect because the proportion of the population who have received the full vaccination course gradually increases throughout the 20 year follow-up (Figure 5.1). Since by the end of this period vaccination coverage in older age groups is still zero, we do not consider the equilibrium that would eventually be reached if vaccination continued indefinitely.

The introduction of vaccination leads to transient behavior that may in principle modify the level of *P. falciparum* transmission. We consider the effects after periods of 5, 10, and 20 years after initiation of the vaccination program. We plot the cumulative numbers of events averted. Where the cumulative number of episodes averted increases approximately linearly over time, (indicating constant effectiveness), we compute the effectiveness of vaccination over the whole 20 year follow-up as

$$E_{cumul} = 1 - \frac{\text{Cumulative number of events in vaccine scenario}}{\text{Cumulative number of events in comparison scenario}}$$

where the comparison scenario is identical to the vaccination scenario in all respects other than the inclusion of vaccination. In addition, we present age-prevalence of parasitemia

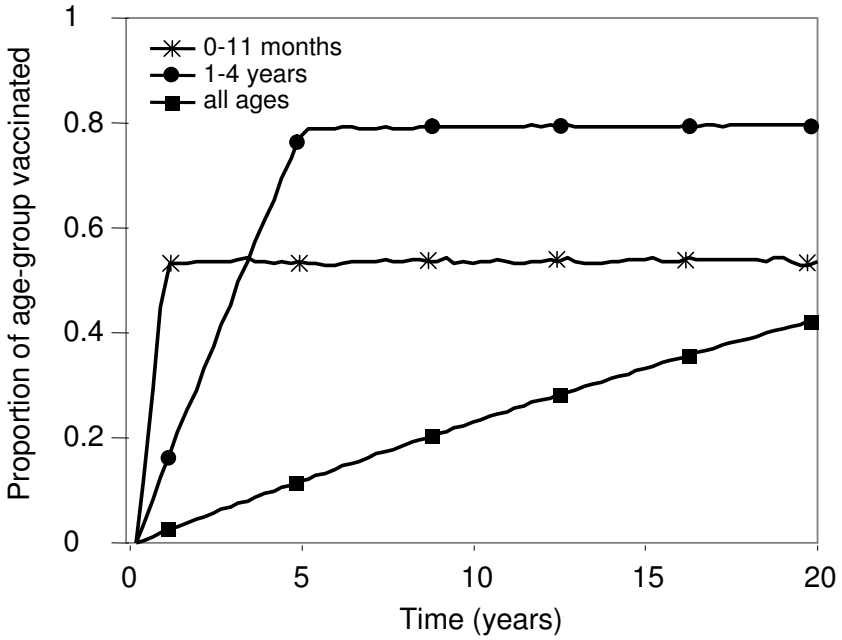

Figure 5.1: Proportion of the age-group that received three doses of vaccination by age and time since start of program.

and anemia as well as age-incidence of different clinical outcomes averaged over one year of simulated follow-up starting 4, 9, and 19 years into the follow-up period.

Effects of vaccine characteristics. We expect the predictions about the effectiveness of the vaccine to depend on assumptions about the key properties of the vaccine. In addition, effectiveness depends on the proportion of the population that has been vaccinated. Effectiveness may be an accelerating function of coverage if vaccination has a community effect through reduction of the infectivity of the human hosts. We therefore modeled a range of different assumptions about the proportion of infections that are prevented after an individual has received one, two, or three doses of the vaccine, the rate of decay of protection against infection, and the variation in efficacy between individuals. To keep the number of simulated scenarios manageable we start from the reference scenario described above and vary one assumption at a time (Table 5.1).

Effects of transmission intensity and seasonality. In addition to the reference scenario we also generate simulation results corresponding to a range of transmission intensities. There are characteristic shifts in the ages distributions of clinical events in *P.*

falciparum at different transmission intensities [Ross et al., 2006b, Smith et al., 2006c] and we wanted to explore how these would modify vaccine effectiveness. Starting from the reference scenario described above, we explore the effect of increasing or decreasing the annual entomologic inoculation rate (EIR) prior to the introduction of the vaccine within a range found in areas of stable endemic malaria. In addition, we study the impact of different seasonal patterns of EIR by simulating the case of a completely non-seasonal environment with the same yearly average EIR as in the reference scenario.

5.3 Results

Reference vaccination scenario. In the reference vaccination scenario the introduction of vaccine leads to lower parasite prevalence for all age groups that had received the vaccine, resulting in a cohort effect with the effect gradually moving into older age groups (Figure 5.2a). Corresponding to the reduction in parasite prevalence, anemia prevalence is also reduced but because the anemia is concentrated in the first few years of life [Carneiro et al., 2006], anemia prevalence becomes stable within the first few years of vaccination (Figure 5.2b).

The incidence of malaria episodes and mortality decrease for children less than five years of age within the first few years of vaccination and remain reduced over the 20-year time span (Figure 5.3). These dynamic effects resulted almost entirely from the cohort effect of introducing vaccination gradually into the population and hardly at all from community effects due to reduction in transmission. The level of transmission was reduced only very slightly in the vaccine scenario compared with the reference. None of the scenarios we studied resulted in major effects on transmission to the vector within the 20-year time span. After 10 years of vaccination, the incidence of uncomplicated episodes in 5-9-year-old children remains lower than in unvaccinated children, while severe episodes and mortality incidence have slightly increased in incidence in this age group (Figure 5.3). This is because the prevention of infections reduces the acquisition of asexual blood stage immunity. By the end of the 20-year follow-up period, all incidence measures are somewhat higher in the 10-19-year-old age group of the vaccinated population, although the cumulative number of events they have experienced over the whole 20-year period is reduced.

The approximately linear increase in cumulative numbers of deaths averted (Figure 5.4c) indicates that the vaccine reduces mortality by a more or less constant amount throughout

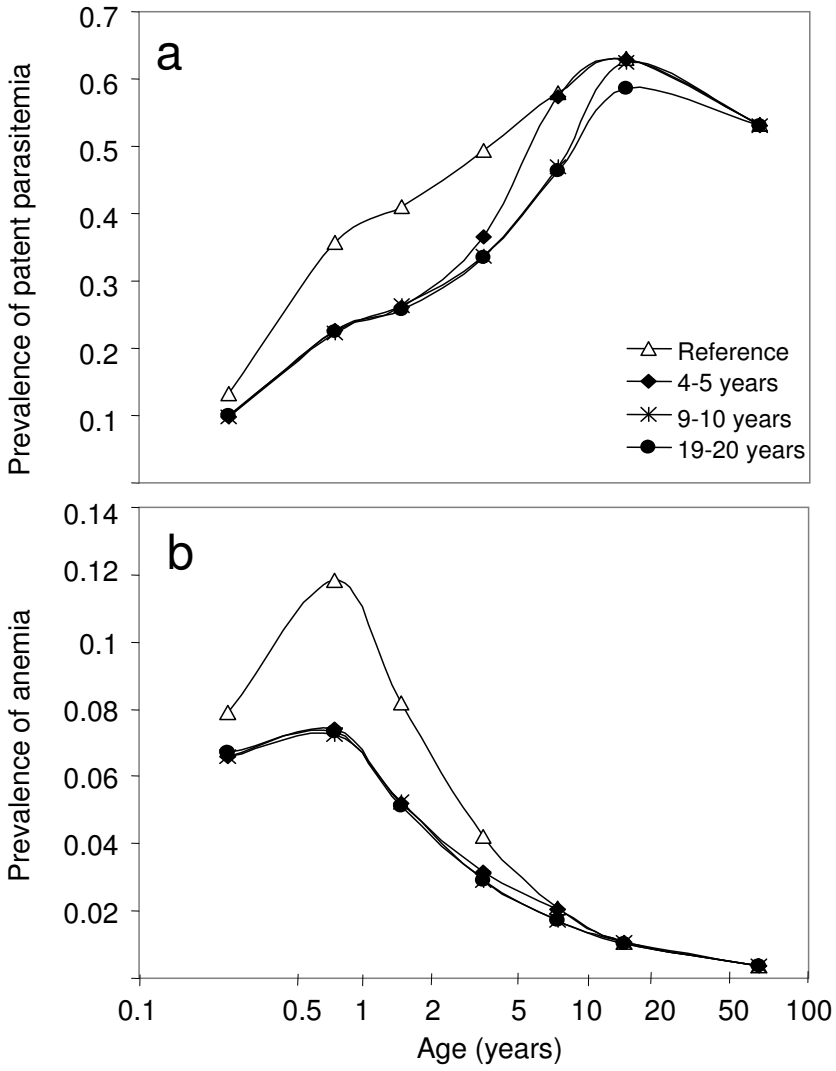

Figure 5.2: Effect of the reference vaccine on prevalence of parasitemia and anemia over time. a) Age-prevalence of parasitemia. b) Age-prevalence of anemia. The data are averaged over periods of one year starting at 4, 9, and 19 years after the onset of the intervention.

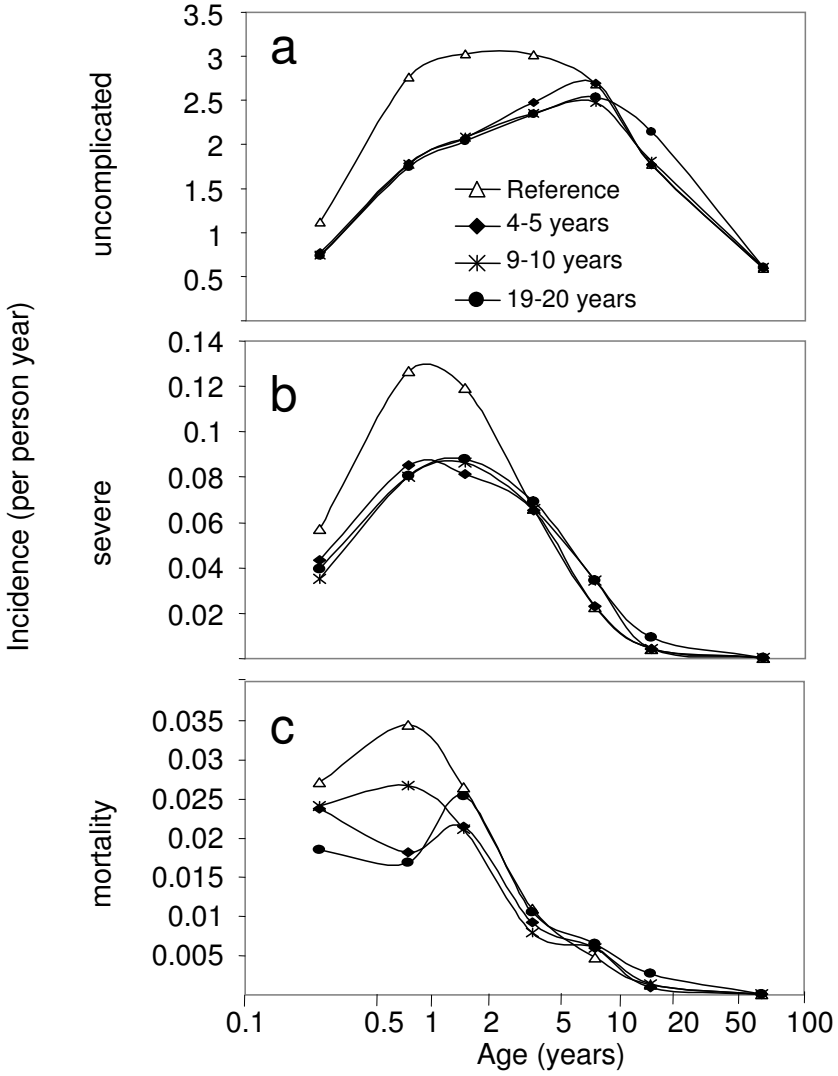

Figure 5.3: Effect of time since the start of the vaccination program on age-incidence patterns. The data are averaged over periods of one year starting at 4, 9, and 19 years after the onset of the intervention. a) Uncomplicated episodes b) Severe episodes. c) Mortality.

the 20-year intervention period. Overall, vaccination also leads to substantial reductions in the incidence of uncomplicated episodes of malaria over the 20-year follow-up (Figure 5.4) but the benefit of the vaccination program in preventing uncomplicated episodes decreases over time, as indicated by a reduction in the gradient of the curve over time (Figure 5.4a).

The decay in the benefit was even more marked when assessed in terms of numbers of severe episodes (Figure 5.4b). After 10 years of vaccination the overall incidence of severe episodes returns to a level similar to that in the absence of vaccination. This is due to the shift in incidence to older ages (Figure 5.3b).

The average effectiveness of the vaccine over the 20-year follow-up period differed for the different clinical outcomes. The average effectiveness in preventing uncomplicated episodes and death were 0.067, and 0.12, respectively (Figure 5.5). The overall effectiveness in preventing severe episodes of 0.052 is difficult to interpret because of the heterogeneity in the effect over time.

Effect of vaccine efficacy. We considered four different values for the initial efficacy of the vaccine (Table 5.1). An efficacy of 30% corresponds approximately to the lower limit that phase IIb clinical trials have so far been powered to detect. Vaccines with lower efficacy than this are unlikely to be considered for further development. An efficacy of 52% corresponds to our best estimate of the initial efficacy of the RTS,S/AS02A vaccine in a recent trial in Mozambique (Chapter 4, this is higher than the average efficacy measured during the trial [Alonso et al., 2004]). An efficacy of 80% corresponds to a rule of thumb often used to evaluate partially efficacious vaccines, while an efficacy of 100% corresponds to a perfect vaccine, and thus allows us to assess the maximum possible effect achievable by our model of vaccine delivery.

An increase in the vaccine efficacy (defined as the proportion of infections averted) results in a near-proportional increase in effectiveness over the whole 20-year follow-up, whether this is measured in terms of prevention of uncomplicated, severe, or fatal episodes (Figure 5.4 and Figure 5.5a). The cumulative number of events averted is highest for the most efficacious vaccine with effects on uncomplicated episodes and mortality approximately proportional to the initial efficacy, but only a vaccine with a very high efficacy remains effective in reducing the incidence of severe episodes in the latter part of the 20-year follow-up period (Figure 5.4). The effects of changes in efficacy on age-prevalence of parasitemia

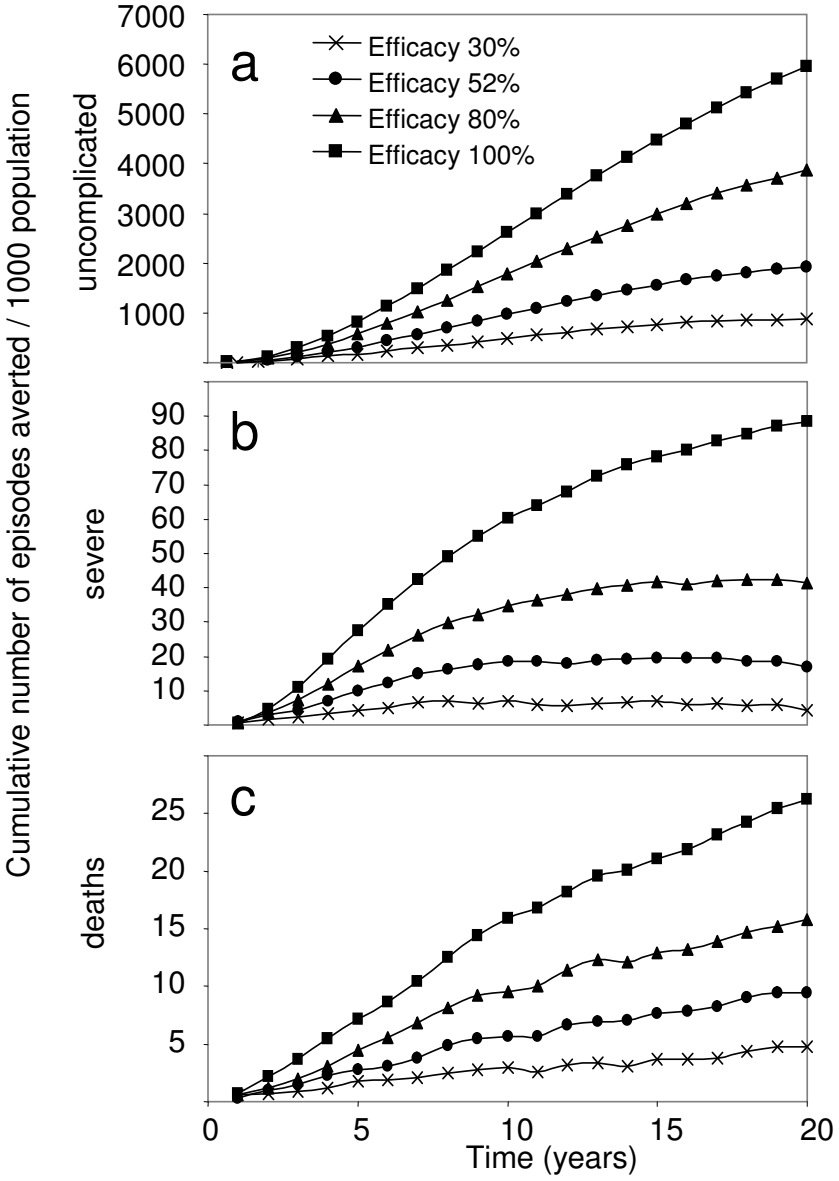

Figure 5.4: Effect of the reference vaccine over time under different assumptions about the initial efficacy of the vaccine (30%, 52%, 80%, and 100% protection against infection after third dose). a) Uncomplicated episodes averted. b) Severe episodes averted. c) Deaths averted.

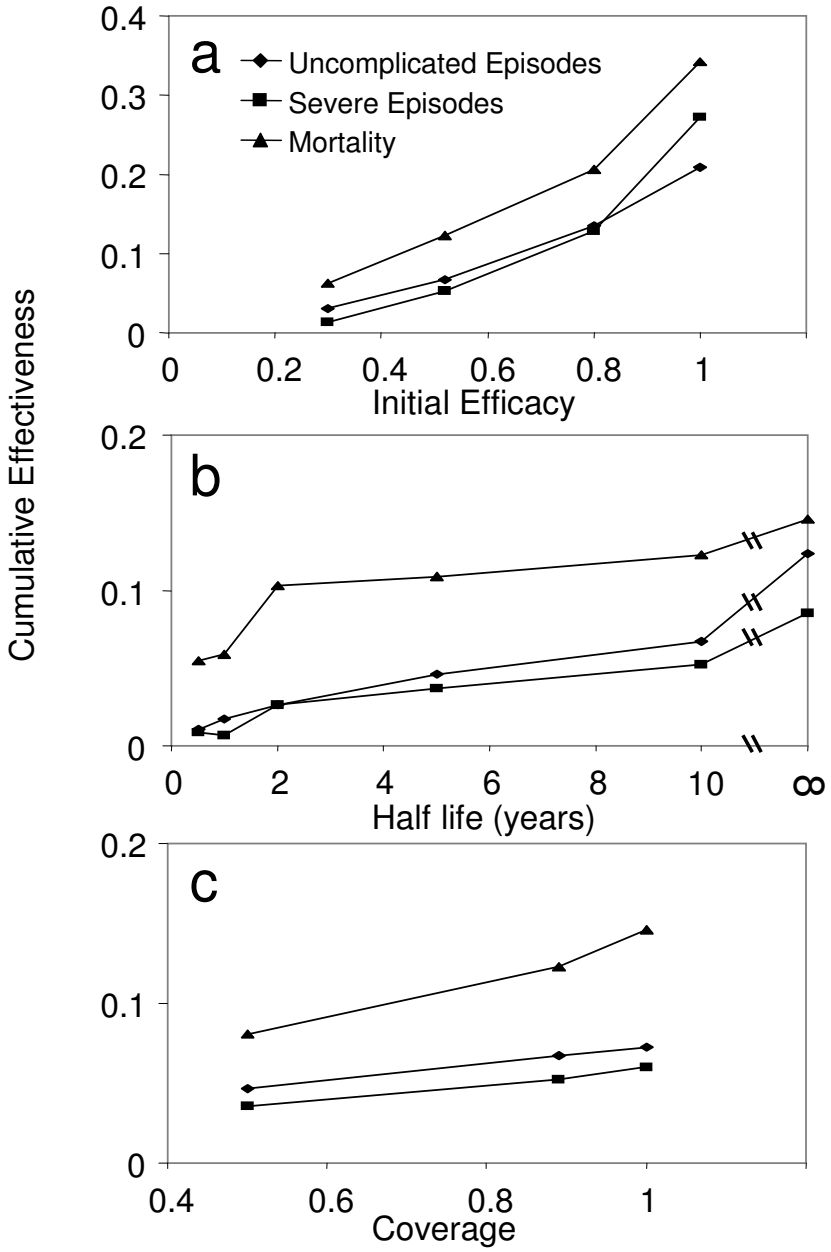

Figure 5.5: Cumulative effectiveness over 20 years against uncomplicated and severe episodes and mortality. a) Effect of different assumptions about the initial efficacy. b) Effect of different assumptions about the decay of the protective effect. c) Effect of different assumptions about the coverage of the vaccination program.

or anemia or in the age-incidence of clinical events in the low and high-efficacy scenarios are similar to those in the reference scenario.

Effects of waning of the protective effect of the vaccine. Assuming a faster decay of the vaccine effect leads to a reduction in all effectiveness measures, and the converse is observed when the rate of decay is decreased. The effectiveness against uncomplicated episodes is roughly proportional to the half-life (Figure 5.5b; Figure 5.6a). However, effectiveness for the other clinical outcomes does not increase linearly with half-life (Figure 5.5). An increase of the half-life from six months to one year has little effect on the effectiveness against severe episodes or mortality, but there is a marked increase in effectiveness if the half-life increases to two years (Figure 5.6bc). There is only a small further improvement in increasing half-life from 2 to 5 or 10 years.

Effect of vaccination coverage. The effect of varying the values of coverage is similar to the effect of varying the initial efficacy, with a low coverage resulting in similar epidemiologic patterns to that of a reduced vaccine efficacy. Although increasing coverage to high levels can be of crucial importance with fully protective vaccines when the objective is to eliminate transmission, the impact of 100% coverage is more or less proportional to that of the 89% coverage in our reference scenario (Figure 5.7).

Effect of variation in efficacy between individuals. An all-or-nothing response to the vaccine (b=0.01) results in a higher number of illness episodes and deaths averted than are found in a scenario with the same mean efficacy, but less variation between individuals. With such a vaccine, the population is equivalent to a mixture of individuals vaccinated with a 100% effective vaccine, together with unvaccinated individuals. As with the simulation of the 100% effective vaccine, however, the number of severe episodes averted decreases over time. This is due to the decay in the efficacy (simulated with a half-life of 10 years). If there is no decay in efficacy we expect the effectiveness of such a vaccine to increase with the coverage throughout the follow-up period.

When there is no heterogeneity in vaccine efficacy (b=100,000), (Figure 5.8), the pattern is very similar to that of the reference vaccine (b=10), in which the degree of heterogeneity was chosen to match the data of the RTS,S/AS02A vaccine trial in Mozambique (Chapter 4).

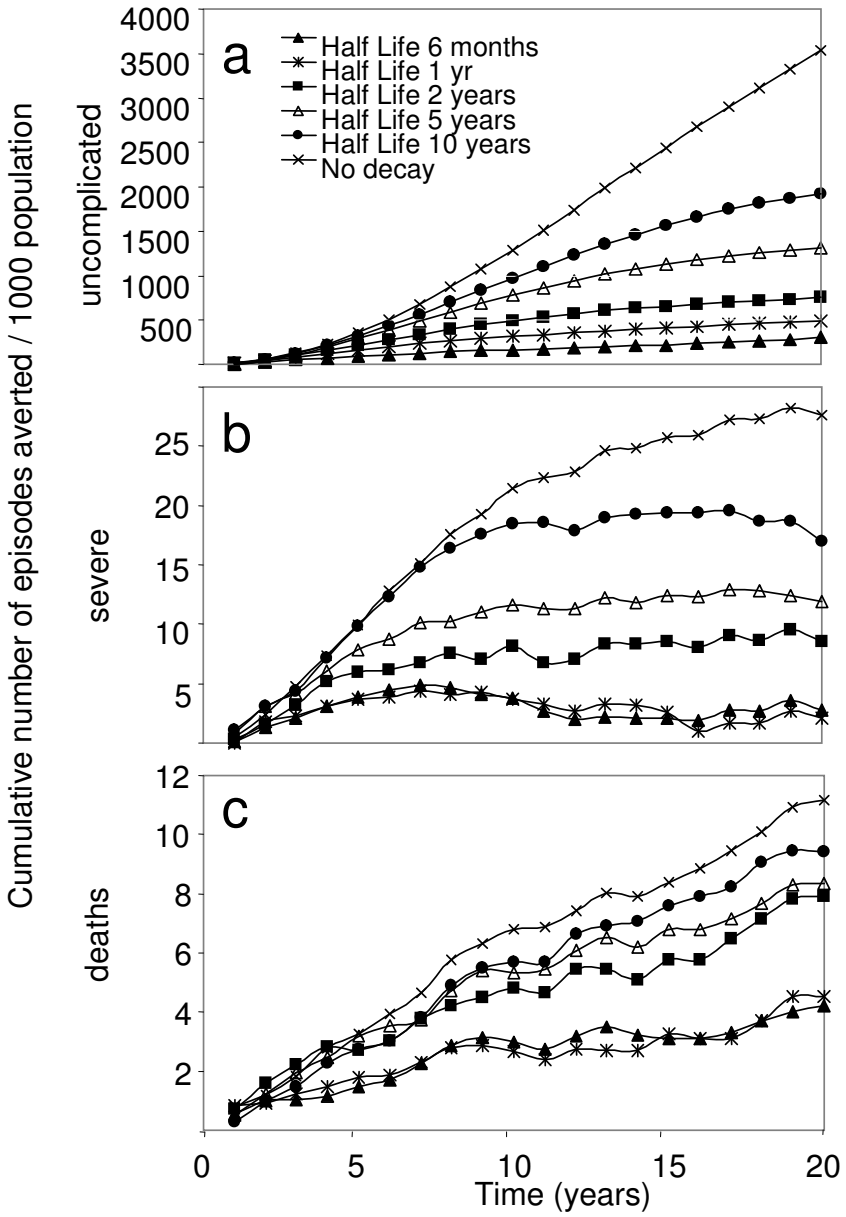

Figure 5.6: Effect of the reference vaccine over time under different assumptions about the decay of the protective effect of the vaccine (half-life = 6 months, 1 year, 2 years, 5 years, and no decay). a) Uncomplicated episodes averted. b) Severe episodes averted. c) Deaths averted.

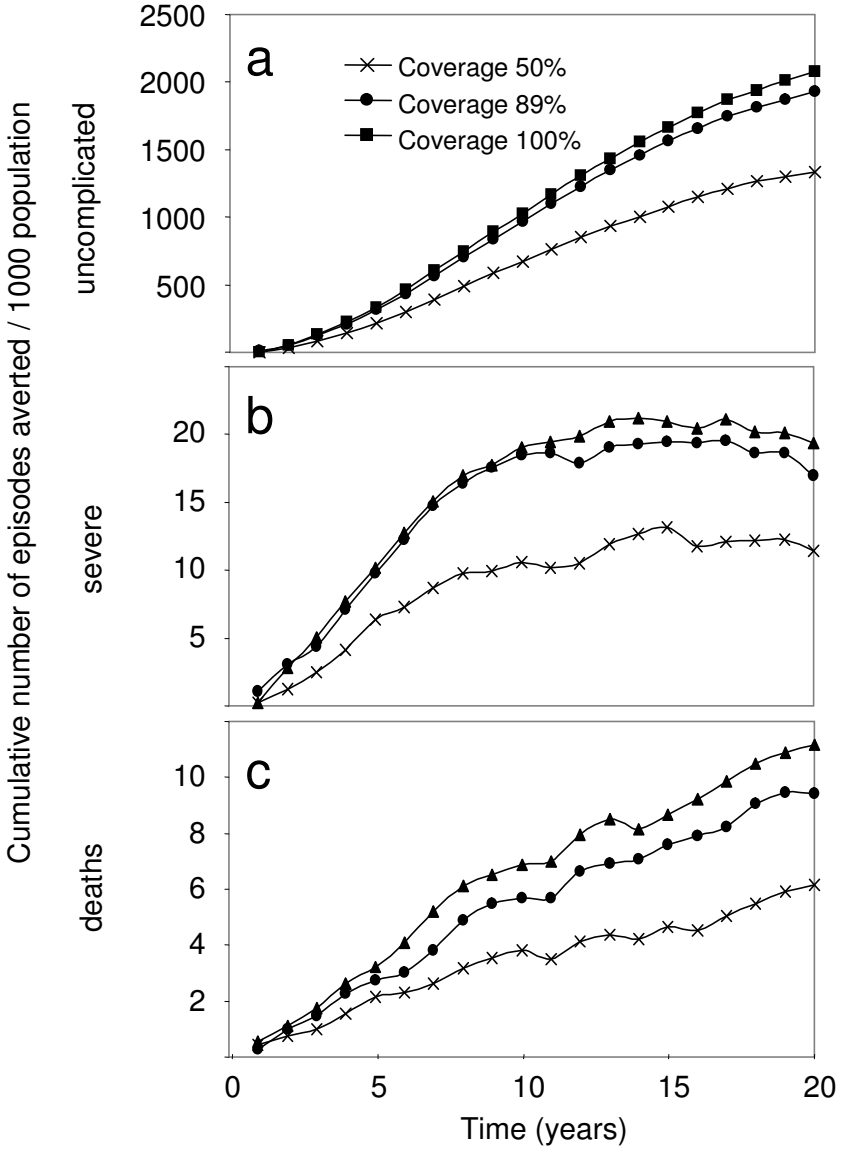

Figure 5.7: Effect of the reference vaccine over time under different assumptions about the proportion of the population covered (50%, 89%, and 100% received all three doses). a) Uncomplicated episodes averted. b) Severe episodes averted. c) Deaths averted.

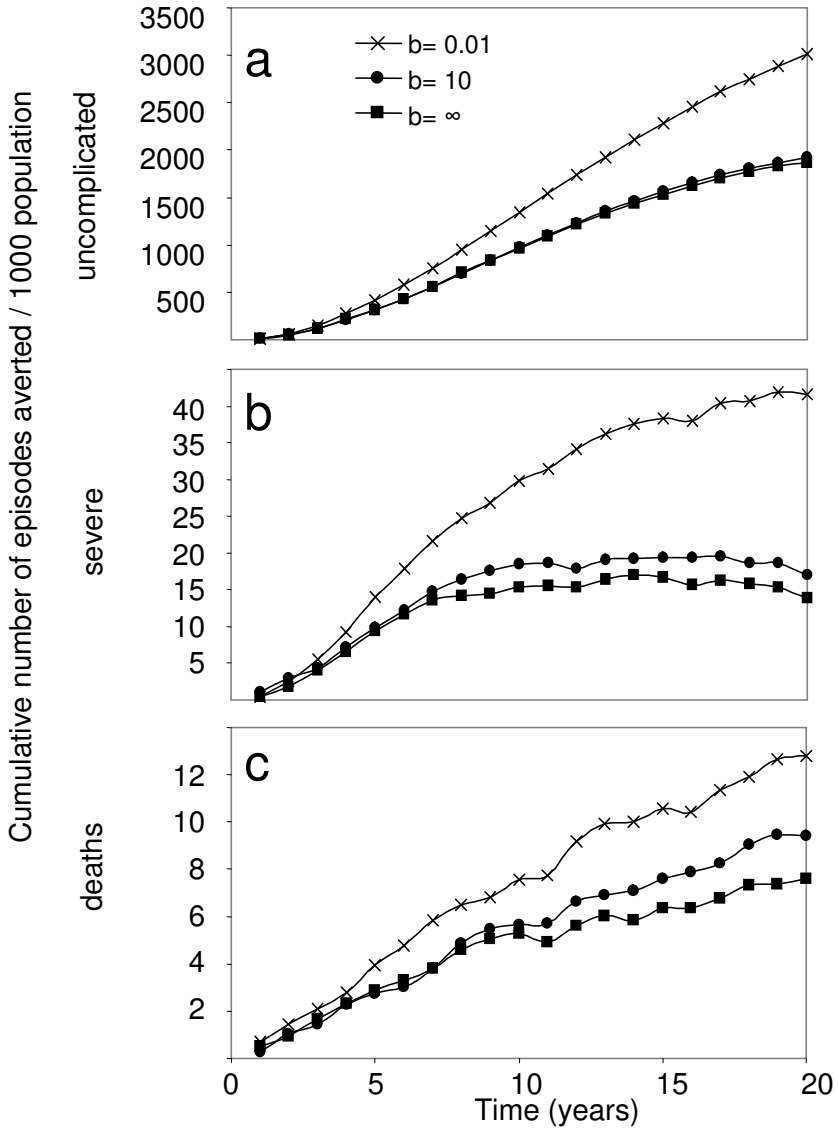

Figure 5.8: Effect of the reference vaccine over time under different assumptions about the distribution of the protective effect of the vaccine among vaccinated individuals (b = 0.01, b=10, b =100,000). a) Uncomplicated episodes averted. b) Severe episodes averted. c) Deaths averted.

Effect of transmission intensity and seasonality. The absolute number of clinical episodes and deaths averted by a vaccine is affected by the transmission intensity in ways that changed over the course of the simulated vaccination program (Figure 5.9). For the

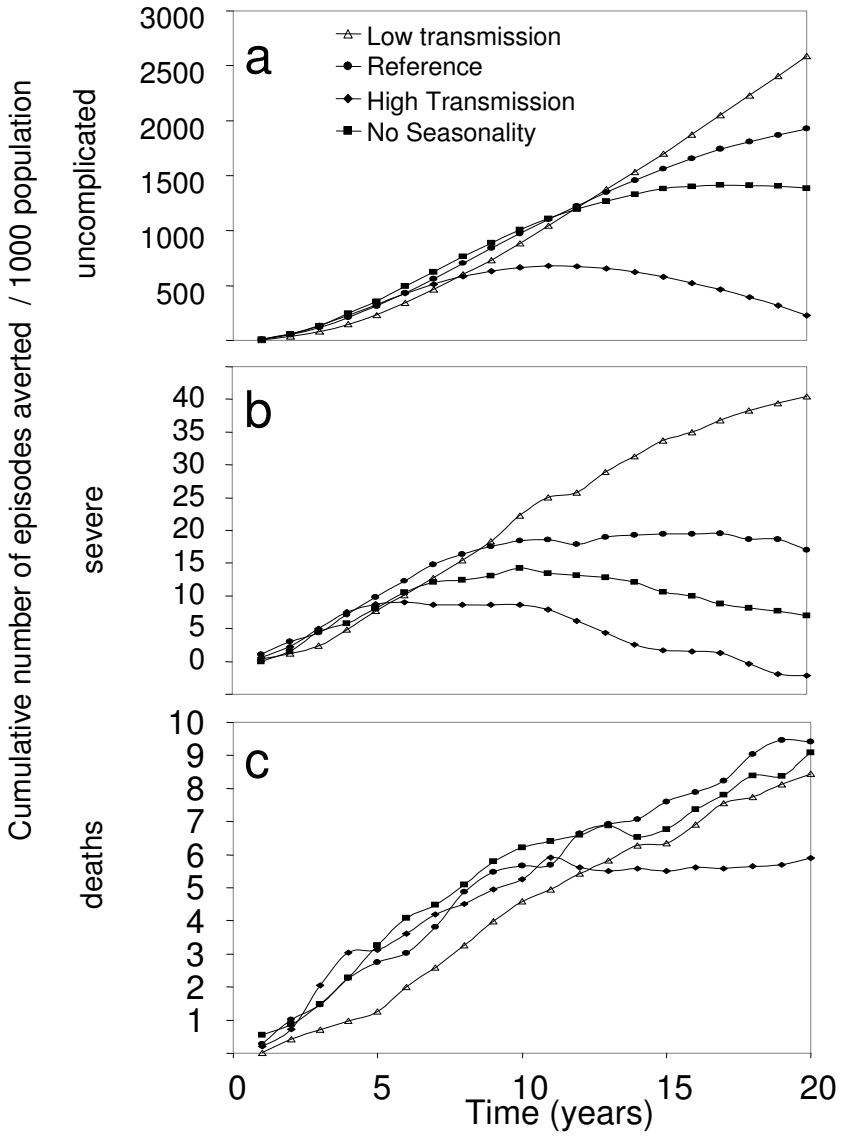

Figure 5.9: Effect of the reference vaccine over time in different transmission intensities. a) Uncomplicated episodes averted. b) Severe episodes averted. c) Deaths averted.

first few years of follow-up the number of events averted was lowest at low transmission intensity due to the lower numbers of events in the vaccinated age group. Protection against uncomplicated episodes increased over time, the effect on mortality remained approximately constant, and that on severe morbidity decayed at a much slower rate than in

the reference scenario. A net reduction in incidence of severe episodes was consequently still evident after 20 years of follow-up, while the total number of deaths averted over the 20-year period was lower than in the reference scenario.

At high transmission the initial gains were similar to those seen for the reference scenario, but the overall incidence of uncomplicated episodes became higher than that in the unvaccinated scenario after about 10 years of the vaccination program (Figure 5.9ab). There was no such adverse effect on mortality rates, but the initial gain seen during the first 10 years of the program did not continue (Figure 5.9c).

Although the degree of seasonality hardly affects the cumulative number of deaths averted, the number of uncomplicated episodes averted is lower in the absence of seasonality than in the reference scenario. The cumulative efficacy against uncomplicated episodes is reduced from 0.067 to 0.050 in the absence of seasonality.

5.4 Discussion

We use a stochastic simulation model of the transmission dynamics and epidemiology of *P. falciparum* malaria in endemic areas to assess the likely impact of a pre-erythrocytic vaccine introduced via the EPI. This is the first major attempt to combine dynamic modeling of malaria transmission with predictions of parasitologic and clinical outcome, using models that have been fitted to field epidemiology data from a range of sites across Africa.

We have based our simulations as much as possible on field data, but many uncertainties and approximations remain, both in our epidemiologic models and our model of vaccination. The uncertainty in the field estimate of efficacy of RTS,S/AS02A is substantial; the efficacy of incomplete courses of vaccination is unknown, as is the rate of waning of vaccine efficacy.

We agree with previous dynamic models of the impact of malaria vaccination [Anderson et al., 1989, Halloran et al., 1989, Koella, 1991, Struchiner et al., 1989] that a leaky anti-infection vaccine will have little effect on transmission in endemic areas. Our estimates of transmission effects are even smaller than those in most previous models because we predict that reduction in human infection will have little effect on infectiousness to vectors (except in the case of complete protection of a sub-set of the population). We nevertheless identify substantial potential public health benefits of vaccination because severe disease

is largely concentrated in the first years of life (in our model this arises largely because of age-dependent cofactors [Ross et al., 2006b]) and can be averted by delaying exposure to blood-stage parasites.

We would expect a pre-erythrocytic vaccine to have much more effect on transmission in areas of unstable malaria such as highland areas of east Africa [Abeku et al., 2004], KwaZulu-Natal [Kleinschmidt et al., 2002], or areas of low transmission outside Africa. This raises the issue of whether the best delivery strategy in such areas might then be a mass vaccination campaign, contributing to local elimination. Mathematical models of the impact of such a vaccination program need not consider the complexities of acquired clinical immunity, and so might reasonably be based on conventional compartment models [Koella, 1991]. Extension of these models to allow appropriately for heterogeneities in transmission [Dye and Hasibeder, 1986] would be of critical importance.

In our model, the dynamics result mainly from a cohort effect on coverage and from the dynamics of immunity, rather than from effects on transmission. The effectiveness of vaccination (the proportion averted of all the events in the population) cannot reach equilibrium until after the oldest people are vaccinated, even 20-year simulations do not approach equilibrium. Effectiveness in the initial years of a program is likely to be much lower than vaccine efficacy because only a small proportion of the people will be vaccinated.

The 20-year time horizon allows us to see that the effect of a vaccine program on illness incidence will change over time, although we predict a roughly constant reduction in the crude mortality rate throughout the follow-up. After approximately 10 years, there is a net reduction in cumulative numbers of clinical episodes only in low transmission scenarios, with a predicted increase in high transmission. This is due to an increase in severe malaria incidence in children greater than five years of age who have accrued less immunity to asexual blood stage parasites during their childhood. This partly results from the models used for predicting uncomplicated episodes [Smith et al., 2006c] and severe malaria [Ross et al., 2006b], which are fitted to data that suggest the lifetime number of clinical episodes [Trape and Rogier, 1996] and the incidence of hospital admissions for severe malaria [Marsh and Snow, 1999] are highest at intermediate levels of transmission.

With a vaccine with high efficacy in a proportion of the population (i.e. with a low value of b), effectiveness continues to increase as the vaccinated proportion increases, although in our simulations this effect is gradually lost due to decay in vaccine efficacy. With vaccines with partial efficacy in all individuals (the model we propose for RTS,S/AS02A, Chapter

4), the factors attenuating the efficacy such as interactions with the epidemiologic effects of acquired immunity become more important as the vaccination program proceeds. In very low-transmission settings, we predict initial increases in effectiveness because the proportion vaccinated increases before the first vaccinees leave the age range of high vulnerability. At higher transmission, there is little evident increase in effectiveness as the number of fully vaccinated individuals increases.

Since no vaccinated child reached more than 20 years of age in our simulations, very long-term effects of vaccination are not captured. This is important when comparing different decays or initial efficacies because the relationship between the duration during protection and the life expectancy of the vaccinated individual may be important in determining the effectiveness. However, we are very uncertain about the risk of severe malaria that such adults would experience. There are few data available from which to estimate severe malaria risk in adolescents or adults with limited previous exposure [Ross et al., 2006b].

Vaccination reduces the incidence of uncomplicated episodes because it leads to fewer successful infections. The reduced exposure to parasites leads to less acquired asexual stage immunity; thus, the longer-term level of clinical protection is lower than the initial efficacy. In our models, the pyrogenic threshold, which determines the parasite density that leads to acute illness, also depends on the recent exposure to parasites and is therefore lower in vaccinated individuals (Chapter 4). Vaccination can also modify the proportion of acute episodes that are severe by leading to a shift in clinical episodes to an older age, when the host is protected from co-morbidity and from other age-dependent factors enhancing susceptibility. With an efficacious vaccine, efficacy against severe malaria may be greater than that against infection. Conversely, if the vaccine does not offer a sufficiently high level of protection for a long enough time, the lower level of asexual stage immunity means that an increased proportion of clinical attacks result in severe malaria.

The application of our models can be extended not only to include other means of deployment (including regimens with booster doses of vaccines), to other types of vaccines (asexual blood stage and transmission blocking), and to consider the inclusion of vaccination within integrated control programs. We have seen that a pre-erythrocytic vaccine will be most effective at low transmission intensities, but that on its own it is unlikely to reduce transmission very much except possibly when this is already low. It may be that such a vaccine will be most effective if deployed in conjunction with vector control measures that reduce the vectorial capacity at the same time.

Chapter 6

Predicting the cost-effectiveness of introducing a pre-erythrocytic vaccine into the Expanded Program on Immunization in Tanzania

Fabrizio Tediosi, Guy Hutton, Nicolas Maire,
Thomas Smith, Amanda Ross, Marcel Tanner
Swiss Tropical Institute, Basel, Switzerland

This article has been published:
American Journal of Tropical Medicine and Hygiene 2006, 75, Suppl 2, 131-143

Abstract

We model the cost-effectiveness of the introduction of a pre-erythrocytic malaria vaccine into the Expanded Program on Immunization. We use a dynamic stochastic simulation model of the epidemiology of *Plasmodium falciparum* in malaria-endemic areas and of case management in Tanzania. We consider a range of vaccine characteristics and a range of transmission settings. At low vaccine prices, the cost-effectiveness of such vaccines may be similar to that of other established preventative and curative interventions against malaria. The cost-effectiveness ratio increases rapidly and approximately linearly with vaccine cost per dose. The approach can be adopted for comparative analyses of the cost effectiveness of different vaccines and other intervention strategies.

6.1 Introduction

The goal of economic evaluation of healthcare interventions in general, and malaria control measures in particular, is to provide policy makers with guidance about how scarce resources can be allocated so that the social and economic benefits are maximized [Drummond et al., 1997, Gold et al., 1996]. Economic evaluation not only shows how efficient it is to spend resources on existing interventions available, but also predicts how efficient new interventions could be if they were to be developed, or if existing interventions had different characteristics. Thus, economic evaluation is an essential part of the appraisal of candidate malaria vaccines. For example, policy makers may wish to know how efficacious a vaccine would need to be to be cost-effective.

Cost-effectiveness analysis (CEA) usually is the method of choice in evaluating alternative health interventions because health decision makers are primarily interested to know what health improvements can be bought with a given budget, and not the overall economic impact *per se.* [Drummond et al., 1997, Gold et al., 1996]. The present paper models the cost-effectiveness of a pre-erythrocytic malaria vaccine, using a dynamic stochastic simulation model of the epidemiology of *Plasmodium falciparum* in malaria-endemic areas and of case management in Tanzania (Chapter 3, Hutton and Tediosi [2006]). Our objective is to assess the potential cost-effectiveness of introducing this malaria vaccine into the Expanded Program on Immunization (EPI) under a range of scenarios, conditions, and assumptions.

We present the vaccine cost-effectiveness for one country, Tanzania. This first stage enables

us to specify model inputs without having to consider simultaneously many heterogeneous settings, as would be the case for sub-Saharan Africa. Even one country does not present a single uniform context for ecologic, epidemiologic, socioeconomic and health system inputs, but there is less heterogeneity than at the multi-country level.

6.2 Materials and Methods

Perspective and boundary. The study is a CEA adopting a societal perspective for both costs and effects, and thus considers all relevant resource inputs to the intervention, and resource consequences and health impacts resulting from the intervention.

The costs of vaccine delivery [Hutton and Tediosi, 2006] include all resource inputs irrespective of whether these costs are borne by government, donors, the patient, the wider community, or a mixture of these. Case management costs (Chapter 3) likewise include all resource inputs irrespective of whether these are borne by government, the patient, or both. Vaccine delivery costs and case management costs include both the direct costs of service provision and costs directly associated with the service, which essentially means the costs for the patient(s) accessing the services, covering additional transport and sustenance costs.

A societal perspective in CEA also requires that direct economic impacts of the intervention should be taken into account. In the case of a vaccine that reduces morbidity episodes as well as mortality, there is a clear impact on productive time either leading to higher income (in the case of market work) or higher unsold production (in the case of non-market work). This can either be through a gain in production of the averted malaria case, or where the patient is a child, the production gained of the care giver who would have cared for the averted malaria case. Therefore, the results include these hypothesized economic impacts.

Given the dynamic nature of the epidemiologic model, and the lower transmission rates to other non-vaccinated individuals associated with an effective vaccine, the health effects of the intervention can also include changes in morbidity and mortality of the non-vaccinated population as a result of reduced transmission. However, our epidemiologic analysis implies that these impacts will be minimal in the epidemiologic settings that we have analyzed (Chapter 5).

Model overview. To predict the cost-effectiveness of the malaria vaccine, we use a stochastic simulation model of the epidemiology of *P. falciparum* in malaria-endemic areas of Africa [Smith et al., 2006a]. This includes a sub-model for the case management of malaria in Tanzania (Chapter 3). We link these elements with costing of vaccine delivery in the Tanzania setting [Hutton and Tediosi, 2006].

The epidemiologic model is a stochastic individual-based simulation of malaria infection in disease-endemic areas that uses a five-day time step. It takes as its input the pattern of the entomologic inoculation rate (EIR) in the absence of interventions, with separate values of the EIR specified for each of the 73 five-day periods during the year. We simulate the reference case management scenario in Tanzania (Chapter 3) to provide a baseline with which to compare simulations where a vaccine is introduced.

The simulated population is maintained as a steady state, and includes individuals of all ages, with immune status depending on their simulated exposure. The denominators for calculation of overall health impacts include individuals who were too old to be vaccinated, and 20-year simulation is thus influenced by cohort effects due to gradual increase in the proportion of the population vaccinated, and by dynamic effects of reduction in exposure on acquisition of natural immunity to asexual parasites.

Alternatives being compared. We compare health outcomes, direct costs, and productivity gains of a combined strategy of a new malaria vaccine delivered through EPI in combination with the reference case management scenario for Tanzania with only the reference case management scenario (Chapter 3).

The EPI was chosen as the channel for vaccine delivery because in most African countries EPI is well established and achieves reasonably high levels of coverage amongst the target population group. Therefore, it is the only reliable mechanism to deliver a vaccine to a high proportion of infants less than one year of age [Edmunds et al., 2000, Griffiths et al., 2005, Hall et al., 1993].

The vaccine modeled is a pre-erythrocytic stage vaccine requiring three doses to fully immunize a child. These doses are administered when infants are one, two, and three months of age, at the same time as the hepatitis B vaccine. Many of the inputs for the CEA are based on data from the case management model (Chapter 3) and epidemiologic scenarios (Chapter 5).

The cost-effectiveness model simulates the health system typical for a rural area of Tanzania (Chapter 3). A set of different scenarios were constructed to reflect different malaria transmission intensities representing the stable, annually recurring pattern of malaria transmission. In all simulations, the seasonal pattern of transmission was assumed to be that recorded in the village of Namawala, Tanzania, during 1989-1991 where exceptionally precise estimates of dry season transmission were made [Smith et al., 1993]. The annual EIR for this site was 329 infectious bites per year. For the reference scenario, we use a seasonal pattern of transmission for a mesoendemic site, which was obtained by dividing the EIR from Namawala for each five-day period by 16. Direct measurement of dry-season transmission in meso-endemic areas is impracticable because of low mosquito densities. To simulate a high-transmission area, we use an EIR of four times that of the reference scenario. This is probably more typical of high-transmission sites in Africa than the extremely high transmission in Namawala. This gives an overall annual EIR of 21 infectious bites per year, which is typical for a mesoendemic area in sub-Saharan Africa [Hay et al., 2000]. The simulations were first run for a warm-up period of 90 years of exposure to define the baseline immune status of the simulated populations, which is highly age-dependent. For the present analyses, the simulations are run in populations of 100,000 individuals, with an approximately stationary age distribution matching that of the demographic surveillance site in Ifakara [INDEPTH Network, 2002].

Measuring health gains. To estimate the number of disability-adjusted life years (DALYs), years of life lived with disability are calculated on the basis of the duration of disability, and respective disability weights (Chapter 3, Murray and Lopez [1996b]). Weights for different malaria attributable disease conditions have been obtained from the global burden of disease (GBD) study [Murray and Lopez, 1996a], and age-weighting is applied as in the GBD method. However, to assess how sensitive results are to the life table used, DALYs are also computed assuming a zero age weighting. The disability associated with anemia is assigned to the same time period as the malaria infections causing it.

Years of life lost (YLLs) and DALYs are calculated assuming age-specific life expectancies based on the life table from Butajira, Ethiopia, with an average life expectancy of 46.6 years at birth [INDEPTH Network, 2004]. This life table represents that of an east African setting with low malaria transmission and is very similar to that for Hai District, a high altitude and low malaria prevalence site in Tanzania [INDEPTH Network, 2002]. We thus compute YLLs for each simulated death under the assumption that this life table would

apply in the absence of malaria.

Assumptions on vaccine efficacy. In the reference scenario, the efficacy of this hypothetical pre-erythrocytic malaria vaccine is assumed to be 52% reduction in infections in naïve individuals (Chapter 4), decaying exponentially with a half-life of 10 years. Since it is likely that the degree of protection provided varies between individuals, in the reference scenario, a value for the initial efficacy is drawn from a beta distribution with parameter b=10 and assigned to each vaccinated individual (Chapter 5).

Coverage. In the reference scenario, it is assumed that the coverage rate is the same as that reported in Tanzania for three doses of diphtheria tetanus pertussis-hepatitis B virus (DTP-HBV) vaccine in the year 2003, which stood at 89%. Given that the coverage for the first dose of DTP-HBV was 95%, the dropout rate from the first to the third dose is 6% [Hutton and Tediosi, 2006].

Case management. The case management model, including both formal and informal treatment, is described elsewhere (Chapter 3). It has implications for health outcomes, both in terms of the potential to reduce rates of severe disease, sequelae and death, but also in the impact on transmission intensity and therefore the potential for new infections in the entire population. The rate of treatment seeking among uncomplicated malaria episodes was assumed to be 5%, which although apparently low, is justified due to the very sensitive definition of clinical episodes used. The clinical episodes simulated thus include very mild fevers that would be unlikely to elicit attendance at a health facility. The model assumes in the reference case a cure rate of 93% for the first-line drug sulfadoxine-pyrimethamine (SP) for uncomplicated malaria (Chapter 5).

Costs presented. We considered both marginal and average costs. The marginal cost reflects most closely the additional financial costs that would be incurred when introducing a new intervention. The average cost includes all those costs involved in delivering a health intervention, including the use of spare capacity or slack in the system, those health care resources diverted from other uses, and existing health sector resources that are shared with other health programs. All cost data are expressed in US$ 2004.

Vaccine delivery costs. The costs of introducing a malaria vaccine into the EPI in Tanzania include those related to an assumed range of vaccine purchase costs, and data collected from Tanzania on likely distribution and cold chain storage costs, management costs, vaccine delivery costs at health facility level, training costs, and social mobilization costs. A detailed description of the methodology used to estimate vaccine delivery costs can be found in an accompanying paper [Hutton and Tediosi, 2006].

The CEA is run under various vaccine price hypotheses ranging from US $1.0 to US $20 per dose. The vaccine delivery cost estimates according to the different price hypotheses are shown in Table 6.1.

Table 6.1: Incremental delivery cost per fully immunized child (FIC) for the vaccine

Vaccine price	Vaccine delivery cost per FIC in US$	
(US$ per dose)	Average cost	Marginal cost
1	4.43	4.24
2	7.43	7.24
4	13.43	13.24
6	19.43	19.24
8	25.43	25.24
10	31.43	31.24
20	61.43	61.24

Case management costs. The costs of treating those seeking health care for malaria episodes are calculated under the two scenarios being modeled: case management alone and vaccine with case management, which allow us to calculate expected cost savings associated with the introduction of an efficacious malaria vaccine.

The direct costs of care seeking for an uncomplicated malaria episode at official facilities include the cost of an outpatient visit (US $1.02 dispensary; US $1.27 health center), a diagnostic test in a proportion of outpatient cases (US $0.30), the cost of a course of SP treatment (varying from US $0.012 to US $0.071, depending on age and weight), the cost of a course of amodiaquine treatment (varying from US $0.018 to US $0.114, depending on age and weight), and other costs incurred by patients when visiting an official health facility (US $0.30).

The direct costs of a severe malaria patient include in-patient hotel costs per day (US$ 7.8),

drug treatment cost during hospitalization (varying from US$ 0.56 to US$ 3.74, depending on age and weight), average length of stay (4.5 days with full recovery), and the costs that patients incur when visiting an official in-patient facility (US$ 1.29 for the average length of stay). The case management cost inputs are presented in detail elsewhere (Chapter 3).

Measuring productivity gains. The productivity costs of malaria relate to the productive time lost due to illness, whether it is the patient or the patient care giver (especially if a child or elderly patient). In this analysis, productivity costs included are those related to time spent by adults seeking official care for their children, time spent by adults caring for children at home, and the time forgone by sick adults due to malaria episodes. Given that inclusion of productivity gains in CEA remains controversial, the reference case results do not include these hypothetical productivity gains.

To measure the value of productive time lost, we use the wage rate method that involves multiplying the time lost per episode (for adults only) by the average daily wage in Tanzania. These estimates are adjusted downwards by an estimate of the unemployment rate in Tanzania, thus taking into account that not all those sick or those caring for the sick would have been working.

The time lost per malaria episode is expected to be highly variable. For example, a recent review of the literature available found that for a sick adult the time off work ranges from one to five days, depending most importantly on severity of disease [Chima et al., 2003]. For this study, uncomplicated adult malaria cases are assumed to lose two working days, while a care taker of a sick child loses one working day. Adults with a severe malaria episode are assumed to lose 4.5 days if not hospitalized, or if hospitalized, 1 day more than their length of stay in hospital. A care giver of a child with severe malaria is assumed not to be able to work during the hospitalization period.

For uncomplicated episodes, productivity costs are computed under two scenarios. In the first scenario, a productivity cost is attached to only those uncomplicated episodes that get treated, presumed to correspond in general to the more severe episodes. In the second scenario, a productivity cost is attached to all malaria episodes. These two scenarios represent the likely upper and lower bounds on the true productivity costs avertable through the introduction of an efficacious vaccine.

The formulae for calculating productivity costs are presented below, and the data inputs

are provided in Table 6.2.

$$I_{cu} = T_{cu}\, w\, (1 - U) \tag{6.1}$$

$$I_{cs} = T_{cs}\, w\, (1 - U) \tag{6.2}$$

$$I_{au} = T_{au}\, w\, (1 - U) \tag{6.3}$$

$$I_{as} = T_{as}\, w\, (1 - U) \tag{6.4}$$

where I_{cu} and I_{cs} are the productivity costs of the care taker for uncomplicated and severe malaria, respectively; I_{au} and I_{as} are the productivity costs of sick adults with uncomplicated and severe malaria, respectively; T_{cu} and T_{cs} are the time lost in days per episode by care taker of sick child for uncomplicated and severe malaria, respectively; T_{au} and T_{as} are the time lost in days for sick adults for uncomplicated and severe malaria, respectively; w is the minimum gross daily wage in Tanzania (US \$3); and U is the assumed unemployment rate in Tanzania (40%).

Table 6.2: Data inputs for calculation of productivity costs*

Item	Value (US$ 2004)
Care taker UM	1.8
Care taker SM if patient dies	3.6
Care taker SM if patient fully recovers	8.1
Care taker SM if patient recovers with sequelae	18.0
Sick adult UM	3.6
Sick adult SM if patient dies	5.4
Sick adult SM if patient fully recovers	9.9
Sick adult SM if patient recovers with sequelae	18.0

*UM = uncomplicated malaria; SM = severe malaria.

Net cost calculations. The net costs associated with current case management and adding the vaccine to case management is computed over time as follows:

$$NC = \sum_{t=1}^{n} \left[\frac{DC(cm_v + v)_t - DC(cm_{nv})_t}{(1 + r)^t} \right] \tag{6.5}$$

where NC is net costs including only direct costs; DC (cm_v+v) is the direct costs in the case of the vaccine plus case management; DC (cm_{nv}) is the direct costs of current case management under a no vaccine scenario; n is the time period of intervention (20 years); and r is the annual discount rate for future costs and health effects.

Reference scenario. In the reference case, results are presented to show cost-effectiveness at four different five-year time periods during the 20-year follow-up period (1-5 years, 6-10 years, 11-15 years, and 16-20 years) to reflect the possible fact that cost-effectiveness changes depending on time after vaccine introduction. The cost-effectiveness ratios (CERs) are presented under seven vaccine price assumptions (in US$): 1, 2, 4, 6, 8, 10, and 20. Incremental CERs are presented using two different definitions of cost: marginal cost to reflect the likely short-term financial impact of the intervention, and average cost to reflect the long-term and full opportunity cost associated with the intervention. In the reference case, only direct costs are included.

Incremental cost-effectiveness ratios are calculated under four health outcomes relevant for decision making: cost per episode averted, cost per DALY averted, cost per YLL, and cost per death averted. Future costs and benefits are presented both undiscounted and at a discount rate of 3% to reflect time preference [Tan-Torres Edejer et al., 2003].

Sensitivity analysis. In addition to the reference case data assumptions and scenarios, the sensitivity analysis runs these same simulations under different assumptions. The rationales for these scenarios and the epidemiologic patterns associated with them are described in Chapter 5. The different transmission intensity patterns used are low stable transmission (Namawala/64, equivalent to 5.2 infectious bites per year and high transmission (Namawala/4, equivalent to 83 infectious bites per year). The reference case is an EIR of 21 infectious bites per year, corresponding to Namawala/16. The different levels of vaccine efficacy are 30%, 80%, and 100%. The reference case is 52% entered in the model. Different decay rates for the efficacy are half-lives of 6 months, 1 year, 2 years, 5 years, and 10,000 years. The reference case is 10 years. Different distributions of vaccine effect in the population are b equals 0.01 and 100,000. The reference case is 10. Different vaccine coverage rates are a low coverage rate, with 70% of the infants receiving their first dose, and 50% receiving their third dose and complete coverage, with 100% of the infants receiving three doses. The reference cases were 89% for the third dose and 95% for the first

dose. Inclusion of productivity cost savings were low productivity costs, where those with uncomplicated episodes who do not seek care are assumed not to lose productive time and high productivity costs, where all those predicted by the model to have a malaria episode are assumed to lose productive time.

6.3 Results

Reference case presentation. *Health effects.* Over 20 years, the number of uncomplicated episodes averted due to the introduction of the vaccine, in the simulated reference population of 100,000 people, is close to 192,485, which corresponds to a rate of 0.1 per capita per year, while the total number of severe episodes averted is 1,697, or 0.0008 per capita per year (Chapter 5). These health effects represent only a small fraction of the total burden of disease because vaccinated children represent only a small proportion of the total population in the early years of the simulation. Since the reference scenario also assumes waning of vaccine-induced immunity, the protected proportion of the population is never very high and increases only gradually. Furthermore, vaccination with a pre-erythrocytic vaccine effectively postpones many illness episodes because it reduces acquisition of asexual stage immunity.

The number of deaths prevented over 20 years is 942. The number of undiscounted DALYs averted over 20 years is 58,579, which corresponds to a rate of 0.029 per capita per year. When DALYs are discounted at 3%, the number of DALY averted is 26,892, or 0.013 per capita per year. The total number of undiscounted DALYs with no age weighting applied is 48,299 DALYs averted, or 0.024 per capita per year. Since most of these DALYs are due to the mortality effects, the number of YLL is very close to that of DALYs. Figure 6.1 presents the distribution of DALYs averted over the 20-year model period, indicating that the health effects of introducing the vaccine vary over time.

Table 6.3 shows that the number of uncomplicated episodes averted is higher in the second and third five-year time periods and lower in the first and fourth five-year time periods since the start of vaccination. Most of the severe episodes averted occur in the first 10 years of the intervention, with a sharp decrease in the third five-year period, even registering a higher number of severe episodes under vaccination scenario in the fourth five-year period. Also, a higher proportion of deaths prevented are concentrated in the first 10 years after vaccine introduction. When health outcomes are discounted, this effect is stronger.

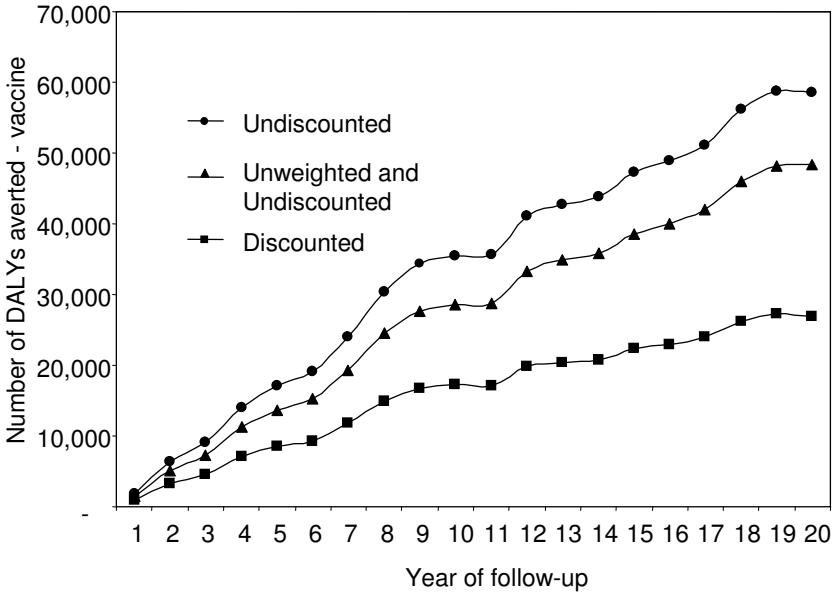

Figure 6.1: Total number of disability-adjusted life years (DALYs) averted after introducing the vaccine (reference case scenario).

Table 6.3: Comparison of discounted and undiscounted health outcomes over the four five-year time period after the vaccine introduction*

	Time period (years)			
	1-5	6-10	11-15	16-20
Uncomplicated episodes averted	31,289	65,810	59,187	36,199
Severe episodes averted	979	867	96	-245
Deaths averted	275	292	193	182
Deaths averted (discounted)	256	236	134	110
YLL averted	16,731	18,454	12,035	11,655
DALYs averted (undiscounted)	17,083	18,426	11,699	11,370
DALYs averted (discounted)	8,507	8,741	5,036	4,608
DALYs averted (unweighted, undiscounted)	13,657	14,953	9,933	9,755

*YLL = Years of life lost; DALY = Disability Adjusted Life Years.

Net costs. The net cost of vaccine introduction for the 20-year period and at a vaccine price of US $1 per dose, is US $447,391, or US $0.22 per capita per year (direct, undiscounted average costs). In the marginal cost analysis, these costs are 3% less at US $433,890. The reference case results are shown in Table 6.4, for discounted and undiscounted costs and at different vaccine price assumptions.

Table 6.4: Net costs in thousand US$, reference case (year 2004)*

Vaccine price per dose	Discounting	Period							
		Years 1-5		Years 6-10		Years 11-15		Years 16-20	
		AC	MC	AC	MC	AC	MC	AC	MC
1	Undiscounted	104	104	211	210	327	320	447	434
	Discounted	97	48	183	182	263	259	336	327
2	Undiscounted	186	182	Neg	366	575	734	779	749
	Discounted	173	121	Neg	318	464	593	586	565
4	Undiscounted	350	337	706	680	1,072	1,028	1,441	1,378
	Discounted	326	265	612	590	866	832	1,088	1,041
6	Undiscounted	513	492	1,035	993	1,568	1,500	2,104	2,008
	Discounted	478	410	899	862	1,268	1,214	1,589	1,518
8	Undiscounted	677	648	1,365	1,307	2,065	1,971	2,767	2,637
	Discounted	630	555	1,185	1,134	1,670	1,595	2,091	1,994
10	Undiscounted	840	803	1,695	1,620	2,561	2,443	3,429	3,267
	Discounted	783	700	1,471	1,406	2,072	1,977	2,592	2,471
20	Undiscounted	1,658	1,580	3,345	3,187	5,044	4,802	6,742	6,414
	Discounted	1,545	1,423	2,903	2,766	4,083	3,887	5,100	4,853

*AC = average cost; MC = marginal cost; Neg = negative. Each figure is the predicted cost for a total population of 100,000 people over the five-year period.

Figure 6.2 shows that the contribution of different cost components remains stable over the 20-year time period after introduction of the vaccine, comprising in-patient costs, outpatient costs, drug costs and patient costs. Before introduction of the vaccine, approximately 30% of direct costs are due to outpatient visits, approximately 10% to drugs, 40% to hospital care, and 20% to patient costs. After the introduction of the vaccine, more than 50% of total direct costs, at a vaccine price of US $1 per dose, would be due to the vaccine delivery costs. This proportion increases significantly as the vaccine price increases.

The number of first-, second-, and third-line drug treatments over time is lower after the introduction of the vaccine (Figure 6.3). The total number of first-line drug treatments averted by the vaccine reaches a maximum in the second five-year interval, then decreases. The number of second- and third-line treatments averted is high in the first five-year

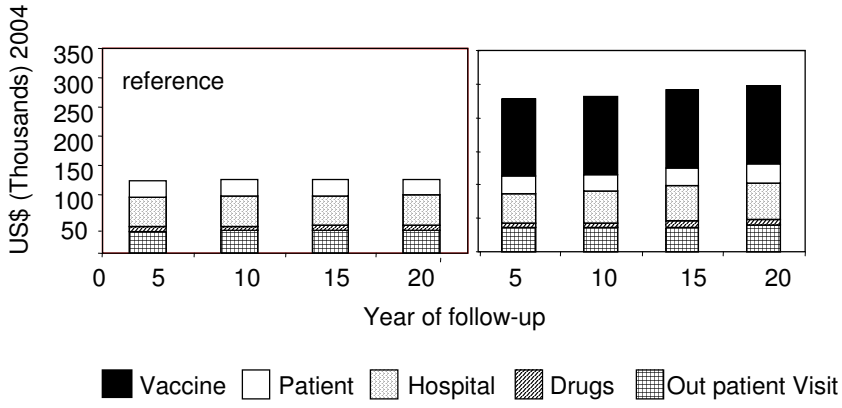

Figure 6.2: Direct cost structure (vaccine price per dose = US $1).

period, after which it decreases to close to zero after 15 years. In the last five-year period the number of first-, second- and third-line drug treatment is higher when the vaccine is introduced. This is due to the fact that in the last five-year period the vaccine does not prevent any severe episodes. There is also a shift in uncomplicated episodes to older ages, where higher drug costs are incurred due to the requirement for a greater dose.

Cost-effectiveness. Cost-effectiveness ratios using undiscounted average cost are presented for the vaccine in Table 6.5 over the entire 20-year intervention period and by vaccine price. The cost per death averted by introducing the vaccine is US $475, under a vaccine price assumption of US $1 per dose, increasing to US $7,158 per death averted at a vaccine dose price of US $20. The cost-effectiveness ratios using the marginal cost are generally between 97% and 99% of the CERs at average cost. Furthermore, discounting costs and health effects makes only a marginal difference to the CER, as shown in Table 6.5.

The undiscounted cost per DALY averted by introducing the vaccine is US $8 under a vaccine price assumption of US $1 per dose, increasing to US$ 115 per death averted at a vaccine dose price of US $20. The effect of discounting increases the cost per DALY averted by around 50% to US$12 per DALY averted at a vaccine price of US$1 per dose. The effect of taking out the age weighting in the DALY calculation reduces the cost per DALY averted back towards undiscounted levels. Figure 6.4 shows the relationship between CERs (for deaths averted and DALYs averted) and vaccine price.

However, the presentation of CERs over the entire 20-year intervention period hides some

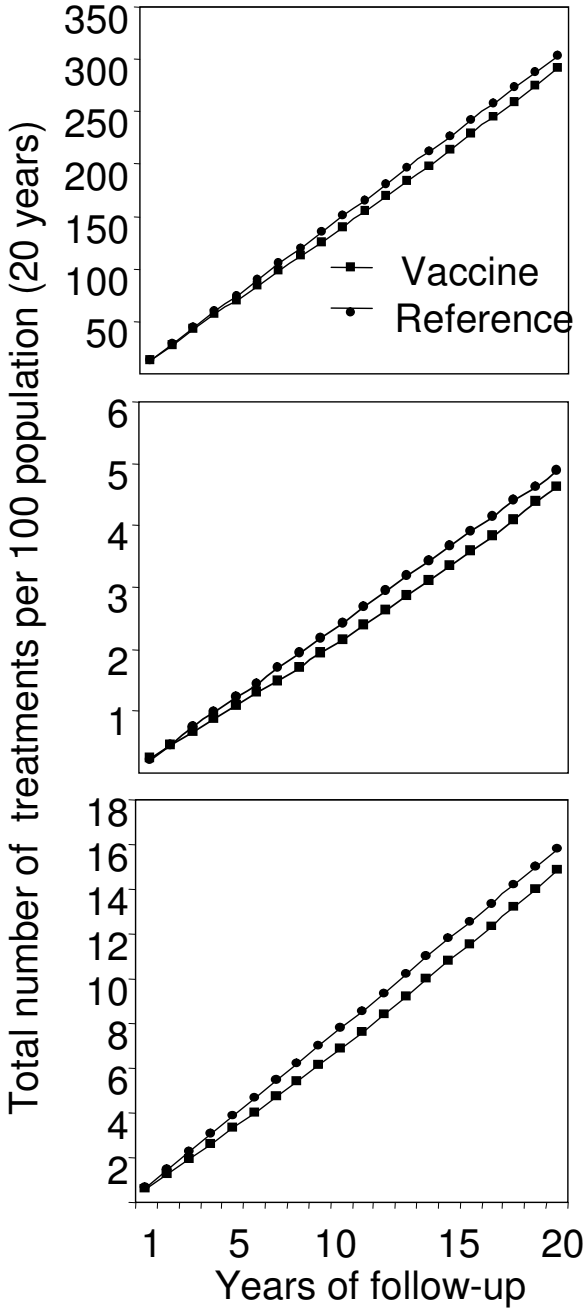

Figure 6.3: Total number of drug treatments under different interventions.

Table 6.5: Cost-effectiveness (average cost) of the vaccine over 20 year intervention period, by vaccine price

Outcome	Vaccine price per dose, in US$ (year 2004)						
	1	2	4	6	8	10	20
Cost per death averted							
Undiscounted	475	827	1,530	2,234	2,937	3,640	7,158
Discounted	456	796	1,477	2,158	2,840	3,521	6,926
Cost per DALY averted							
Undiscounted	8	13	25	36	47	59	115
Discounted	12	22	40	59	78	96	190
Undiscounted, unweighted	9	16	30	44	57	71	140

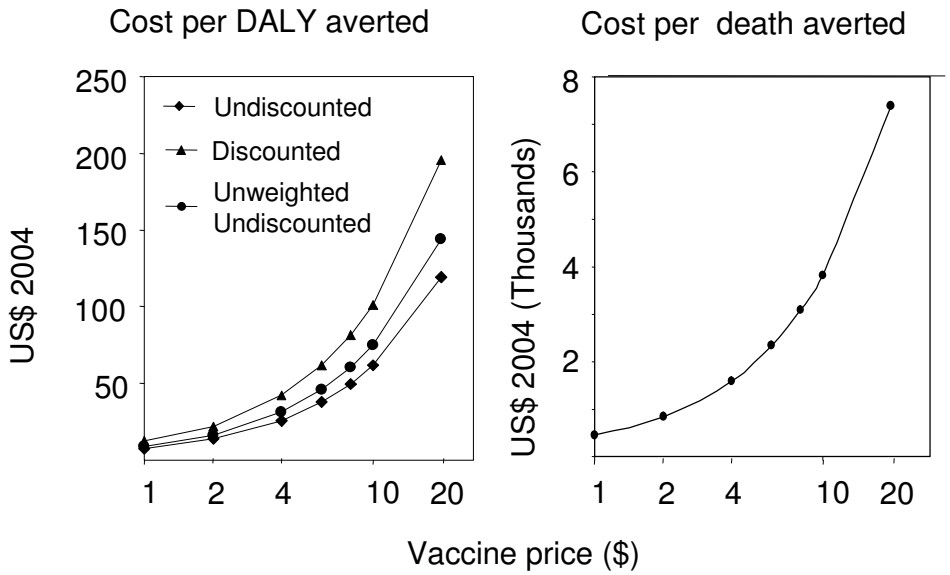

Figure 6.4: Relationship between cost-effectiveness ratios and vaccine price over the entire 20-year intervention period. DALY = disability-adjusted life year.

important variations across five-year time intervals. Furthermore, variations in cost-effectiveness between the four different periods do not show a similar pattern across health outcome measures. Table 6.6 shows CERs for selected health outcomes over the four time intervals, and at different vaccine price assumptions.

Table 6.6: Cost-effectiveness ratios for selected health outcomes, disaggregated by 5-year time intervals and by vaccine price*

		Cost-effectiveness ratios (direct cost) for different health outcomes											
		Uncomplicated episodes averted		Severe episodes averted		Deaths prevented		DALYs averted (UD)		DALYs averted (D)		DALYs averted (UD, UW)	
Vaccine price†	Time interval	AC	MC	AC	MC	AC	MC	AC	MC	AC	MC	AC	MC
1	1-5	3	3	106	106	379	378	6	6	11	11	8	8
	6-10	2	2	123	122	364	362	6	6	10	10	7	7
	11-15	2	2	1,209	1,152	601	573	10	9	16	15	12	11
	16-20	3	3	Neg	Neg	663	625	11	10	16	15	12	12
2	1-5	6	6	190	186	676	661	11	11	20	20	14	13
	6-10	3	3	219	213	649	632	10	10	17	17	13	12
	11-15	3	3	2,077	1,977	1,033	983	17	16	27	26	20	19
	16-20	6	5	Neg	Neg	1,119	1,058	18	17	26	25	21	20
4	1-5	11	11	357	344	1,271	1,226	20	20	38	37	26	25
	6-10	5	5	411	395	1,219	1,174	19	19	33	32	24	23
	11-15	6	6	3,813	3,626	1,897	1,803	31	30	50	48	37	35
	16-20	10	10	Neg	Neg	2,032	1,925	33	31	48	46	38	36

Continued on next page

Vaccine price†	Time interval	AC	MC	AC	MC	AC	MC	AC	MC	AC	MC	AC	MC
6	1-5	16	16	524	503	1,866	1,790	30	29	56	54	38	36
	6-10	8	8	603	578	1,789	1,715	28	27	48	46	35	33
	11-15	9	9	5,549	5,275	2,760	2,624	46	43	73	70	54	51
	16-20	15	14	Neg	Neg	2,944	2,792	47	45	70	66	55	52
8	1-5	22	21	691	662	2,460	2,355	40	38	74	71	50	47
	6-10	10	10	794	760	2,359	2,256	37	36	63	61	46	44
	11-15	12	11	7,285	6,924	3,623	3,444	60	57	96	92	70	67
	16-20	19	18	Neg	Neg	3,857	3,659	62	59	91	87	72	68
10	1-5	27	26	858	820	3,055	2,920	49	47	92	88	62	59
	6-10	13	12	986	942	2,928	2,798	46	44	79	75	57	55
	11-15	15	14	9,020	8,573	4,487	4,264	74	70	119	113	87	83
	16-20	24	23	Neg	Neg	4,769	4,526	76	72	113	107	89	84
20	1-5	53	50	1,693	1,614	6,028	5,745	97	92	182	173	121	116
	6-10	26	24	1,946	1,854	5,777	5,504	92	87	155	148	113	107
	11-15	29	27	17,700	16,818	8,804	8,366	145	138	234	223	171	163
	16-20	47	45	Neg	Neg	9,332	8,860	149	142	221	210	174	165

* DALYs = disability-adjusted life years; D = discounted; UD = undiscounted; UW = unweighted; AC = average cost; MC = marginal cost; Neg = negative.

† Price per dose (US$)

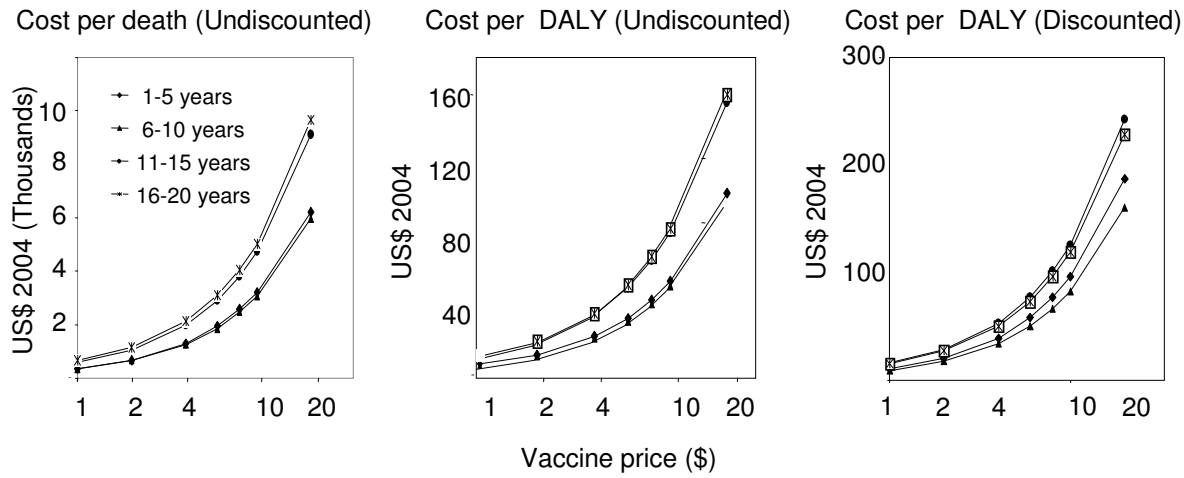

Figure 6.5: Cost-effectiveness ratios for different time periods and vaccine prices. DALY = disability-adjusted life year.

The CERs for cost per death averted are similar in the first two five-year intervals, but considerably higher in the second two five-year intervals. At a vaccine price of US $1 per dose, the cost per death averted ranges between US $364 and US $601 over the four time intervals (Figure 6.5). The cost per death increases almost linearly with the vaccine price and at US $20 per dose it ranges between US $6,028 and US $9,332 per death averted at different time periods.

The undiscounted cost per DALY averted follows the same pattern over time as the cost per death averted, with a substantial difference between the first two five-year periods and the second two five-year periods (Figure 6.5). At vaccine price of US $1 the cost per DALY averted varied between US $6 and US $11 over time, but it increases with the vaccine price up to a range of US $92 to US $149 at US $20 per dose.

The discounted cost per DALY averted is higher, ranging between US $11 and US $16 at US $1 per dose (Figure 6.5). When DALYs are computed undiscounted and assuming zero age weighting, the average direct cost per DALY averted over the four time intervals ranges between US $7 and US $12 at this vaccine price. The cost per DALY averted by the vaccination program is thus lower in the first two five-year time periods than in the latter. The CER is much higher if both costs and DALYs are discounted at 3% while excluding the age weighting from the DALY calculation leads to a CER that is somewhere in between.

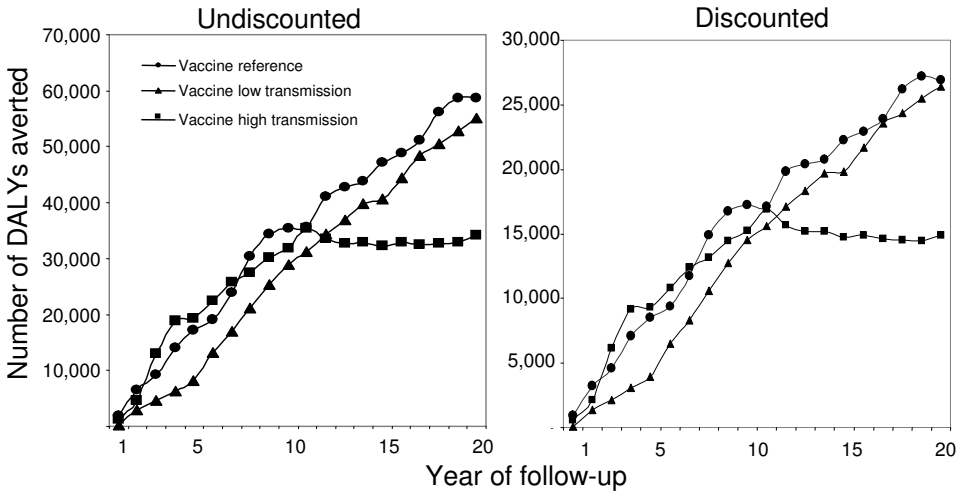

Figure 6.6: Number of disability-adjusted life years (DALYs) averted due to vaccine introduction in different transmission settings.

Cost-effectiveness ratios for cost per episode averted demonstrate yet another pattern. As most uncomplicated episodes are prevented after a few years from vaccine introduction and before the end of the third five-year interval, the cost per uncomplicated episode averted is higher in the first and last five years (US $3 at a vaccine price of US $1 per dose) and lower in the second and third five-year periods (US $2 at a vaccine price of US $1 per dose). This finding is even stronger for the severe episodes, since most of them are averted in the first 10 years, and in the last five years the number of severe episodes is higher in the vaccination scenario than under no vaccination. The cost per severe episode averted is US $106 in the first five-year period, US $123 in the second five-year period, and US $1209 in the third. In the fourth five-year period, the health effect is negative, thus giving a negative CER.

Effect of transmission intensity. The number of deaths and DALYs averted in the first 10 years of the simulation is lower in a low-transmission setting (5.2 infectious bites per year) than in the reference scenario, while in a high-transmission setting (83 infectious bites per year) is close to the number reported in the reference scenario (Figure 6.6). However, in a high-transmission setting, almost all deaths prevented (approximately 90%) and DALYs averted (approximately 93%) occur in the first 10 years.

The cost per death averted and per DALY averted in a high-transmission setting is thus

equal to that in the reference scenario in the first five-year period, but it is almost twice the cost per death averted in the second five-year period, and then the CER increases dramatically in the following years (Table 6.7). In a low-transmission setting, the cost per death prevented and per DALY (both undiscounted and discounted) averted are twice as high as those in the reference scenario in the first five years, and lower in the following years (Table 6.7).

Table 6.7: Cost-effectiveness under different scenarios.*

		Cost per DALY averted				Cost per Death prevented			
Scenario	Assumption* / Time period	1-5	6-10	11-15	16-20	1-5	6-10	11-15	16-20
Reference case	UD	6.1	5.8	9.9	10.6	378.9	364.5	601.4	663.1
	D	11.4	9.8	16.0	15.7	379.6	362.4	599.7	657.4
	UD,UW	7.6	7.1	11.7	12.4				
Low transmission	UD	13.0	4.7	8.8	7.4	845.4	293.7	579.9	512.1
	D	25.3	7.4	13.3	9.8	421.8	122.7	104.4	74.7
	UD,UW	16.2	5.9	10.6	9.0				
High transmission	UD	5.5	9.5	309.7	68.1	339.4	559.4	4,965.7	3,281.7
	D	10.6	16.2	Neg	725.7	234.7	171.3	146.9	97.7
	UD,UW	6.8	11.4	128.3	59.4				
Half-life 6 months	UD	12.6	13.5	Neg	17.8	744.8	795.9	9,798.5	1,067.5
	D	23.5	23.0	Neg	21.3	729.1	779.5	8,568.5	1,079.5
	UD,UW	15.8	16.5	827.8	22.3				
Half-life 1 year	UD	9.9	22.4	37.9	13.9	618.6	1,332.0	2,080.8	909.2
	D	18.5	41.5	62.5	19.4	607.5	1,299.3	2,212.6	938.3
	UD,UW	12.3	26.4	42.8	16.7				
Half-life 2 years	UD	6.4	9.2	19.3	9.3	401.4	552.9	1,201.0	554.8
	D	12.0	15.6	31.7	12.4	391.9	548.0	1,212.3	555.7
	UD,UW	8.1	11.2	22.8	11.2				

Continued on next page

Table 6.7: Cost-effectiveness under different scenarios.*

Scenario	Assumption* / Time period	Cost per DALY averted				Cost per Death prevented			
		1-5	6-10	11-15	16-20	1-5	6-10	11-15	16-20
Half-life 5 years	UD	5.5	8.2	13.1	11.8	336.7	517.3	804.0	761.3
	D	10.3	14.0	21.3	16.8	336.1	514.1	801.5	766.2
	UD,UW	6.9	10.0	15.3	13.9				
Half-life 10,000 years	UD	5.2	4.5	11.2	6.2	323.0	287.3	673.8	406.0
	D	9.9	7.5	18.1	8.6	321.6	285.7	671.4	403.8
	UD,UW	6.5	5.6	5.6	5.6				
Efficacy 30%	UD	9.7	14.1	26.8	15.7	625.9	917.9	1,706.5	1,080.6
	D	18.2	23.7	45.1	23.6	622.1	921.1	1,768.3	1,092.1
	UD,UW	12.1	17.5	30.9	18.7				
Efficacy 80%	UD	3.5	3.0	5.0	6.2	219.9	187.3	318.9	407.2
	D	6.7	5.0	7.9	9.5	222.4	184.8	315.2	408.5
	UD,UW	4.3	3.7	3.7	3.7				
Efficacy 100%	UD	1.9	1.4	2.8	3.2	120.2	89.8	175.4	205.4
	D	3.7	2.3	4.3	4.5	121.5	89.3	173.8	204.7
	UD,UW	2.4	1.8	3.3	3.7				
Coverage 50%	UD	5.1	6.8	15.6	8.2	325.0	437.8	916.2	529.1
	D	9.7	11.7	27.3	11.8	326.6	441.3	934.5	535.8
	UD,UW	6.4	8.3	17.3	9.8				

Continued on next page

Table 6.7: Cost-effectiveness under different scenarios.*

Scenario	Assumption* / Time period	Cost per DALY averted				Cost per Death prevented			
		1-5	6-10	11-15	16-20	1-5	6-10	11-15	16-20
Coverage 100%	UD	5.7	5.0	11.6	8.0	355.0	316.3	698.8	517.0
	D	10.7	8.3	18.4	11.2	354.6	310.7	689.7	512.8
	UD,UW	7.1	6.2	13.7	9.6				
b=0.01†	UD	4.0	4.3	5.7	7.6	253.1	272.1	354.6	503.3
	D	7.5	7.2	8.6	10.9	254.4	269.6	350.2	506.1
	UD,UW	4.6	4.8	6.6	8.6				
b=100,000†	UD	5.4	6.8	17.9	15.3	348.1	430.5	1056.4	980.9
	D	10.2	11.7	31.3	27.5	324.9	345.5	733.5	587.5
	UD,UW	6.7	8.4	8.4	8.4				

* Using US $, year 2004, average costs, vaccine price US $1 per dose. DALY = disability-adjusted life year; D = discounted; UD = undiscounted; UW = unweighted; Neg = a negative cost-effectiveness ratio.

† b is the parameter of the beta distribution used to model variation between individuals in the efficacy of the vaccine.

Effects of different vaccine efficacy. The cost-effectiveness simulations in the reference scenario assume that vaccination reduces the force of infection by 52%. Figure 6.7 shows the number of DALYs averted over the 20-year period at different levels of vaccine efficacy. The impact on deaths averted shows a similar pattern.

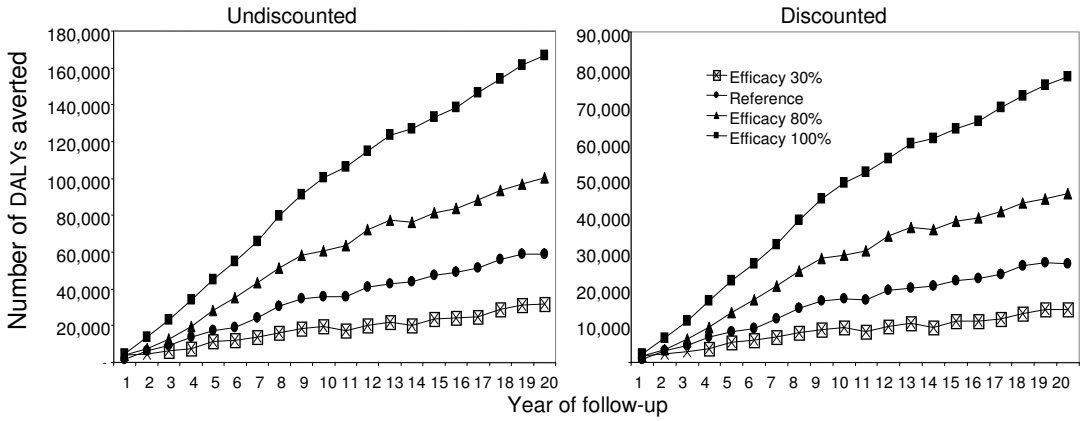

Figure 6.7: Total number of disability-adjusted life years (DALYs) averted at different levels of vaccine efficacy.

Table 6.7 shows the cost-effectiveness results under different efficacy assumptions. If the efficacy of the vaccine is 30% instead of 52%, the direct costs per death prevented and per DALY averted would be considerably higher, with the highest difference being in the second and third five-year periods where it is over 200%. Increasing the efficacy to 80% would reduce the CERs by approximately 50% to between US $3 and US $6 per DALY averted and to between US $200 and US $400 per death averted. The cost-effectiveness of a completely efficacious vaccine would result in a considerable further improvement in the CER to US $1.4-$3.2 per DALY averted.

Effects of decay of efficacy. The reference scenario assumes a half-life of protection against infection of 10 years. The cost-effectiveness simulations are run assuming different duration of vaccine protection from six months up to 10,000 years, approximating a non-decaying efficacy. The impact on DALYs averted is shown in Figure 6.8.

As expected, the longer the duration of efficacy the lower the CERs (Table 6.7). However, the improvements in cost effectiveness ratios are not linear. Improving the half-life from six months to five years leads to substantial improvements in the CER, but the differences in cost-effectiveness between five and 10 years efficacy duration are slightly smaller.

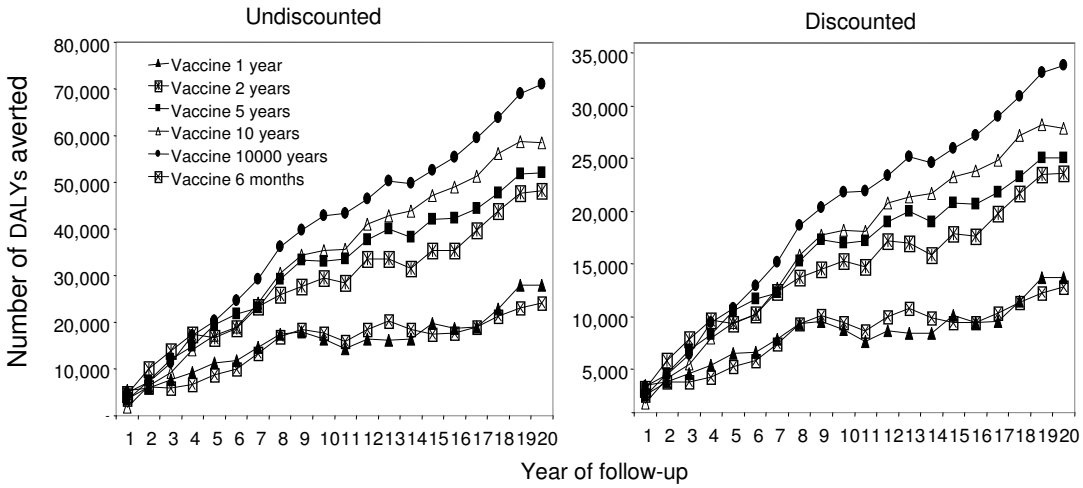

Figure 6.8: Total disability-adjusted life years (DALYs) averted at different levels of vaccine efficacy decay (half-life).

Effects of variation in vaccine efficacy between individuals. The distribution of vaccine efficacy among the vaccinated infants has a moderate effect on the number of deaths and DALYs that can be averted introducing the vaccine. The two alternative scenarios modeled, assuming either an all-or-nothing response or complete heterogeneity, show that the more the efficacy is concentrated in a few vaccinated subjects, the more deaths and DALYs can be prevented.

This finding is also reflected in the CERs that are more favorable than the reference case if b=0.01 (i.e. efficacy concentrated among fewer individuals), and less favorable if the effect was completely dispersed (Figure 6.9).

Effects of the coverage rate. The reference scenario assumes a fairly high vaccine coverage rate (89%) as reported in Tanzania for DTP-HBV vaccine in year 2003 [Hutton and Tediosi, 2006]. We also simulate a coverage rate of 50%, which is likely to be closer to that in many malaria-endemic countries, and coverage of 100%, which allows us to analyze which effects are due to incomplete coverage. The cost-effectiveness simulations are thus run assuming a low coverage rate (50%) and complete coverage (100%). A lower coverage rate leads to significant reduction in the total number of deaths and of DALYs averted over the 20-year simulation (Figure 6.10).

The cost per death prevented and per DALY averted assuming a coverage rate of 50%

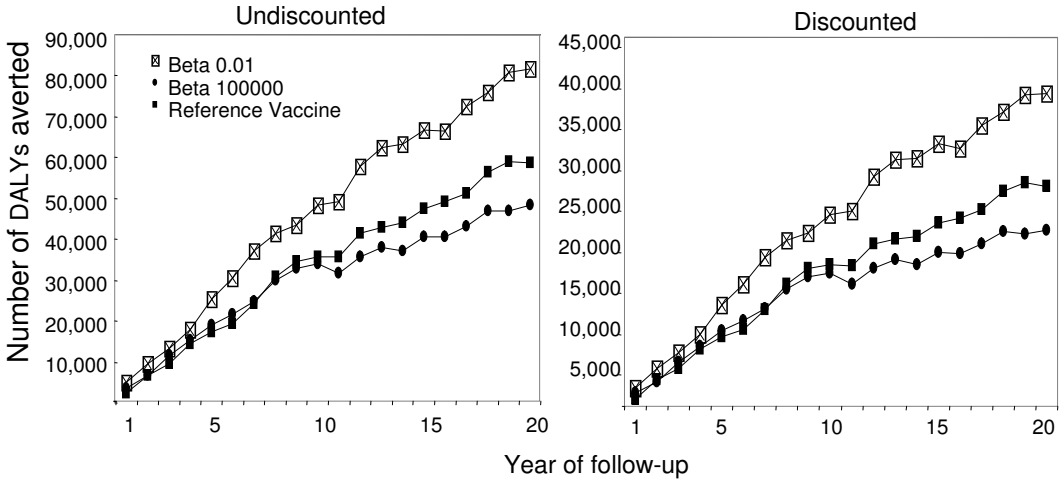

Figure 6.9: Total disability-adjusted life years (DALYs) averted under different assumptions about heterogeneity in initial efficacy.

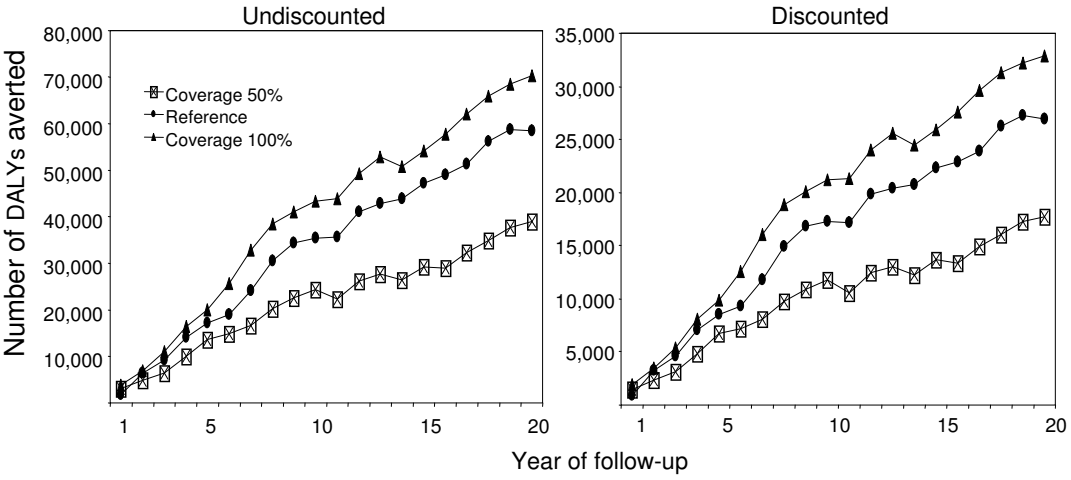

Figure 6.10: Disability-adjusted life years (DALYs) averted under different assumptions about vaccine coverage.

is between 20% and 50% higher than in the reference scenario in the central 10 years of simulation, and is slightly lower in the first and last five years (Table 6.7). A complete coverage would increase slightly the number of deaths prevented and more significantly the number of DALY averted compared to the reference scenario, while the cost per deaths and DALY averted would be slightly lower.

Inclusion of productivity costs. The economic implications of reducing the burden of malaria go beyond the direct costs due to health care treatment. In the sensitivity analysis, we model the cost-effectiveness results including the productivity costs of productive time lost due to the disease. Results are presented for two assumptions of the proportion of malaria episodes where there is a productivity cost associated with the disease: the high productivity cost case where productivity costs are incurred by all episodes predicted by the epidemiologic model, and the low productivity cost case where there are no productivity costs associated with uncomplicated episodes unless the patient seeks treatment.

Over the entire 20-year follow-up period, introducing the vaccine would lead to savings in productivity costs of approximately US $263,634 in the high productivity cost scenario and US $28,443 in the low productivity cost scenario. However, since effects of the vaccine vary over time, the savings in productivity costs also vary over time (Table 6.8). Under the high productivity cost scenario, the savings in productivity costs reduce the total net cost of introducing the vaccine by between 49% and 90% in different time periods at a vaccine price of US $1 per dose. The savings are significantly reduced to an impact on total net cost of 3% to 4% when the vaccine price increases to US $20 per dose.

Table 6.8: Hypothetical value of production time gained due to less time spent ill after vaccine introduction (US $, year 2004)

Time period (years)	High productivity cost scenario		Low productivity cost scenario	
	Undiscounted	Discounted	Undiscounted	Discounted
1-5	63,478	57,173	15,260	14,074
6-10	124,743	98,807	18,603	15,114
11-15	105,779	72,440	6,238	4,407
16-20	59,366	35,214	-8,771	-5,153

Under the low productivity cost scenario, the reductions in the net cost of introducing the vaccine are significantly lower than under the high productivity cost scenario. Total net

cost reductions would occur only in the first three five-year periods, giving reductions of 5% to 7% and 5% at US $1 per dose and under 1% at US $20 per dose. In the fourth five-year period productivity costs would be higher with the vaccine. This leads to an increase in the net cost of introducing the vaccine in the last 10 year of follow-up.

As a consequence, the cost per DALY averted (discounted) is lower when productivity costs are included, as shown in Table 6.9. Under the high productivity cost scenario, the total cost per DALY averted would be between US $1.7 and US $8.1 at a vaccine price of US $1 per dose. These figures represent a reduction in cost per DALY averted of between 63% and 89% when compared to the CER containing only direct costs. However, since the vaccine price increases, the cost per DALY becomes closer to the reference case analysis CER. For example, at US $20 per dose, the cost per DALY averted would be between US $148 and US $227 in different time periods, which is similar to that including only direct costs.

Table 6.9: Cost per DALY averted including direct and productivity costs (US $, year 2004)*

Vaccine price per dose	Time period (years)	Cost per discounted DALY averted	
		High productivity cost scenario	Low productivity cost scenario
1	1-5	3.98	9.76
	6-10	Neg	8.07
	11-15	1.66	15.12
	16-20	8.12	16.80
2	1-5	13.50	18.72
	6-10	6.15	15.73
	11-15	13.88	26.61
	16-20	19.60	27.59
4	1-5	32.55	36.63
	6-10	22.44	31.05
	11-15	38.31	49.59
	16-20	42.56	49.18
6	1-5	51.60	54.54
	6-10	38.73	46.37
	11-15	62.75	72.56
	16-20	65.51	70.77
8	1-5	70.65	72.46
	6-10	55.02	61.69
	11-15	87.18	95.54
	16-20	88.47	92.36
10	1-5	89.70	90.37
	6-10	71.32	77.01
	11-15	111.61	118.52
	16-20	111.43	113.95
20	1-5	180.41	179.93
	6-10	148.91	153.62
	11-15	227.97	233.40
	16-20	220.77	221.91

*DALY = disability-adjusted life year; Neg = cost saving and a health benefit.

6.4 Discussion

We have used a stochastic simulation of *P. falciparum* epidemiology combined with a case management model for a Tanzanian setting (Chapter 3) to explore the potential cost-effectiveness of a pre-erythrocytic malaria vaccine. To our knowledge, this is the first time that dynamic models of malaria transmission and disease have been used to evaluate the cost-effectiveness of malaria vaccines. We have used vaccines with different characteristics introduced by the EPI in Tanzania to illustrate the approach. The models can readily be extended to other types of vaccine and to different epidemiologic and socioeconomic settings.

Over the vaccine price range of US $1.0 to US $20 per dose, the CER is almost proportional to the price per dose, ranging (in the reference analyses) between US $12 and US $190 per (discounted) DALY averted. In the sub-Saharan African context, CERs towards the lower end of this range would be very attractive for health ministries [Goodman et al., 1999, Tan-Torres Edejer et al., 2003]. Up to a vaccine price per dose of almost US $10, the cost per discounted DALY averted remains under US $100. When productivity costs due to morbidity are included, our CERs are even lower than those estimated including only direct costs. However, this difference decreases with the increase of vaccine price. There is little difference between marginal and average costs, which means that substantial savings cannot be achieved by taking up spare capacity in the health system; thus, the cost of the vaccine is the major determinant of costs.

These results should be interpreted in the context of CEA of other malaria control strategies. At vaccine price towards the lower end of the range used, our cost-effectiveness estimates of vaccination compare favorably with those of several other malaria control interventions estimated for the Global Forum for Health Research (GFHR) [Goodman et al., 2000], but these comparisons are problematical because of differences in the methodology. Although the GFHR study used DALY calculations based on an African life table with similar life expectancies to those that we use, our models differ by including dynamic effects that result in age and time shifts in the burden of disease.

The indirect economic impact of malaria is clearly important and we aimed to capture these effects by including productivity costs in some analyses. However, there are many pitfalls in measuring potential or actual economic impact in the context of rural Africa where most of the population is subsistence farmers, child care is often performed by older siblings, work is seasonal, and work inputs may be shifted over time and between household members.

We had no empirical studies available for our estimates of time use or on the impact of malaria episodes on productive capacity. Concerns about equity effects, inadequate data, or methods for estimating economic benefits mean that indirect costs are often excluded from CEA [Chima et al., 2003, Gold et al., 1996]. Indirect costs were not included in the GFHR study [Goodman et al., 2000], or in any other cost-effectiveness studies to date of malaria interventions, and were not included in the analyses underpinning World Health Organization guidelines for CER thresholds for considering health interventions as attractive or very attractive [Tan-Torres Edejer et al., 2003]. Our analyses that include productivity costs are thus even less comparable with those of other studies.

A major impact of malaria on productivity is likely to be by the effects on premature mortality, but it is inappropriate to include in a CEA the costs of mortality, as available from estimates of life-time earnings forgone or willingness to pay studies, since this would result in double counting of the benefits of averting deaths [Drummond et al., 1997, Gold et al., 1996, Weinstein et al., 1996]. Among the microeconomic studies on the economic consequences of malaria published, only one [Shepard et al., 1991] has included productivity costs due to premature mortality. That study estimated the economic burden of malaria and not the cost-effectiveness of interventions.

A malaria vaccine may also have positive impacts on social and economic development that are not captured by the productivity cost savings. Endemic malaria is associated with substantially lower indices of economic development at the national level [Malaney et al., 2004, Sachs and Malaney, 2002], and reducing the burden of malaria might have macroeconomic benefits that are not captured in micro-economic analyses. However the epidemiologic analyses (Chapter 5) clearly indicate that on their own vaccine programs with profiles like those we investigated will avert a proportion of illness events that is much lower than the primary vaccine efficacy, and will have little or no effect on malaria endemicity. In this context, it would be surprising if they had substantial effects on economic development.

We obtain only modest estimates of the wider economic benefits of a vaccination program if we apply the recently suggested approach [Sachs, 2001] of estimating these benefits by multiplying the number of DALYs averted by the average GDP per capita. Using our prediction that a pre-erythrocytic malaria vaccine would avert between 0.013 and 0.029 DALYs per capita per year and the GDP per capita of Tanzania (US $322 in 2005), the annual per capita economic benefits would be between US $4.2 and US $9.3 (according to whether DALYs are discounted and aged weighted).

These conclusions reflect the reference case, but the CER is highly sensitive to assumptions about the epidemiologic setting and vaccine characteristics including the transmission intensity, the efficacy, and duration of protection (Table 6.7). The CER varied with the time since the start of the vaccination program because the epidemiologic model does not reach equilibrium within the time scale of the simulation (Chapter 5). In general, the cost per DALY averted is lower in the first phase of the vaccination program than later, with the highest cost per DALY in the third five-year time period after the start of the program. Extending the duration of protection increases the CERs in the third and fourth five-year time periods. A vaccine boost at some specified time point may have a similar effect, although this would involve additional costs that would be included in calculation of the CER. We have not addressed the emerging problem of drug resistance, which could be included in the case management model and would presumably increase the cost per DALY averted.

Our simulations considered only a limited set of sources of heterogeneity. In particular, we assumed that each person in the simulation was exposed to the same entomologic challenge, and that the chances of being vaccinated were independent of individual susceptibility to disease. We also assumed homogeneous probabilities of accessing health care. Over a period of 20 years, the introduction of a new malaria vaccine would have an impact on the health system and on the case management of malaria. It would be possible to simulate more realistic patterns of heterogeneity but the field data on which to base such models are very limited.

Some counter-intuitive behavior in CERs corresponds to health effects in the model. When episodes are delayed rather than averted, they occur in older individuals who may require larger drug dosages. Thus, the health benefit of delaying illness may be partially offset by increased costs. Since the epidemiologic model also corresponds with field data that suggests a maximum incidence of clinical episodes (though not mortality) at intermediate transmission intensities [Marsh and Snow, 1999, Ross et al., 2006b, Smith et al., 2006c, Trape and Rogier, 1996], it is possible for reductions in malaria transmission to lead to increased case loads.

The proportion of clinical episodes averted varies by transmission intensity (Chapter 5), as do the numbers of DALYs averted. The numbers of clinical episodes continues to decrease after 10 years of the vaccine introduction only in low-transmission scenarios. This is explained by the fact that in high-transmission settings there is an increase in

severe malaria incidence in children more than five years of age, due to reduced accrual of immunity to asexual blood stage parasites during early childhood. In addition, the pyrogenic threshold, which determines the parasite density that leads to acute illness, depends on the recent exposure to parasite and can be lower in vaccinated individuals (Chapter 4). In the model, the lower level of acquired immunity in vaccinated individuals and the resulting inability to effectively control parasite densities also leads to higher proportion of the acute episodes being severe.

An extension to the current work will be to carry out a full probabilistic sensitivity analysis. This will enable us to present acceptability curves in addition to the presentation of CERs in this report. However, the present analyses already indicate that a pre-erythrocytic malaria vaccine, even one with moderate efficacy and minimal effectiveness in reducing transmission to the vector, could be a cost-effective intervention in reducing the intolerable burden of malaria in sub-Saharan Africa.

Chapter 7

Discussion

This thesis discusses some components of an integrated mathematical model for predicting the epidemiologic effects of malaria control interventions. The model provides a unique platform for predicting both the short- and long-term effects of malaria control interventions on the burden of disease, allowing for the temporal dynamics of effects on immunity and transmission.

Chapters 3, 5, and 6 illustrate the application of the integrated set of models. Chapter 3 describes an attempt to use a dynamic model for case management of malaria in sub-Saharan Africa. This model allows the simulation of different rates of treatment coverage and parasitologic cure rates, and makes it possible to look at how variations in transmission intensity might affect the impact of changes in the health system. The case management model also is an important part of simulations that predict the consequences of other control interventions. The epidemiologic impact of an intervention depends on the health system in place, and the net cost of the intervention can be affected by possible savings in health system expenditures due to a reduction in the case load.

Chapter 5 reports the first major attempt to combine dynamic modeling of malaria transmission and control with predictions of parasitologic and clinical outcome. The predictions of the impact of control interventions presented in this chapter focus on malaria control using a pre-erythrocytic vaccine delivered via the Expanded Program on Immunization (EPI). The results suggest a significant impact on morbidity and mortality for a range of assumptions about the vaccine characteristics, but only small effects on transmission intensities.

Chapter 6 explores the potential cost-effectiveness of a pre-erythrocytic malaria vaccine. Depending on the assumed vaccine characteristics and cost, the predicted cost-effectiveness ratios would make vaccination campaigns an attractive choice for health planners compared with other malaria control interventions [Goodman et al., 1999, Tan-Torres Edejer et al., 2003]. These conclusions reflect the reference case, but the cost-effectiveness ratio is sensitive to assumptions about the epidemiologic setting and vaccine characteristics including the transmission intensity, the efficacy and duration of protection (Table 6.7).

Chapters 2 and 4 discuss two components that are important building blocks of the comprehensive model. In addition, the analysis of some of their predictions can also provide insights into the epidemiology and control of malaria. Chapter 2 presents a model for the processes involved in controlling the asexual blood stages of *P. falciparum* infections. This is a central component of the comprehensive model as the densities of asexual blood parasites in part determine the clinical outcomes predicted. In addition, the infectivity of humans to mosquitoes and therefore the modeled effect of an intervention on transmission intensity follows from the simulated blood stage parasite densities (gametocytogenesis is not explicitly modeled [Ross et al., 2006a]). The analysis of models for the control of asexual blood stages can also be used to test hypotheses about the nature of acquired immunity and malaria transmission dynamics. As an example, the model is able to reproduce the shift in peak prevalence as a function of age as transmission intensity increases which is characteristic for diseases with acquired immunity. A good fit to the data requires the consideration of the cumulative parasite densities to which a human host had been exposed. This suggests that the number of parasite strains a host has encountered alone is a poor predictor of acquired immunity. In general, the model appears to reproduce reasonably well the parasitologic patterns seen in malariologic surveys in endemic areas.

Chapter 4 demonstrates that an adequate simulation of the first two RTS,S/AS02A trials published (Bojang et al. [2001], Alonso et al. [2004]) can be achieved by assuming that vaccination completely blocks a certain fraction of infections that would otherwise reach the erythrocytic stages. No additional terms need to be added to modify those infections that survive. The different efficacy estimates against the different outcomes in the two field trials can all be reconciled with the same efficacy in terms of the relative reduction of the force of infection. The close match of the model with the data suggests that the interplay of vaccine-induced and naturally acquired immunity are the main causes of the variations in efficacy between the different outcomes and trials.

The integrated model creates a sound foundation for measuring the effects of introducing new antimalarial interventions (e.g. malaria vaccines), or scaling-up those that are already known to be efficacious and cost-effective. The remainder of this chapter discusses some limitations of the model, and proposes alternatives and extensions of both the model and the analysis of the predictions.

So far, no attempt has been made to simulate immunologic processes in more detail than via the proposed proxies. The longitudinal patterns of blood-stage parasites might be better reproduced by fitting within-host models explicitly incorporating effects of antigenic variation to repeated assessments of parasitemia with short time-intervals. This may be important if interventions that affect the blood stages of the parasite are to be modeled, such as blood stage vaccines or Intermittent Preventive Treatment. Such within-host models have been fitted to data from malariatherapy patients [Molineaux et al., 2001, Paget-McNicol et al., 2002, Recker et al., 2004] but so far there is no agreement that any particular such model is appropriate. Because the modeling approach of the present model is individual-based, it would be possible to amend it to include a more realistic model of within-host dynamics. However, there are few datasets from endemic areas to which longitudinal patterns of parasitemia with short time-intervals can be fitted.

The model for immunity against asexual blood stages assumes that the main mechanisms controlling parasite densities do not decay in the absence of a stimulus. Some immune responses are known to be short lived [Kinyanjui et al., 2003], but it is not obvious which of the immune proxies in the model would correspond to these effectors. The best way to get an estimate of such a decay would be to attempt to fit models with a decay parameter of immunity. It is not clear whether this parameter would be identifiable when fitting such models to the datasets used so far. Such an improved model would have to be validated against longitudinal patterns of parasitemia in semi-immune individuals. In particular, data from people whose exposure is interrupted by well-documented periods of protection from infection would be important to consider if the model is to be applied for predicting the impact of interventions such as vaccination in the context of non-continual exposure to *P. falciparum*. An example of such a dataset is the study of the malaria epidemic in the Madagascar Highlands in the years 1986-1988 [Mouchet et al., 1997].

So far the possibilities for the development and fitting of alternative models have been limited by the need to re-estimate model parameters as a consequence of the modifications. Fitting models to data in these models requires massive computational power, for the

following reasons:

1. The simulations use short time steps of five days because relatively short term fluctuations, for instance in mosquito densities, are very important in driving the epidemiology of malaria, and because the parasite life cycle involves time delays of the order of five days.

2. It is assumed that the simulated populations are in an (immunologic) equilibrium state at the outset of a simulated parasitologic or epidemiologic survey. This requires long warm-up periods prior to the start of the actual simulation.

3. Many of the relevant predictions depend on relatively rare events. A key epidemiologic outcome is the number of malaria-related deaths. Simulations of large numbers of individuals are required to obtain precise predictions of the frequency at which these events would occur.

4. The dimensionality of the parameter-space is relatively high, and therefore requires a large number of iterations of the optimization algorithm for convergence. This can be improved by sequentially fitting parameters of different model components. Parameters of more downstream components are fitted conditional on parameter estimates of upstream modules. Still the process of fitting a single complete model can require several months.

This leads to the need for many millions of individual-based simulation runs, each of which requires in the order of a few hours of CPU time on current mid-range PC. The project has now started using a Volunteer Computing approach to access the necessary computing power. The model implementation was adapted to the Berkeley Open Infrastructure for Network Computing [BOINC]. This platform for Volunteer Computing allows to make use of many thousands of privately owned PCs to run simulations. The first phase of the project had demonstrated the feasibility of such a distributed approach. At that time a desktop grid infrastructure was used to harness the idle time of a few dozen office PCs connected through the intranet at the Swiss Tropical Institute. This showed that the problem lent itself to easy parallelization and distribution.

The tasks can easily be distributed over the internet because the data for individual simulation runs is mostly independent. Moreover the data-to-compute ratio is not limiting: the input data for a single simulation is in the order of just a few kilobytes, and the same is true for the results that are sent back from the clients which run the simulations. Bandwidth is

therefore not limiting even under the assumption that some of the volunteer users connect to the project server over a slow dial-up line. While the turnaround time for results is preferably short, the usual period of a few days to get back most of the results is sufficient for the modeling study.

The port of the simulation software to make use of the virtually unlimited computing power donated by volunteers has removed one limiting factor, and will allow the exploration of a whole ensemble of alternative models in the future. There still remain challenges in efficiently exploiting this resource. Due to the high parallelity of the system, the performance of the process of fitting model parameters to field data is very sensitive to the choice of the underlying optimization algorithm. While the prospect of unlimited computer power can inspire new modeling approaches and allows the study of a number of alternative model specifications, one has to be careful to avoid the pitfalls of overparameterized models with very limited predictive power.

The model for case management presented in Chapter 3 has some limitations because its temporal resolution is the five-day time steps underlying all other model components. However, prompt treatment of malaria episodes is an important determinant of their clinical outcome. Therefore, the case management model is currently being amended to explicitly model case referral, and allow for a more finegrained classification of treatment histories. The main predictions in Chapter 3 assume that sulfadoxine-pyrimethamine (SP) is used as the first-line drug to treat uncomplicated malaria. Parasite resistance to SP has reached critical levels in many parts of Central and East Africa, including Tanzania [Mugittu et al., 2004, Talisuna et al., 2004] and this places a question mark against some of the longer-term predictions of cost-effectiveness, which assume that treatment using SP remains efficacious. By now, many African countries including Tanzania have replaced SP with artemisinin-based combination therapy (ACT) as the first line treatment for uncomplicated malaria [World Health Organization, 2004]. This change to a highly efficacious drug has implications for both the epidemiologic predictions of the model (Chapter 3, Effective treatment scenario), and more importantly on the cost of treatment and therefore the predicted cost-effectiveness of control interventions if they result in a lower number of treatments. Future predictions will therefore be based on case management with ACT as the first line treatment of malaria as the default.

With the renewed interest in malaria elimination, the question arises whether the modeling approach chosen can go beyond its original goal of predicting the comparative cost-

effectiveness of malaria control interventions in endemic settings. The models described in this thesis should not be used in this context, for at least two reasons. One reason why one should have more confidence in predictions in intermediate or high transmission settings is that most of the data used for the parameter estimation comes from locations with these transmission characteristics. In addition, it is likely that heterogeneity in transmission is an important aspect in marginal settings, i.e. that transmission is focal, and differentially affects humans. Alternative models for the infection of human hosts that address this issue are currently being developed (Smith, in preparation).

While the model parameters were estimated from field data where this was possible, many uncertainties and approximations regarding the vaccine characteristics remain. The assumptions about the profile of the reference vaccine scenario in the previous chapters were based on the data from clinical trials of RTS,S/AS02A that were available at that time (Bojang et al. [2001], Alonso et al. [2004]). New data from vaccine trials has since then become available, and should be taken into account when discussing the simulation predictions. The half life of the protective efficacy of the vaccine was identified as an important driver of the cumulative effectiveness. Alonso and colleagues [2005] report that there was no significant reduction in the protective effect when they followed the cohorts from the RTS,S/AS02A trial in Manhiça [Alonso et al., 2004] for a total of 21 months. The power of this analysis is relatively small, but at least the data does not indicate that there is substantial waning of the protective efficacy within the first 21 months. The predictions in Chapter 5 suggest that a pre-erythrocytic vaccine with a half life of less than 2 years shows relatively little effectiveness. A recent analysis of simulation results with a bigger sample size and refitted parameters (see below) confirm these predictions (data not shown). The uncertainty in the field estimate of the initial efficacy of RTS,S/AS02A remains substantial. In addition, the efficacy of incomplete courses of vaccination are unknown. This may be a critical factor if there is a high drop out rate, for example if the vaccine is delivered outside the EPI. The best one can do here is to explore and document the sensitivity of the model predictions to a range of input values.

The latest results from a clinical trial of RTS,S/AS02A show that the vaccine is safe and efficacious in infants [Aponte et al., 2007]. This is important because all current predictions of the epidemiologic impact and cost-effectiveness assume that the vaccine will be delivered through the EPI, and therefore that the vaccine will be administered to children during the first months of their life.

Since no vaccinated child reached more than 20 years of age in the simulations which predict the impact of introducing a vaccine into the EPI, very long-term effects of vaccination are not captured. This is important when comparing different decays or initial efficacies, as the relationship between the duration during of protection and the life-expectancy of the vaccinated individual may be important in determining the effectiveness. However, we are very uncertain about the risk of severe malaria that such adults would experience. There are few data available from which to estimate severe malaria risk in adolescents or adults with limited previous exposure [Ross et al., 2006b].

All the predictions presented in Chapter 5 are point estimates. This presentation is appropriate as the model, despite its stochastic nature, should deliver predictions with an arbitrary precision for any scenario for a given set of input parameters. Given the simulations assume a homogenous population of human individuals, the simulated population size can in principle be as large as necessary, thus removing any noise that will affect the predictions due to stochasticity. However, at the time of publication of the predictions of the impact of improved case management (Chapter 3) and the impact of a pre-erythrocytic vaccine (Chapters 5,6), the computing resources for running simulations and analyzing the results were limiting. Therefore all these predictions were based on single runs of any scenario with a population size of 100,000 simulated individuals. While this is likely to be appropriate for the prediction of frequent events like uncomplicated malaria episodes, some of the result indicate that the simulation of larger populations may be appropriate for prediction rare outcomes like mortality (see Figures 5.5, 5.6).

The predictive simulations of the impact of a pre-erythrocytic vaccine have now been rerun for the reference vaccine case (Table 5.1). These new predictions are based on 100 simulation runs with a simulated human population of 100,000 individuals each. All model parameters were previously re-estimated by simultaneously fitting all model components to the 61 parasitologic and epidemiologic datasets available. In general, the results (data not shown) confirm the results reported in Chapter 5.

As the cost-effectiveness analysis of the vaccine (Chapter 6) was based on the predictions of the epidemiologic impact of the vaccine, there are also only point estimates available. Table 6.7 suggests considerable stochastic variation in the prediction of the cost per death averted. Using the same set of predictions as above, this analysis has been repeated. Again, the result (not shown) confirms that the estimates presented in Chapter 6 are in the correct range for most outcomes. This indicates that the simulated population sizes

are appropriate for most outcomes, but reveals that accurate predictions of mortality may need bigger sample sizes. The predictions of neurologic sequelae are very noisy even with a simulated population size of 10 million individuals. Point estimates may not be appropriate when simulating scenarios where stochasticity is important, i.e. very low transmission settings where elimination is likely (the limitations of the model under these circumstances were discussed previously).

That these results more or less confirm the earlier findings is reassuring for a number of reasons. First, the point estimates in Chapters 5 and 6, in most cases, do not seem to be too noisy. Second, the simulation software has undergone significant changes during the port to the BOINC volunteer computing platform. This did not seem to affect the results. The same is true for the software that is now in use to allow a more automated analysis of simulation predictions. Finally, the predictions are not substantially affected by the refitting of the model parameters using a different approach.

These new predictions using bigger sample sizes also provide an opportunity for a more detailed analysis of some of the epidemiologic outcomes. Chapter 5 reports only the total number of deaths, or deaths averted by the vaccine. This includes both direct and indirect deaths averted [Ross et al., 2006b]. The disaggregation into the two components reveals that the evaluation of a real world vaccine intervention will miss an important effect of the vaccine if only malaria-specific mortality is considered (data not shown). The simulations suggest that the effectiveness due the prevention of indirect deaths may be much more important. Indirect deaths will, by definition, not be included in malaria-specific mortality statistics [Ross et al., 2006b]. At the end of the 20-year intervention period, a rebound of direct mortality is observed, while the predicted incidence of the all malaria-related deaths (direct plus indirect) is still lower in the vaccine scenario. However, one should be cautious in interpreting this prediction. The 20-year time span, chosen to cover the maximum planning phase a policy maker would reasonably consider, means that some of the vaccinated children reach an age for which data to appropriately fit the relevant model parameters is rare, and may not be as reliable as the data for young children [Ross et al., 2006b].

Most results in previous chapters that were presented over time used a temporal resolution of one or more years. This is useful for readability, but ignores the fact that the transmission intensity or potential is usually seasonal. A higher temporal resolution brings up an interesting prediction of potential importance if the simulation model is to be used for

health planning. By analyzing the number of events averted in quarterly intervals (data not shown) the impact of the seasonal changes in transmission intensity becomes apparent. During the second half of the 20-year intervention period, the number of events averted is negative for some time during each year. This could be either because the annual peak incidence is shifted to another time of the year, or because the incidence becomes either more or less seasonal. This observation merits closer investigation, as it may have important implications for the accuracy of malaria diagnosis. It has been suggested that algorithms for clinical diagnosis of malaria should take seasonality into account in low endemicity settings [Breman, 2001].

One factor that is a potential driver of the cost-effectiveness of a vaccine was not taken into account in the previous analysis. In order to maintain a stable age-distribution in the simulated population, the demographic model (Chapter 2) relies on out-migration of human individuals. Note, that while the process of removing individuals from the population is called out-migration here, this simply implies that individuals are removed from the population due to events that are not related to malaria. The cost of a vaccination program, and therefore its cost-effectiveness, depends on the number of vaccine doses delivered. Out-migration may cause the observed cost-effectiveness ratio for a vaccine to appear less favorable if some of the protective effect is lost to out-migrating individuals. Because out-migration in this demographic model mostly affects young individuals, and the vaccine is assumed to be delivered via the EPI in the simulations discussed here, a significant proportion of vaccinees is removed from the population shortly after receiving the vaccine. With the current model and associated parameters for demography, more than half of the vaccine doses remain in the population for less than one year (data not shown). The effect of this on cost-effectiveness is difficult to quantify, and will vary for different epidemiologic outcomes. On one hand, there are a number of vaccine doses lost before the full potential benefit is reached, on the other hand the outmigrated individuals are part of the predictions while the vaccine still has a high level of efficacy and at the same time do not contribute to the observed rebound. In addition, the simulated out-migrations include non-malaria specific deaths as well as migration events. The two would need to be separated in order to predict the proportion of vaccine doses that are lost versus the vaccine benefits that would simply be missed when locally evaluating the impact of a vaccine program. Further analysis is needed to learn more about the dependence of the cost-effectiveness on the details of the demographic model. It may be necessary to more explicitly distinguish between different demographic processes in order to separate births

and deaths from migration.

The main objective of the malaria model described here is to make quantitative predictions. In addition to that, a good model should provide a means of identifying current gaps in knowledge that need to be filled for rational planning of malaria control strategies by identifying the most important drivers of the predicted outcomes. Sensitivity analysis of the predictions due to input data is a powerful tool to identify potential weaknesses in the data required to make accurate predictions. While confidence intervals for the fitted parameters of the mathematical model have been calculated (Table 2.3), this information has not been used to do a sensitivity analysis of the predictions reported in previous chapters. A thorough sensitivity analysis is still outstanding, but preliminary results of a probabilistic sensitivity analysis suggest that some of the epidemiologic outcomes are sensitive to parameters that define age-specific effects (e.g. the risk of severe malaria or indirect mortality due to co-morbidity). All such parameters, as well as non-parametric age-specific functions like the case-fatality rate, are potentially important because the main effect of an intervention like a pre-erythrocytic vaccine is to reduce the force of infection in vaccinated individuals, and therefore to shift malaria-related events to a later age. These findings emphasize the importance of good data on malaria of adolescents and adults.

The focus of this thesis is on the predictions of the impact and cost-effectiveness of pre-erythrocytic vaccines delivered via the EPI. The application of the models described can be extended to include other means of deployment (including regimens with booster doses of vaccines or mass-vaccination campaigns), to other types of vaccines (asexual blood stage and transmission blocking), and other control interventions listed in Chapter 1. It will be interesting to evaluate and compare different interventions, but also to investigate the effect of combining several interventions into an integrated control program. The predictions of the impact of a pre-erythrocytic vaccine have shown that such a vaccine will be most effective at low transmission intensities, but that on its own it is unlikely to significantly reduce transmission except, possibly, when this is already low. In areas with moderate to high transmission, it may be that such a vaccine will be most effective if it is deployed in conjunction with measures that reduce the vectorial capacity at the same time.

As a consequence of the computational demands and the resulting complexity of the software environment, the integrated model does not allow for real-time exploratory analysis. The process of preparing input data for simulation runs, running the simulations, and

analyzing the results can take several days depending on the nature and scope of the desired predictions. Enabling health planners and decision makers to effectively work with the products of the simulation models despite these constraints remains one of the great challenges. The project is therefore developing a web-based computer platform that will enable stakeholder groups to prioritize both strategies to be simulated and the outputs generated. This will complement the planned publication of future model predictions in the peer-reviewed literature, which will always be restricted to a subset of the findings that can be of interest to the scientific community. The epidemiologic predictions will be linked with estimated intervention and case management costs for these scenarios to generate comparative analyzes of the cost-effectiveness of all the interventions, when delivered via different plausible delivery strategies. Summaries of the organizational, financial, and economic implications of implementing and/or scaling them up will be derived, as well as approximate estimates of populations at risk at different levels of endemicity. These will together make it possible to predict the disease burden likely to be averted by any particular intervention strategy. Predictions will be made with as many different validated models as are available, eventually leading to ensembles of predictions for each scenario.

The web-interface to a comprehensive set of model predictions can be valuable both for informing malaria control strategies and research funding policy. The acceptability among decision makers will depend on more than the scientific quality of the data made available. This point is reinforced by a statement of Habbema and colleagues [1992], who emphasize that usability and adaptability are central if models are to be an integral part of a disease control program. The authors were responsible for the modeling part of the Onchocerciasis Control Program in West Africa. Mathematical modeling made a significant contribution to the success of that program. Usability of the interface and high-level documentation accessible to a non-modeler audience will be important success factors for the model predictions to make a contribution to the control of malaria.

Bibliography

T. A. Abeku, S. I. Hay, S. Ochola, P. Langi, B. Beard, S. J. de Vlas, and J. Cox. Malaria epidemic early warning and detection in African highlands. *Trends Parasitol*, 20:400–405, 2004.

T. Adam, C. Kakundwa, F. Manzi, J. A. Schellenberg, L. Mgalula, D. de Savigny, C. Mbuya, and K. Wilczynska. Analysis Report on the Costs of IMCI in Tanzania. Multi-Country Evaluation of the Integrated Management of Childhood Illness (IMCI). Technical report, WHO, Geneva, 2004.

P. L. Alonso, T. Smith, J. R. Schellenberg, H. Masanja, S. Mwankusye, H. Urassa, I. Bastos de Azevedo, J. Chongela, S. Kobero, and C. Menendez. Randomised trial of efficacy of SPf66 vaccine against Plasmodium falciparum malaria in children in southern Tanzania. *Lancet*, 344:1175–1181, 1994.

P. L. Alonso, M. E. Molyneux, and T. Smith. Design and methodology of field-based intervention trials of malaria vaccines. *Parasitol Today*, 11:197–200, 1995.

P. L. Alonso, F. Saute, J. Aponte, F. X. Gomez-Olive, A. Nhacalo, R. Thompson, E. Macete, F. Abacassamo, P. J. Ventura, X. Bosch, C. Mendendez, and M. Dgedge. *Manhiça DSS, Mozambique*. Population and Health in Developing Countries. IDRC, Ottawa, 2002.

P. L. Alonso, J. Sacarlal, J. Aponte, A. Leach, E. Macete, J. Milman, I. Mandomando, B. Spiessens, C. Guinovart, M. Espasa, Q. Bassat, P. Aide, O. Ofori-Anyinam, M. M. Navia, S. Corachan, M. Ceuppens, M. C. Dubois, M. A. Demoitie, F. Dubovsky, C. Menendez, N. Tornieporth, W. R. Ballou, R. Thompson, and J. Cohen. Efficacy of the RTS,S/AS02A vaccine against Plasmodium falciparum infection and disease in young African children: randomised controlled trial. *Lancet*, 364:1411–1420, 2004.

P. L. Alonso, J. Sacarlal, J. J. Aponte, A. Leach, E. Macete, P. Aide, B. Sigauque, J. Milman, I. Mandomando, Q. Bassat, C. Guinovart, M. Espasa, S. Corachan, M. Lievens, M. M. Navia, M.-C. Dubois, C. Menendez, F. Dubovsky, J. Cohen, R. Thompson, and W. R. Ballou. Duration of protection with RTS,S/AS02A malaria vaccine in prevention of Plasmodium falciparum disease in Mozambican children: single-blind extended follow-up of a randomised controlled trial. *Lancet*, 366:2012–2018, 2005.

M. Alonso-Gonzalez, C. Menendez, F. Font, E. Kahigwa, J. Kimario, H. Mshinda, M. Tanner, X. Bosch-Capblanch, and P. L. Alonso. Cost-effectiveness of iron supplementation and malaria chemoprophylaxis in the prevention of anaemia and malaria among Tanzanian infants. *Bull World Health Organ*, 78:97–107, 2000.

R. M. Anderson and R. M. May. *Infectious Diseases of Humans: Dynamics and Control.* Oxford University Press, Oxford, 1991.

R. M. Anderson, R. M. May, and S. Gupta. Non-linear phenomena in host-parasite interactions. *Parasitology*, 99 Suppl:S59–S79, 1989.

J. J. Aponte, P. Aide, M. Renom, I. Mandomando, Q. Bassat, J. Sacarlal, M. N. Manaca, S. Lafuente, A. Barbosa, A. Leach, M. Lievens, J. Vekemans, B. Sigauque, M. Dubois, M. Demoiti, M. Sillman, B. Savarese, J. G. McNeil, E. Macete, W. R. Ballou, J. Cohen, and P. L. Alonso. Safety of the RTS,S/AS02D candidate malaria vaccine in infants living in a highly endemic area of Mozambique: a double blind randomised controlled phase I/IIb trial. *Lancet*, 370:1543–1551, 2007.

C. Aranda, J. J. Aponte, F. Saute, S. Casimiro, J. Pinto, C. Sousa, V. do Rosario, V. Petrarca, M. Dgedge, and P. Alonso. Entomological characteristics of malaria transmission in Manhiça, a rural area in southern Mozambique. *J Med Entomol*, 42:180–186, 2005.

J. L. Aron. Mathematical modeling of immunity to malaria. *Math Biosci*, 90:385–396, 1988.

H. Babiker, L. Ranford-Cartwright, D. Currie, J. D. Charlwood, P. Billingsley, T. Teuscher, and D. Walliker. Random mating in a natural population of the malaria parasite Plasmodium falciparum. *Parasitology*, 109:413–421, 1994.

W. R. Ballou, M. Arevalo-Herrera, D. Carucci, T. L. Richie, G. Corradin, C. Diggs, P. Druilhe, B. K. Giersing, A. Saul, D. G. Heppner, K. E. Kester, D. E. Lanar, J. Lyon,

A. V. Hill, W. Pan, and J. D. Cohen. Update on the clinical development of candidate malaria vaccines. *Am J Trop Med Hyg*, 71 (Suppl 2):239–247, 2004.

J. C. Beier, C. N. Oster, F. K. Onyango, J. D. Bales, J. A. Sherwood, P. V. Perkins, D. K. Chumo, D. V. Koech, R. E. Whitmire, and C. R. Roberts. Plasmodium falciparum incidence relative to entomologic inoculation rates at a site proposed for testing malaria vaccines in western Kenya. *Am J Trop Med Hyg*, 50:529–536, 1994.

J. C. Beier, G. Killeen, and J. I. Githure. Short report: entomologic inoculation rates and Plasmodium falciparum malaria prevalence in Africa. *Am J Trop Med Hyg*, 61:109–113, 1999.

F. Binka, A. Nazzar, and J. F. Phillips. The Navrongo Community Health and Family Planning Project. *Stud Fam Plann*, 26:121–139, 1995.

F. Binka, A. Kubaje, M. Adjuik, L. A. Williams, C. Lengeler, G. Maude, G. E. Armah, B. Kajihara, J. H. Adiamah, and P. G. Smith. Impact of permethrin impregnated bednets on child mortality in Kassena-Nankana district, Ghana: a randomized controlled trial. *Trop Med Int Health*, 1:147–154, 1996.

BOINC. Berkeley Open Infrastructure for Network Computing. `http://boinc.berkeley.edu`.

K. Bojang, P. J. M. Milligan, M. Pinder, L. Vigneron, A. Alloueche, K. E. Kester, W. R. Ballou, D. Conway, W. H. H. Reece, P. Gothard, L. Yamuah, M. Delchambre, G. Voss, B. M. Greenwood, A. Hill, K. P. McAdam, N. Tornieporth, J. D. Cohen, and T. Doherty. Efficacy of RTS,S/AS02 malaria vaccine against Plasmodium falciparum infection in semi-immune adult men in The Gambia: a randomised trial. *Lancet*, 358:1927–1934, 2001.

J. G. Breman. The ears of the hippopotamus: manifestations, determinants, and estimates of the malaria burden. *Am J Trop Med Hyg*, 64 (Suppl):1–11, 2001.

J. G. Breman, A. Egan, and G. T. Keusch. The intolerable burden of malaria: a new look at the numbers. *Am J Trop Med Hyg*, 64 (Suppl):iv–vii, 2001.

D. R. Brewster, D. Kwiatkowski, and N. J. White. Neurological sequelae of celebral malaria in children. *Lancet*, 336:1039–1043, 1990.

G. A. Butcher. Antimalarial drugs and the mosquito transmission of Plasmodium. *Int J Parasitol*, 27:975–987, 1997.

I. A. Carneiro, T. Smith, J. P. A. Lusingu, R. Malima, J. Utzinger, and C. J. Drakeley. Modeling the relationship between the population prevalence of Plasmodium falciparum malaria and anemia. *Am J Trop Med Hyg*, 75 (Suppl 2):82–89, 2006.

J. D. Charlwood, T. Smith, E. Lyimo, A. Kitua, H. Masanja, M. Booth, P. L. Alonso, and M. Tanner. Incidence of Plasmodium falciparum infection in infants in relation to exposure to sporozoite-infected anophelines. *Am J Trop Med Hyg*, 59:243–251, 1998.

R. I. Chima, C. A. Goodman, and A. Mills. The economic impact of malaria in Africa: a critical review of the evidence. *Health Policy*, 63:17–36, 2003.

D. F. Clyde. *Malaria in Tanzania*. Oxford University Press, London, Oxford, 1967.

W. E. Collins and G. M. Jeffery. A retrospective examination of the patterns of recrudescence in patients infected with Plasmodium falciparum. *Am J Trop Med Hyg*, 61:44–48, 1999a.

W. E. Collins and G. M. Jeffery. A retrospective examination of sporozoite- and trophozoite-induced infections with Plasmodium falciparum in patients previously infected with heterologous species of Plasmodium: effect on development of parasitologic and clinical immunity. *Am J Trop Med Hyg*, 61:36–43, 1999b.

B. Cooper and M. Lipsitch. The analysis of hospital infection data using hidden Markov models. *Biostatistics*, 5:223–237, 2004.

M. Craig, R. Snow, and D. Le Sueur. A climate-based distribution model of malaria transmission in sub-Saharan Africa. *Parasitol Today*, 15:105–111, 1999.

D. de Savigny, C. Mayombana, E. Mwageni, H. Masanja, A. Minhaj, Y. Mkilindi, C. Mbuya, H. Kasale, and G. Reid. Care-seeking patterns for fatal malaria in Tanzania. *Malar J*, 3:27, 2004.

P. Deloron and C. Chougnet. Is immunity to malaria really short-lived? *Parasitol Today*, 8:375–378, 1992.

K. Dietz, L. Molineaux, and A. Thomas. A malaria model tested in the African savannah. *Bull World Health Org*, 50:347–357, 1974.

C. Drakeley, D. Schellenberg, J. Kihonda, C. A. Sousa, A. P. Arez, D. Lopes, J. Lines, H. Mshinda, C. Lengeler, S. J. Armstrong, M. Tanner, and P. Alonso. An estimation of the entomological inoculation rate for Ifakara: a semi-urban area in a region of intense malaria transmission in Tanzania. *Trop Med Int Health*, 8:767–774, 2003.

M. B. Drummond, B. O'Brien, G. L. Stoddart, and G. Torrance. *Methods for the economic evaluation of health care programmes.*, volume 2. Oxford University Press, Oxford, 1997.

C. Dye and G. Hasibeder. Population dynamics of mosquito-borne disease: effects of flies which bite some people more frequently than others. *Trans R Soc Trop Med Hyg*, 80: 69–77, 1986.

W. C. Earle and M. Perez. Enumeration of parasites in the blood of malarial patients. *J Lab Clin Med*, 17:1124–1132, 1932.

W. J. Edmunds, A. Dejene, Y. Mekonnen, M. Haile, W. Alemnu, and D. J. Nokes. The cost of integrating Hepatitis B virus vaccine into national immunization programmes: a case study from Addis Ababa. *Health Policy Plan*, 15:408–16, 2000.

R. H. Elderkin, D. P. Berkowitz, F. A. Farris, C. F. Gunn, F. J. Hickernell, S. N. Kass, F. I. Mansfield, and R. G. Taranto. *On the steady state of an age-dependent model for malaria*, pages 491 –512. Nonlinear Systems and Applications. Academic Press, New York, 1977.

D. E. Eyles and M. Young. The duration of untreated or inadequately treated Plasmodium falciparum infections in the human host. *J Natl Malar Soc*, 10:327–336, 1951.

J. Fox-Rushby and K. Hanson. Calculating and presenting disability adjusted life years (DALYs) in cost-effectiveness analysis. *Health Policy Plan*, 16:326–331, 2001.

J. L. Gallup and J. Sachs. The economic burden of malaria. *Am J Trop Med Hyg*, 64: 85–96, 2001.

M. L. Gatton and Q. Cheng. Investigating antigenic variation and other host-parasite interactions in Plasmodium falciparum infection in naive hosts. *Parasitology*, 128:367–376, 2004.

Y. Geissbuehler, P. Chaki, B. Emidi, N. Govella, R. Shirima, V. Mayagaya, , D. Mtasiwa, H. Mshinda, U. Fillinger, S. Lindsay, K. Kannady, M. de Castro, M. Tanner, and

G. Killeen. Interdependence of domestic malaria prevention measures and mosquito-human interactions in urban Dar es Salaam, Tanzania. *Malar J*, 6:126, 2007.

GFATM. http://www.theglobalfund.org/search/portfolio.aspx?countryid=tnz. 2004.

H. M. Gilles and D. A. Warrell. *Bruce-Chwatt's Essential Malariology, Third Edition*. Edward Arnold, London, 1993.

M. T. Gillies. *Anophiline mosquitos: vector behaviour and bionomics. In: Malaria. Principles and Practice of Malariology (Editors: W.H. Wernsdorfer and I. McGregor)*, pages 453–485. Churchill Livingstone, Edinburgh, 1988.

J. R. Glynn and D. J. Bradley. Inoculum size, incubation period and severity of malaria. analysis of data from malaria therapy records. *Parasitology*, 110:7–19, 1995.

M. R. Gold, S. R. Gold, and M. C. Weinstein. *Cost-effectiveness in health and medicine*. Oxford University Press, Oxford, 1996.

C. A. Goodman, P. G. Coleman, and A. Mills. Cost-effectiveness of malaria control in sub-Saharan Africa. *Lancet*, 354:378–385, 1999.

C. A. Goodman, P. G. Coleman, and A. Mills. *Economic analysis of malaria control in sub-Saharan Africa*. Global Forum for Health Research, Geneva, 2000.

B. Greenwood. Review: Intermittent preventive treatment - a new approach to the prevention of malaria in children in areas with seasonal malaria transmission. *Trop Med Int Health*, 11:983–991, 2006.

B. Greenwood, K. Bojang, C. Whitty, and G. Targett. Malaria. *Lancet*, 365:1487–1498, 2005.

B. M. Greenwood, F. Groenendaal, A. K. Bradley, A. M. Greenwood, F. Shenton, S. Tulloch, and R. Hayes. Ethnic differences in the prevalence of splenomegaly and malaria in The Gambia. *Ann Trop Med Parasitol*, 81:345–354, 1987.

U. Griffiths, G. Hutton, and E. das Dores Pascoal. Cost-effectiveness of introducing Hepatitis B vaccine into the infant immunization schedule in Mozambique. *Health Policy Plan*, 20:50–59, 2005.

V. Grimm and S. F. Railsback. *Individual-based Modeling and Ecology*. Princeton University Press, Princeton, 2005.

S. Gupta and K. P. Day. A theoretical framework for the immunoepidemiology of Plasmodium falciparum malaria. *Parasite Immunol*, 16:361–370, 1994.

J. D. F. Habbema, E. S. Alley, A. P. Plaisier, G. J. van Oortmarssen, and J. H. F. Remme. Epidemiological modeling for onchocerciasis control. *Parasitol Today*, 8:99–103, 1992.

A. J. Hall, R. L. Robertson, P. E. Crivelli, Y. Lowe, H. Inskip, S. K. Snow, and H. Whittle. Cost-effectiveness of hepatitis B vaccine in The Gambia. *Trans R Soc Trop Med Hyg*, 87:333–6, 1993.

M. E. Halloran, C. J. Struchiner, and A. Spielman. Modeling malaria vaccines. ii: Population effects of stage-specific malaria vaccines dependent on natural boosting. *Math Biosci*, 94:115–149, 1989.

M. E. Halloran, M. Haber, and I. M. J. Longini. Interpretation and estimation of vaccine efficacy under heterogeneity. *Am J Epidemiol*, 136:328–343, 1992.

M. E. Halloran, L. Watelet, and C. J. Struchiner. Epidemiologic effects of vaccines with complex direct effects in an age-structured population. *Math Biosci*, 121:193–225, 1994.

M. E. Halloran, I. M. J. Longini, and C. J. Struchiner. Estimability and interpretation of vaccine efficacy using frailty mixing models. *Am J Epidemiol*, 144:83–97, 1996.

S. I. Hay, D. J. Rogers, J. F. Toomer, and R. Snow. Annual Plasmodium falciparum entomological inoculation rates (EIR) across Africa: literature survey, Internet access and review. *Trans R Soc Trop Med Hyg*, 94:113–127, 2000.

Health Research for Action. Health Care Financing in Tanzania: Costing study of health services. Final Report. Technical report, Laarstraat, Belgium, 1999.

P. A. Holding and R. Snow. Impact of Plasmodium falciparum malaria on performance and learning: review of the evidence. *Am J Trop Med Hyg*, 64:68–75, 2001.

M. G. Hudgens, P. B. Gilbert, and S. G. Self. Endpoints in vaccine trials. *Stat Meth Med Res*, 13:89–114, 2004.

G. Hutton and F. Tediosi. The costs of introducing a malaria vaccine through the expanded program on immunization in Tanzania. *Am J Trop Med Hyg*, 75 (Suppl 2):119–130, 2006.

INDEPTH Network. *Population, Health and Survival at INDEPTH Sites*. IDRC, Ottawa, 2002.

INDEPTH Network. *Model Life Tables for Sub-Saharan Africa*. Ashgate, Aldershot, England, 2004.

J. Keiser, J. Utzinger, M. C. De Castro, T. A. Smith, M. Tanner, and B. Singer. Urbanization in sub-Saharan Africa and implication for malaria control. *Am J Trop Med Hyg*, 71:118–127, 2004.

K. E. Kester, D. A. McKinney, N. Tornieporth, C. F. Ockenhouse, D. G. Heppner, T. Hall, U. Krzych, M. Delchambre, G. Voss, M. G. Dowler, J. Palensky, J. Wittes, J. Cohen, and W. R. Ballou. Efficacy of recombinant circumsporozoite protein vaccine regimens against experimental Plasmodium falciparum malaria. *J Infect Dis*, 183:640–647, 2001.

G. F. Killeen, A. Ross, and T. Smith. Infectiousness of malaria-endemic human populations to vectors. *Am J Trop Med Hyg*, 76 (Suppl 2):38–45, 2006.

S. M. Kinyanjui, P. Bull, C. Newbold, and K. Marsh. Kinetics of antibody responses to Plasmodium falciparum-infected erythrocyte variant surface antigens. *J Infect Dis*, 187: 667–674, 2003.

S. Kirkpatrick, C. D. J. Gelatt, and M. P. Vecchi. Optimization by simulated annealing. *Science*, 220:671–680, 1983.

A. Kitua, T. Smith, P. L. Alonso, H. Masanja, H. Urassa, C. Menendez, J. Kimario, and M. Tanner. Plasmodium falciparum malaria in the first year of life in an area of intense and perennial transmission. *Trop Med Int Health*, 1:475–484, 1996.

I. Kleinschmidt, B. Sharp, I. Mueller, and P. Vounatsou. Rise in malaria incidence rates in south africa: a small-area spatial analysis of variation in time trends. *Am J Epidemiol*, 155:257–264, 2002.

J. C. Koella. On the use of mathematical models of malaria transmission. *Acta Trop*, 49: 1–25, 1991.

C. Lengeler. Insecticide-treated bed nets and curtains for preventing malaria. *Cochrane Database of Systematic Reviews*, 2004.

M. Lipsitch, T. Cohen, B. Cooper, J. M. Robins, S. Ma, L. James, G. Gopalakrishna, S. K. Chew, C. C. Tan, M. H. Samore, D. Fisman, and M. Murray. Transmission dynamics and control of severe acute respiratory syndrome. *Science*, 300:1966–1970, 2003.

G. Macdonald. *The epidemiology and control of malaria*. Oxford University Press, London, 1957.

G. Macdonald, C. B. Cuellar, and C. V. Foll. The dynamics of malaria. *Bull World Health Org*, 38:743–755, 1968.

P. Malaney, A. Spielman, and J. Sachs. The malaria gap. *Am J Trop Med Hyg*, 71(Suppl 2):141–146, 2004.

K. Marsh and R. Snow. Malaria transmission and morbidity. *Parassitologia*, 41:241–246, 1999.

S. C. McCombie. Treatment seeking for malaria: a review of recent research. *Soc Sci Med*, 43:933–945, 1996.

S. C. McCombie. Self-treatment for malaria: the evidence and methodological issues. *Health Policy Plan*, 17:333–344, 2002.

F. E. McKenzie. Why model malaria? *Parasitol Today*, 16:511–516, 2000.

F. E. McKenzie and E. M. Samba. The role of mathematical modeling in evidence-based malaria control. *Am J Trop Med Hyg*, 71 (Suppl 2):94–96, 2004.

M. M. Meremikwu, A. A. A. Omari, and P. Garner. Chemoprophylaxis and intermittent treatment for preventing malaria in children (review). *The Cochrane Library*, 2006.

Ministry of Health, Tanzania. National Guidelines for Malaria Diagnosis and Treatment. Malaria Control Series 2000. Technical report, Dar es Salaam, Tanzania, 2000.

D. Modiano, V. Petrarca, B. S. Sirima, I. Nebie, D. Diallo, F. Esposito, and M. Coluzzi. Different response to Plasmodium falciparum malaria in West African sympatric ethnic groups. *Proc Natl Acad Sci USA*, 93:13206–13211, 1996.

L. Molineaux and K. Dietz. Review of intra-host models of malaria. *Parassitologia*, 41: 221–231, 1999.

L. Molineaux and G. Gramiccia. *The Garki Project*. World Health Organisation, Geneva, 1980.

L. Molineaux, D. A. Muir, H. C. Spencer, and W. H. Wernsdorfer. *The epidemiology of malaria and its measurement. In: Malaria. Principles and Practice of Malariology (Editors: W.H. Wernsdorfer and I. McGregor)*, pages 999–1089. Churchill Livingstone, Edinburgh, 1988.

L. Molineaux, H. H. Diebner, M. Eichner, W. E. Collins, G. M. Jeffery, and K. Dietz. Plasmodium falciparum parasitaemia described by a new mathematical model. *Parasitology*, 122:379–391, 2001.

J. Mouchet, S. Laventure, S. Blanchy, R. Fioramonti, A. Rakotonjanabelo, P. Rabarison, J. Sircoulon, and J. Roux. La reconquête des Hautes Terres de Madagascar par le paludisme. *Bull Soc Pathol Exot*, 90:162–168, 1997.

MSD. Medical store department price catalog. 2004.

S. H. Muela, J. M. Ribera, A. K. Mushi, and M. Tanner. Medical syncretism with reference to malaria in a Tanzanian community. *Soc Sci Med*, 55:403–413, 2002.

K. Mugittu, M. Ndejembi, A. Malisa, M. Lemnge, Z. Premji, A. Mwita, W. Nkya, J. Kataraihya, S. Abdulla, H. P. Beck, and H. Mshinda. Therapeutic efficacy of sulfadoxine-pyrimethamine and prevalence of resistance markers in Tanzania prior to revision of malaria treatment policy: Plasmodium falciparum dihydrofolate reductase and dihydropteroate synthase mutations in monitoring in vivo resistance. *Am J Trop Med Hyg*, 71:696–702, 2004.

C. J. L. Murray and A. D. Lopez. *The global burden of disease: a comprehensive assessment of mortality and disability from diseases, injuries, and risk factors in 1990 and projected to 2020*. Harvard University Press, Harvard, 1996a.

C. J. L. Murray and A. D. Lopez. *Estimating Causes of Death: New Methods and Global and Regional Applications for 1990*. World Health Organisation, Geneva, 1996b.

NMCP. National Malaria Medium Term Strategic Plan 2002-2007. National Malaria Control Programme, Ministry of Health Tanzania. 2003.

NMCP. Monitoring Malaria situation and control activities in Tanzania 2001-2003. Health Facility and Community survey. National Malaria Control Programme Monitoring and Evaluation Unit. Technical report, Dar es Salaam, Tanzania, 2004.

S. Owusu-Agyei, T. Smith, H. P. Beck, L. Amenga-Etego, and I. Felger. Molecular epidemiology of Plasmodium falciparum infections among asymptomatic inhabitants of a holoendemic malarious area in northern Ghana. *Trop Med Int Health*, 7:421–428, 2002.

S. Paget-McNicol, M. Gatton, I. Hastings, and A. Saul. The Plasmodium falciparum var gene switching rate, switching mechanism and patterns of parasite recrudescence described by mathematical modelling. *Parasitology*, 124:225–235, 2002.

R. E. Paul, M. J. Packer, M. Walmsley, M. Lagog, L. Ranford-Cartwright, R. Paru, and K. P. Day. Mating patterns in malaria parasite populations of Papua New Guinea. *Science*, 269:1709–1711, 1995.

W. H. Press, B. P. Flannery, S. A. Teukolsky, and W. T. Vetterling. *Numerical recipes in C: the art of scientific computing*. Cambridge University Press, Cambridge, 1988.

RBM WHO. Economic costs of malaria. `http://www.rbm.who.int/cmc_upload/0/000/015/363/RBMInfosheet_10.htm`, 2006.

M. Recker, S. Nee, P. Bull, S. Kinyanjui, K. Marsh, C. Newbold, and S. Gupta. Transient cross-reactive immune responses can orchestrate antigenic variation in malaria. *Nature*, 429:555–558, 2004.

H. Reyburn, C. Drakeley, I. Carneiro, C. Jones, J. Cox, J. Bruce, E. Riley, B. Greenwood, and C. Whitty. *The epidemiology of severe malaria due to Plasmodium falciparum at different transmission intensities in NE Tanzania. LSHTM Malaria Centre Report 2002-2003*, pages 6–7. 2004.

V. Robert, K. Macintyre, J. Keating, J. F. Trape, J. B. Duchemin, M. Warren, and J. C. Beier. Malaria transmission in urban sub-Saharan Africa. *Am J Trop Med Hyg*, 68: 169–176, 2003.

C. Rogier and J. F. Trape. Study of premunition development in holo- and meso-endemic malaria areas in Dielmo and Ndiop (Senegal): preliminary results, 1990-1994. *Med Trop (Mars)*, 55:71–76, 1995.

A. Ross and T. Smith. The effect of malaria transmission intensity on neonatal mortality in endemic areas. *Am J Trop Med Hyg*, 75 (Suppl 2):74–81, 2006.

A. Ross, G. F. Killeen, and T. Smith. Relationships between host infectivity to mosquitoes and asexual parasite density in Plasmodium falciparum. *Am J Trop Med Hyg*, 75 (Suppl 2):32–37, 2006a.

A. Ross, N. Maire, L. Molineaux, and T. Smith. An epidemiologic model of severe morbidity and mortality caused by Plasmodium falciparum. *Am J Trop Med Hyg*, 75 (Suppl 2): 63–73, Aug 2006b.

R. Ross. *The prevention of malaria*, volume 2. Murray, London, 1911.

A. K. Rowe, R. W. Steketee, F. Arnold, T. Wardlaw, S. Basu, N. Bakyaita, M. Lama, C. A. Winston, M. Lynch, R. Cibulskis, K. Shibuya, A. A. Ratcliffe, B. L. Nahlen, and Group for the Roll Back Malaria Monitoring and Evaluation Reference. Evaluating the impact of malaria control efforts on mortality in sub-Saharan Africa. *Trop Med Int Health, submitted*, 2007.

J. Sachs and P. Malaney. The economic and social burden of malaria. *Nature*, 415:680–685, 2002.

J. D. Sachs. Macroeconomics and health: investing in health for economic development. Technical report, Geneva, 2001.

W. Sama, G. Killeen, and T. Smith. Estimating the duration of Plasmodium falciparum infection from trials of indoor residual spraying. *Am J Trop Med Hyg*, 70:625–634, 2004.

A. Saul. Models for the in-host dynamics of malaria revisited: errors in some basic models lead to large over-estimates of growth rates. *Parasitology*, 117:405–407, 1998.

F. Saute, J. Aponte, J. Almeda, C. Ascaso, N. Vaz, M. Dgedge, and P. Alonso. Malaria in southern Mozambique: incidence of clinical malaria in children living in a rural community in Manhiça district. *Trans R Soc Trop Med Hyg*, 97:655–660, 2003.

J. R. Schellenberg, T. Smith, P. L. Alonso, and R. Hayes. What is clinical malaria? finding case definitions for field research in highly endemic areas. *Parasitol Today*, 10:439–442, 1994.

D. S. Shepard, M. B. Ettling, U. Brinkmann, and R. Sauerborn. The economic cost of malaria in africa. *Trop Med Parasitol*, 42:199–203, 1991.

G. T. Shute. *The microscopic diagnosis of malaria. In: Malaria. Principles and Practice of Malariology (Editors: W.H. Wernsdorfer and I. McGregor)*, pages 781–784. Churchill Livingstone, Edinburgh, 1988.

T. Smith and P. Vounatsou. Estimation of infection and recovery rates for highly polymorphic parasites when detectability is imperfect, using hidden markov models. *Stat Med*, 22:1709–1724, 2003.

T. Smith, J. D. Charlwood, J. Kihonda, S. Mwankusye, P. Billingsley, J. Meuwissen, E. Lyimo, W. Takken, T. Teuscher, and M. Tanner. Absence of seasonal variation in malaria parasitaemia in an area of intense seasonal transmission. *Acta Trop*, 54:55–72, 1993.

T. Smith, J. A. Schellenberg, and R. Hayes. Attributable fraction estimates and case definitions for malaria in endemic areas. *Stat Med*, 13:2345–2358, 1994.

T. Smith, H. P. Beck, A. Kitua, S. Mwankusye, I. Felger, N. Fraser-Hurt, A. Irion, P. L. Alonso, T. Teuscher, and M. Tanner. Age dependence of the multiplicity of Plasmodium falciparum infections and of other malariological indices in an area of high endemicity. *Trans R Soc Trop Med Hyg*, 93 (Suppl 1):15–20, 1999.

T. Smith, G. F. Killeen, N. Maire, A. Ross, L. Molineaux, F. Tediosi, G. Hutton, J. Utzinger, K. Dietz, and M. Tanner. Mathematical modeling of the impact of malaria vaccines on the clinical epidemiology and natural history of Plasmodium falciparum malaria: Overview. *Am J Trop Med Hyg*, 75 (Suppl 2):1–10, Aug 2006a.

T. Smith, N. Maire, K. Dietz, G. F. Killeen, P. Vounatsou, L. Molineaux, and M. Tanner. Relationship between the entomological inoculation rate and the force of infection for Plasmodium falciparum malaria. *Am J Trop Med Hyg*, 75 (Suppl 2):11–18, 2006b.

T. Smith, A. Ross, N. Maire, C. Rogier, J. F. Trape, and L. Molineaux. An epidemiological model of the incidence of acute illness in Plasmodium falciparum malaria. *Am J Trop Med Hyg*, 75 (Suppl 2):56–62, 2006c.

R. W. Snow, C. A. Guerra, A. M. Noor, H. Y. Myint, and S. I. Hay. The global distribution of clinical episodes of Plasmodium falciparum malaria. *Nature*, 434:214–217, 2005.

C. J. Struchiner, M. E. Halloran, and A. Spielman. Modeling malaria vaccines. i: New uses for old ideas. *Math Biosci*, 94:87–113, 1989.

A. O. Talisuna, P. Bloland, and U. D'Alessandro. History, dynamics, and public health importance of malaria parasite resistance. *Clin Microbiol Rev*, 17:235–254, 2004.

T. Tan-Torres Edejer, R. Baltussen, T. Adam, R. Hutubessy, A. Acharya, D. B. Evans, and C. J. L. Murray. *Making choices in health: WHO guide to cost-effectiveness analysis*. World Health Organization, Geneva, 2003.

M. Tanner and C. Vlassoff. Treatment-seeking behaviour for malaria: a typology based on endemicity and gender. *Soc Sci Med*, 46:523–532, 1998.

J. F. Trape and C. Rogier. Combating malaria morbidity and mortality by reducing transmission. *Parasitol Today*, 12:236–240, 1996.

United Nations. *Demographic Yearbook 2000*. United Nations, New York, 2002.

P. Vounatsou, T. Smith, A. Kitua, P. L. Alonso, and M. Tanner. Apparent tolerance of Plasmodium falciparum in infants in a highly endemic area. *Parasitology*, 120:1–9, 2000.

M. Weinstein, J. Siegel, M. Gold, M. Kamlet, and L. Russell. Recommendations of the panel of cost-effectiveness in medicine. *Journal of the American Medical Association*, 276:1253–1341, 1996.

M. E. Woolhouse. Patterns in parasite epidemiology: The peak shift. *Parasitol Today*, 14: 428–434, 1998.

World Health Organization. A global strategy for malaria control. Technical report, Geneva, 1993.

World Health Organization. Investing in Health Research and Development. Report of the ad hoc committee on health research relating to future intervention options. Technical report, Geneva, 1996.

World Health Organization. Malaria vector control and personal protection. `http://www.who.int/malaria/docs/WHO-TRS-936s.pdf`, 2006.

World Health Organization. Progress report on implementation of the plan of action of the abuja declaration. `http://www.afro.who.int/malaria/publications/section3.pdf`, 2004.

G. Zhou, N. Minakawa, A. K. Githeko, and G. Yan. Association between climate variability and malaria epidemics in the East African highlands. *Proc Natl Acad Sci USA*, 101: 2375–2380, 2004.